INTERNATIONAL SCIENTIFIC JOURNAL

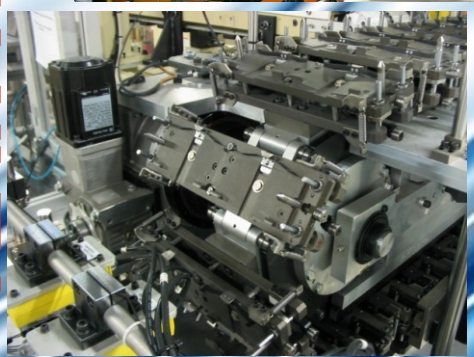
trans & MOTAUTO WORLD

ISSN PRINT 2367-8399
ISSN WEB 2534-8493

YEAR VI, ISSUE 2/2021









SCIENTIFIC TECHNICAL UNION OF MECHANICAL INGENEERING "INDUSTRY 4.0"
108 RAKOVSKI STR., SOFIA 1000, BULGARIA

INTERNATIONAL SCIENTIFIC JOURNAL

TRANS MOTAUTO WORLD

PUBLISHER:

SCIENTIFIC TECHNICAL UNION OF MECHANICAL ENGINEERING INDUSTRY-4.0

108, Rakovski Str., 1000 Sofia, Bulgaria
tel. (+359 2) 987 72 90,
tel./fax (+359 2) 986 22 40**,**
office@stumejournals.com
www.stumejournals.com

ISSN PRINT 2367-8399
ISSN WEB 2534-8493
YEAR VI, ISSUE 2 / 2021

EDITORIAL BOARD

CHIEF EDITOR
Prof. Petar Kolev, Bulgaria

MEMBERS:

Prof. Ahmet H. Ertas, TR
Prof. Aleksandar Kostikj, MK
Prof. Andrey Ferenets, RU
Prof. Angel Dimitrov, BG
Prof. Beti Angelevska, MK
Prof. Dainis Berjoza, LV
Prof. Dan Scarpete, RO
Prof. Daniela Todorova, BG
Prof. Emilia Andreeva-Moschen, AT
Prof. Gordana Marunic, HR
Prof. Hristo Stanchev, BG
Prof. Igor Penkov, EE
Prof. Igor Smirnov, UA
Prof. Igor Taratorkin, RU
Prof. Iliyan Lilov, BG
Prof. Lech Sitnik, PL
Prof. Ljudmila Boyko, UA
Prof. Madaminjon Aripdzanov, UZ
Prof. Martin Kendra, SK
Prof. Massimo Borghi, IT
Prof. Miho Mihow, BG
Prof. Murat Dogruel, TR
Prof. Natalia Sidenko, LV
Prof. Natasa Tomic-Petrovic, RS
Prof. Nikolay Georgiev, BG
Prof. Nikolay Ovchenkov, RU
Prof. Oleg Sharkov, RU
Prof. Pepo Yordanov, BG
Prof. Polatbeg Zhunisbekov, KZ
Prof. Rinat Kurmaev, RU
Prof. Rosen Ivanov, BG
Prof. Teymuraz Kochadze, GE
Prof. Tomaz Morchadze, GE
Prof. Vadim Zhmud, RU
Prof. Valyo Nikolov, BG
Prof. Zoran Jovanovic, RS

RESPONSIBLE SECRETARY:
Prof. Nikolay Tonchev, Bulgaria

C O N T E N T S

TRANSPORT TECHNICS. INVESTIGATION OF ELEMENTS. RELIABILITY

Exergy analysis of three cylinder steam turbine from supercritical coal-fired power plant
Mrzljak Vedran, Prpić-Oršić Jasna, Lorencin Ivan, Anđelić Nikola 34

Scissor lift dynamic analysis and motion regulation for the case of lifting with maximum load
Ilir Doçi, Shpetim Lajqi, Shkumbin Makolli, Burim Bibaj 38

Experimental Results of the Hybrid Electric Vehicle Energy Efficiency in Urban Transportation
Slavcho Bozhkov, Georgi Tonkov, Vladislav Boinovski, Petar Chernev 43

Design of a sailplane based on modern computational methods
Ivo Angelov, Simeon Simeonov 47

TRANSPORT. SAFETY AND ECOLOGY. LOGISTICS AND MANAGEMENT

Characteristics and state of road traffic safety in Montenegro
Marko Lučić 51

Common dimensions of European transport policy and the "Belt-Road" initiative
Antoaneta Kirova, Dimitar Todorov 54

Modeling travel behavior onboard of privately autonomous vehicle and shared autonomous vehicle
Jamil Hamadneh, Domokos Esztergár-Kiss 57

Determination of pre-collision travel speed in the event of a frontal collision between a vehicle and a fixed obstacle, using video recordings
Irina Duma, Nicolae Burnete, Adrian Todoruț, Daniel Truşcă 62

Ride comfort in road vehicles: a literature review
Diana Dacova 65

VEHICLE ENGINES. APPLICATION OF FUELS TYPES. EFFICIENCY

Fuel economy of off-road vehicles in respect to recuperation of vehicle's kinetic energy
Jasna Glišović1, Saša Vasiljević, Nenad Miloradović, Nadica Stojanović, Ivan Grujić 70

Exergy analysis of three cylinder steam turbine from supercritical coal-fired power plant

Mrzljak Vedran, Prpić-Oršić Jasna, Lorencin Ivan, Anđelić Nikola
Faculty of Engineering, University of Rijeka, Vukovarska 58, 51000 Rijeka, Croatia
E-mail: vedran.mrzljak@riteh.hr, jasna.prpic-orsic@riteh.hr, ilorencin@riteh.hr, nandelic@riteh.hr

Abstract: *In this paper is performed exergy analysis of three cylinder steam turbine from the supercritical coal-fired power plant. Exergy analysis parameters were calculated for the whole turbine and each cylinder for the ambient temperature range between 5 °C and 45 °C. The dominant mechanical power producer of all the cylinders is a low pressure cylinder (LPC) which produces 262.06 MW of mechanical power. An increase in the ambient temperature increases exergy destructions and decreases exergy efficiencies of the whole turbine and each cylinder. Exergy analysis shows that LPC is a cylinder with the highest exergy destruction (between 24.67 MW and 28.24 MW) and the lowest exergy efficiency (between 82.27% and 84.16%) in comparison to the other cylinders. Exergy destruction of the whole observed turbine is between 67.85 MW and 77.62 MW, while the whole turbine exergy efficiency ranges between 89.47% and 90.67%. Inside the observed steam turbine, LPC is the most influenced by the ambient temperature change, therefore future research and possible optimization should be specifically based on this cylinder.*

KEYWORDS*: EXERGY ANALYSIS, THREE CYLINDER STEAM TURBINE, SUPERCRITICAL POWER PLANT, THE AMBIENT TEMPERATURE VARIATION*

1. Introduction

The dominant function of steam turbines worldwide is electrical generator drive and electrical power production [1-3]. Steam turbines can today be found in various power plants, such as conventional, cogeneration, combined, marine, as a part of energy systems in various industries, etc. [4-10].

Improvement of steam power plants is today obtained in various different ways [11, 12]. One of important improvements is steam superheating on the temperatures and pressures above the water critical point parameters. Such steam power plants are named supercritical and ultra-supercritical power plants [13, 14]. Due to steam high temperature and pressure, steam turbines in such power plants (especially high pressure steam turbine cylinders) must be carefully designed and maintained with an aim to minimize all the possible losses [15]. Supercritical and ultra-supercritical steam power plants have various disadvantages, but its highest benefit is much higher overall plant efficiency in comparison to conventional steam power plants [16].

From the exergy viewpoint, in this paper is analyzed three cylinder steam turbine, which operates in supercritical coal-fired power plant. Along with calculation of produced mechanical power, it is analyzed exergy destruction (exergy power loss) and exergy efficiency of each cylinder and the whole turbine during the ambient temperature change. A special attention is paid to finding of the component which is the most influenced by the ambient temperature change.

2. Description and characteristics of the analyzed three cylinder steam turbine

Scheme and operating points required for the exergy analysis of three cylinder steam turbine from supercritical coal-fired power plant are presented in Fig. 1. Nominal mechanical power produced by the whole turbine, according to [17], is 660 MW.

High Pressure Cylinder (HPC) is a single flow cylinder which consists of one steam extraction. After HPC, a small part of the steam mass flow rate is delivered to high pressure feed water heating system (operating point 4), while the remaining steam mass flow rate is delivered to steam reheater. Steam reheater in the power plant is mounted in the steam generator (due to better visibility, in Fig. 1 reheater is shown as an independent component).

After steam reheating (increasing of steam temperature), steam expands through Intermediate Pressure Cylinder (IPC) which also has one steam extraction (identical to HPC). As HPC, IPC is also a single flow cylinder. After IPC, a certain steam mass flow rates are delivered to deaerator and Main Feed water Pump Turbine (MFPT) [18], operating points 7 and 8, while the remaining steam mass flow rate (operating point 9) is delivered to Low Pressure Cylinder (LPC).

LPC is a dual flow steam turbine, which means that the steam mass flow rate enters in the middle of the cylinder, one half expand through the left part (LPC-1), while the other part of the steam mass flow rate expand through the right part (LPC-2). In Fig. 1 LPC is divided in two parts, but all the considerations related to LPC will be performed by using only one part of LPC (the same results will be obtained if considering LPC-1 or LPC-2). The only attention is required during the calculation of LPC produced mechanical power – it will be calculated for LPC-1 and multiplied by two. After expansion in LPC, remaining steam mass flow rate from both parts of the LPC, is delivered to steam condenser for condensation [19].

The scheme shown in Fig. 1 is the most common arrangement of multi-cylinder steam turbines in thermal power plants [20]. Such arrangement is especially beneficial from the viewpoint of steam axial force self-balancing [21].

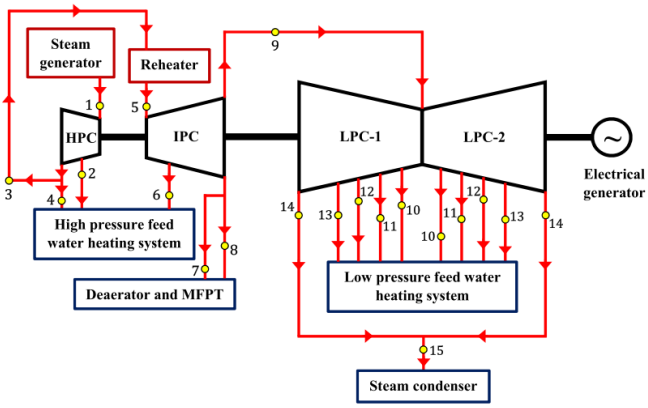


Fig. 1. *Three cylinder steam turbine from coal-fired supercritical power plant along with operating points*

3. Exergy analysis equations

3.1. General exergy equations, balances and principles

Exergy analysis of any component or a system is based on the second law of thermodynamics and it takes into consideration parameters of the ambient in which component or system operates [22, 23]. From this viewpoint, exergy analysis has the advantage over the energy analysis, which is based on the first law of thermodynamics and which did not take into consideration parameters of the ambient in which component or a system operates [24, 25]. Therefore, energy analysis will provide the same results if any component or a system operates at the ambient temperature of 5 °C or at the ambient temperature of 45 °C, while exergy analysis will show clear differences in the obtained results.

While disregarding kinetic and potential energies, which have a small impact on the overall balance, the overall exergy balance equation, valid for any component or a system, can be written according to recommendations from [26] as:

$$\dot{X}_{\mathrm{HEAT}} + P_{\mathrm{INLET}} + \sum \dot{E}x_{\mathrm{INLET}} = P_{\mathrm{OUTLET}} + \sum \dot{E}x_{\mathrm{OUTLET}} + \dot{E}x_{\mathrm{D}}. \qquad (1)$$

In Eq. (1), P is used or produced mechanical power in (kW), while $\dot{E}x_{\mathrm{D}}$ is exergy destruction (exergy power loss) in (kW). Other two undefined variables from Eq. (1) are firstly $\dot{X}_{\mathrm{HEAT}}$ - the exergy transfer by heat at the temperature T in (kW), defined as [27]:

$$\dot{X}_{\mathrm{HEAT}} = \sum(1 - \frac{T_0}{T}) \cdot \dot{Q}, \tag{2}$$

where T is temperature in (K), $\dot{Q}$ is an energy transfer by heat in (kW) and 0 is the index related to the ambient state. $\dot{E}x$ is a total exergy power of fluid flow in (kW) defined by an equation [28]:

$$\dot{E}x = \dot{m} \cdot \varepsilon. \tag{3}$$

In Eq. (3) $\dot{m}$ is the fluid mass flow rate in (kg/s), while ε is fluid specific exergy in (kJ/kg), defined according to [29] as:

$$\varepsilon = (h - h_0) - T_0 \cdot (s - s_0). \tag{4}$$

In Eq. (4), h is fluid specific enthalpy in (kJ/kg) and s is fluid specific entropy in (kJ/kg·K). The overall definition of any component or a system exergy efficiency is:

$$\eta x = \frac{\mathrm{CUMULATIVE\ \ EXERGY\ \ OUTLET}}{\mathrm{CUMULATIVE\ \ EXERGY\ \ INLET}}, \tag{5}$$

but is should be highlighted that for any component or a system, the proper exergy efficiency definition varies according to operating characteristics and type. In a standard operation, fluid mass flow rate leakage did not occur in any component or a system, so the valid mass flow rate balance is [30]:

$$\sum \dot{m}_{\mathrm{INLET}} = \sum \dot{m}_{\mathrm{OUTLET}}\ . \tag{6}$$

These equations, balances and principles will be used in exergy analysis of the whole observed steam turbine and each cylinder.

3.2. Exergy analysis equations of the whole observed turbine and each of its cylinders

Markings in all of the equations from this subsection are performed in relation to Fig. 1.

High Pressure Cylinder (HPC)

- Produced mechanical power:

$$P_{\mathrm{HPC}} = \dot{m}_1 \cdot (h_1 - h_2) + (\dot{m}_1 - \dot{m}_2) \cdot (h_2 - h_3). \tag{7}$$

- Exergy destruction:

$$\dot{E}x_{\mathrm{D,HPC}} = \dot{E}x_1 - \dot{E}x_2 - \dot{E}x_3 - \dot{E}x_4 - P_{\mathrm{HPC}}\,. \tag{8}$$

- Exergy efficiency:

$$\eta x_{\mathrm{HPC}} = \frac{P_{\mathrm{HPC}}}{\dot{E}x_{\mathrm{D,HPC}} + P_{\mathrm{HPC}}}. \tag{9}$$

Intermediate Pressure Cylinder (IPC)

- Produced mechanical power:

$$P_{\mathrm{IPC}} = \dot{m}_5 \cdot (h_5 - h_6) + (\dot{m}_5 - \dot{m}_6) \cdot (h_6 - h_7). \tag{10}$$

- Exergy destruction:

$$\dot{E}x_{\mathrm{D,IPC}} = \dot{E}x_5 - \dot{E}x_6 - \dot{E}x_7 - \dot{E}x_8 - \dot{E}x_9 - P_{\mathrm{IPC}}\,. \tag{11}$$

- Exergy efficiency:

$$\eta x_{\mathrm{IPC}} = \frac{P_{\mathrm{IPC}}}{\dot{E}x_{\mathrm{D,IPC}} + P_{\mathrm{IPC}}}. \tag{12}$$

Low Pressure Cylinder – left part (LPC-1); the same for right part (LPC-2)

- Produced mechanical power:

$$P_{\mathrm{LPC-1}} = \frac{\dot{m}_9}{2} \cdot (h_9 - h_{10}) + \left(\frac{\dot{m}_9}{2} - \dot{m}_{10}\right) \cdot (h_{10} - h_{11}) + \left(\frac{\dot{m}_9}{2} - \dot{m}_{10} - \dot{m}_{11}\right) \cdot (h_{11} - h_{12}) + \left(\frac{\dot{m}_9}{2} - \dot{m}_{10} - \dot{m}_{11} - \dot{m}_{12}\right) \cdot (h_{12} - h_{13}) + \left(\frac{\dot{m}_9}{2} - \dot{m}_{10} - \dot{m}_{11} - \dot{m}_{12} - \dot{m}_{13}\right) \cdot (h_{13} - h_{14}). \tag{13}$$

- Exergy destruction:

$$\dot{E}x_{\mathrm{D,LPC-1}} = \frac{\dot{E}x_9}{2} - \dot{E}x_{10} - \dot{E}x_{11} - \dot{E}x_{12} - \dot{E}x_{13} - \dot{E}x_{14} - P_{\mathrm{LPC-1}}. \tag{14}$$

- Exergy efficiency:

$$\eta x_{\mathrm{LPC-1}} = \frac{P_{\mathrm{LPC-1}}}{\dot{E}x_{\mathrm{D,LPC-1}} + P_{\mathrm{LPC-1}}}. \tag{15}$$

Whole Turbine (WT)

- Produced mechanical power:

$$P_{\mathrm{WT}} = P_{\mathrm{HPC}} + P_{\mathrm{IPC}} + 2 \cdot P_{\mathrm{LPC-1}}. \tag{16}$$

- Exergy destruction:

$$\dot{E}x_{\mathrm{D,WT}} = \dot{E}x_{\mathrm{D,HPC}} + \dot{E}x_{\mathrm{D,IPC}} + 2 \cdot \dot{E}x_{\mathrm{D,LPC-1}}. \tag{17}$$

- Exergy efficiency:

$$\eta x_{\mathrm{WT}} = \frac{P_{\mathrm{WT}}}{\dot{E}x_{\mathrm{D,WT}} + P_{\mathrm{WT}}}. \tag{18}$$

4. Steam parameters required for the exergy analysis

Required steam parameters in each operating point from Fig. 1 (steam temperature, steam pressure and steam mass flow rate) are found in [17] and presented in Table 1. Other steam parameters required for the exergy analysis (steam specific enthalpy, steam specific entropy and steam quality) in each operating point of Fig. 1, are calculated from the parameters presented in Table 1, by using NIST REFPROP 9.0 software [31].

From Table 1 can be seen that HPC and IPC of the observed steam turbine operates with a superheated steam, while the last few stages of both LPC parts (LPC-1 and LPC-2) operates with wet steam (steam under the saturation line – operating points 13 and 14). Steam quality of, for example 0.97, means that in that operating point exist 97% of steam and 3% of water droplets.

Steam specific exergies in each operating point from Fig. 1 are calculated by using Eq. (4). The defined ambient parameters for steam specific exergies calculation are always the same ambient pressure equal to 1 bar, while the ambient temperature is varied from 5 °C up to 45 °C, in steps of 10 °C.

Table 1. *Steam operating parameters for the exergy analysis*

O.P.*	Mass flow rate (kg/s)	Temperature (°C)	Pressure (bar)	Quality
1	532.00	566.0	242.000	Superheated
2	35.50	367.2	67.970	Superheated
3	448.40	315.1	45.670	Superheated
4	48.10	315.1	45.670	Superheated
5	448.40	566.0	41.100	Superheated
6	20.10	457.0	20.580	Superheated
7	25.40	362.9	10.650	Superheated
8	27.90	362.9	10.650	Superheated
9	375.00	362.9	10.650	Superheated
10	13.15	253.6	4.374	Superheated
11	6.55	128.8	1.333	Superheated
12	8.70	88.2	0.655	Superheated
13	6.60	60.9	0.208	0.970
14	152.50	35.8	0.059	0.940
15	305.00	35.8	0.059	0.940

*O.P. = Operating Point (according to Fig. 1)

5. Results and discussion

Produced mechanical power for the whole analyzed turbine and each cylinder is presented in Fig. 2.

LPC of the analyzed turbine produces the highest mechanical power of 262.06 MW (each part of the LPC produces 131.03 MW), while the lowest mechanical power is produced in IPC (180.77 MW). HPC produces mechanical power of 216.57 MW.

The whole analyzed turbine produces mechanical power of 659.40 MW. As the nominal mechanical power of the whole analyzed steam turbine is 660 MW, it can be concluded that data from Table 1 are given for the nominal turbine operating conditions.

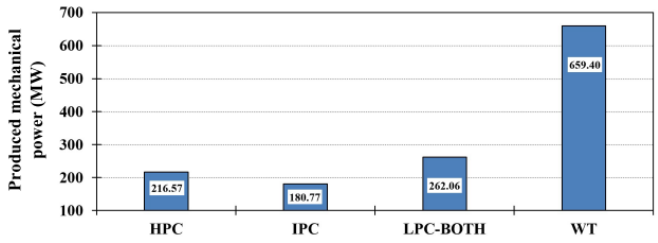


Fig. 2. *Produced mechanical power of the whole analyzed turbine and each cylinder*

Exergy destruction (exergy power loss) of the whole analyzed steam turbine and each cylinder at the various ambient temperatures is presented in Fig. 3.

By observing turbine cylinders, it can be seen that the highest exergy destruction is observed in LPC (between 24.67 MW and 28.24 MW), while the lowest exergy destruction is observed in IPC (between 6.11 MW and 6.94 MW). The whole analyzed steam turbine has exergy destruction between 67.85 MW and 77.62 MW.

From the ambient temperature viewpoint, it can be concluded that an increase in the ambient temperature results with increase in the exergy destruction of the whole turbine and each turbine cylinder.

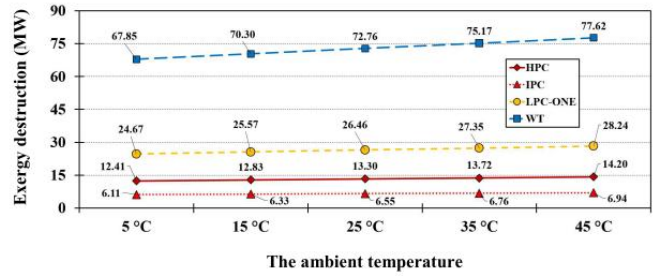


Fig. 3. *Exergy destruction of the whole analyzed turbine and each cylinder at the various ambient temperatures*

For the most components from steam power plant, exergy destruction and exergy efficiency are reverse proportional during the ambient temperature change. The same reverse proportionality can be seen for the analyzed steam turbine and all of its cylinders by comparing Fig. 3 and Fig. 4.

When observing exergy efficiency of the whole turbine, Fig. 4, it can be noted that the whole turbine has a much higher exergy efficiency than LPC, regardless of much higher exergy destruction, Fig. 3 and Fig. 4, at any ambient temperature.

In the considered ambient temperature range, exergy efficiency of HPC varies between 93.85% and 94.58%, of IPC between 96.30% and 96.73%, while exergy efficiency of the LPC varies between 82.27% and 84.16%. The whole turbine, in the considered ambient temperature range, has an exergy efficiency between 89.47% and 90.67%, what is expected exergy efficiency range of the whole steam turbine from supercritical steam power plant.

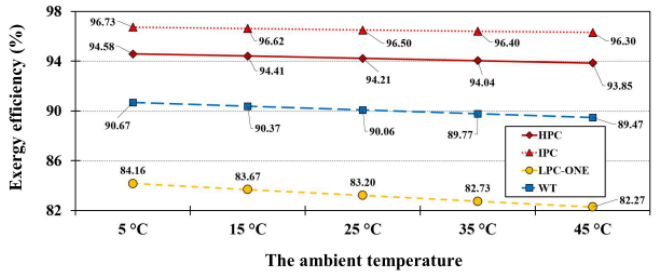


Fig. 4. *The exergy efficiency of the whole analyzed turbine and each cylinder at the various ambient temperatures*

The final goal of this paper is to investigate which cylinder of the observed steam turbine is the most influenced by the ambient temperature change. Therefore, the average percentage change in exergy destruction and in exergy efficiency of the whole analyzed turbine and each cylinder between ambient temperatures 5 °C and 45 °C is presented in Fig. 5.

While observing turbine cylinders during the ambient temperature change, it should be noted that the average percentage change in exergy destruction is the highest for HPC and LPC (3.16%), while average exergy destruction percentage change of IPC is much smaller (3.02%). Therefore, from the exergy destruction viewpoint, HPC and LPC are the most influenced by the ambient temperature change.

Average percentage change in exergy efficiency of each cylinder shows that LPC exergy efficiency is much more influenced by the ambient temperature change (0.56%) in comparison to HPC (0.19%), while the IPC is the lowest influenced by the ambient temperature change also from the exergy efficiency viewpoint (0.11%).

During the ambient temperature change, average exergy destruction change of the whole analyzed turbine is equal to 3.15%, while the average exergy efficiency change is equal to 0.33%.

Therefore, the conclusion which can be derived from Fig. 5 is that in the whole observed steam turbine, LPC is the most influenced by the ambient temperature change.

Further analysis of the observed steam turbine and all of its cylinders will be performed by using various artificial intelligence methods already developed by our research team [32-34].

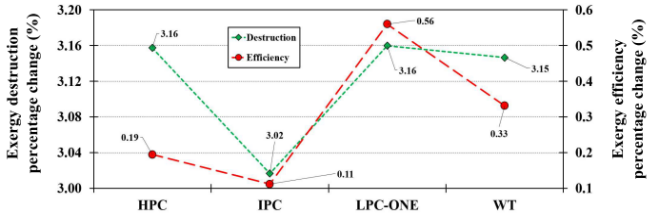


Fig. 5. *Average percentage change in exergy destruction and in exergy efficiency of the whole analyzed steam turbine and each cylinder between ambient temperatures 5 °C and 45 °C*

6. Conclusions

In this paper is performed an analysis of three cylinder steam turbine from the supercritical coal-fired power plant. Exergy destruction (exergy power loss) and exergy efficiency of each cylinder and the whole turbine during the ambient temperature change were analyzed. The most important conclusions from the performed analysis are:

- Considering all the cylinders, LPC produces the highest mechanical power equal to 262.06 MW (each part of the LPC produces 131.03 MW), followed by HPC (216.57 MW), while the lowest mechanical power is produced in IPC (180.77 MW).
- Exergy destruction and exergy efficiency of turbine cylinders are reverse proportional. LPC has the highest exergy destruction (between 24.67 MW and 28.24 MW) and the lowest exergy efficiency (between 82.27% and 84.16%). IPC has the lowest exergy destruction (between 6.11 MW and 6.94 MW) and consequentially the highest exergy efficiency (between 96.30% and 96.73%).
- The exergy destruction of the whole observed turbine is between 67.85 MW and 77.62 MW, while the whole turbine exergy efficiency ranges between 89.47% and 90.67%, what are expected values for steam turbine from supercritical steam power plant.
- Inside the whole observed steam turbine, LPC is the most influenced by the ambient temperature change, followed by HPC, while IPC is the cylinder which exergy efficiency and exergy destruction will be the lowest influenced by the ambient temperature change.

7. Acknowledgment

This research has been supported by the Croatian Science Foundation under the project IP-2018-01-3739, CEEPUS network CIII-HR-0108, European Regional Development Fund under the grant KK.01.1.1.01.0009 (DATACROSS), project CEKOM under the grant KK.01.2.2.03.0004, CEI project "COVIDAi" (305.6019-

20), University of Rijeka scientific grant uniri-tehnic-18-275-1447, University of Rijeka scientific grant uniri-tehnic-18-18-1146 and University of Rijeka scientific grant uniri-tehnic-18-14.

8. References

[1] Muhammad Ashraf, W., Moeen Uddin, G., Muhammad Arafat, S., Afghan, S., Hassan Kamal, A., Asim, M., ... & Krzywanski, J. (2020). Optimization of a 660 MWe Supercritical Power Plant Performance—A Case of Industry 4.0 in the Data-Driven Operational Management Part 1. Thermal Efficiency. Energies, 13(21), 5592. (doi:10.3390/en13215592)

[2] Muhammad Ashraf, W., Moeen Uddin, G., Hassan Kamal, A., Haider Khan, M., Khan, A. A., Afroze Ahmad, H., ... & Krzywanski, J. (2020). Optimization of a 660 MWe Supercritical Power Plant Performance—A Case of Industry 4.0 in the Data-Driven Operational Management. Part 2. Power Generation. Energies, 13(21), 5619. (doi:10.3390/en13215619)

[3] Lorencin, I., Anđelić, N., Mrzljak, V., & Car, Z. (2019). Genetic Algorithm Approach to Design of Multi-Layer Perceptron for Combined Cycle Power Plant Electrical Power Output Estimation. Energies, 12(22), 4352. (doi:10.3390/en12224352)

[4] Behrendt, C., & Stoyanov, R. (2018). Operational Characteristic of Selected Marine Turbounits Powered by Steam from Auxiliary Oil-Fired Boilers. New Trends in Production Engineering, 1(1), 495-501. (doi:10.2478/ntpe-2018-0061)

[5] Elhelw, M., Al Dahma, K. S., & el Hamid Attia, A. (2019). Utilizing exergy analysis in studying the performance of steam power plant at two different operation mode. Applied Thermal Engineering, 150, 285-293. (doi:10.1016/j.applthermaleng.2019.01.003)

[6] Mrzljak, V., Poljak, I., & Prpić-Oršić, J. (2019). Exergy analysis of the main propulsion steam turbine from marine propulsion plant. Brodogradnja: Teorija i praksa brodogradnje i pomorske tehnike, 70(1), 59-77. (doi:10.21278/brod70105)

[7] Burin, E. K., Vogel, T., Multhaupt, S., Thelen, A., Oeljeklaus, G., Gorner, K., & Bazzo, E. (2016). Thermodynamic and economic evaluation of a solar aided sugarcane bagasse cogeneration power plant. Energy, 117, 416-428. (doi:10.1016/j.energy.2016.06.071)

[8] Mrzljak, V., & Poljak, I. (2019). Energy Analysis of Main Propulsion Steam Turbine from Conventional LNG Carrier at Three Different Loads. NAŠE MORE: znanstveno-stručni časopis za more i pomorstvo, 66(1), 10-18. (doi:10.17818/NM/2019/1.2)

[9] Mrzljak, V., Poljak, I., & Mrakovčić, T. (2017). Energy and exergy analysis of the turbo-generators and steam turbine for the main feed water pump drive on LNG carrier. Energy conversion and management, 140, 307-323. (doi:10.1016/j.enconman.2017.03.007)

[10] Medica-Viola, V., Mrzljak, V., Anđelić, N., & Jelić, M. (2020). Analysis of Low-Power Steam Turbine With One Extraction for Marine Applications. NAŠE MORE: znanstveni časopis za more i pomorstvo, 67(2), 87-95. (doi:10.17818/NM/2020/2.1)

[11] Noroozian, A., Mohammadi, A., Bidi, M., & Ahmadi, M. H. (2017). Energy, exergy and economic analyses of a novel system to recover waste heat and water in steam power plants. Energy conversion and management, 144, 351-360. (doi:10.1016/j.enconman.2017.04.067)

[12] Baressi Šegota, S., Lorencin, I., Anđelić, N., Mrzljak, V., & Car, Z. (2020). Improvement of Marine Steam Turbine Conventional Exergy Analysis by Neural Network Application. Journal of Marine Science and Engineering, 8(11), 884. (doi:10.3390/jmse8110884)

[13] Tumanovskii, A. G., Shvarts, A. L., Somova, E. V., Verbovetskii, E. K., Avrutskii, G. D., Ermakova, S. V., ... & Lazarev, M. V. (2017). Review of the coal-fired, over-supercritical and ultra-supercritical steam power plants. Thermal Engineering, 64(2), 83-96. (doi:10.1134/S0040601517020082)

[14] Viswanathan, R., Henry, J. F., Tanzosh, J., Stanko, G., Shingledecker, J., Vitalis, B., & Purgert, R. (2005). US program on materials technology for ultra-supercritical coal power plants. Journal of materials engineering and performance, 14(3), 281-292. (doi:10.1361/10599490524039)

[15] Kocijel, L., Poljak, I., Mrzljak, V., & Car, Z. (2020). Energy Loss Analysis at the Gland Seals of a Marine Turbo-Generator Steam Turbine. Tehnički glasnik, 14(1), 19-26. (doi:10.31803/tg-20191031094436)

[16] Surywanshi, G. D., Pillai, B. B. K., Patnaikuni, V. S., Vooradi, R., & Anne, S. B. (2019). 4-E analyses of chemical looping combustion based subcritical, supercritical and ultra-supercritical coal-fired power plants. Energy Conversion and Management, 200, 112050. (doi:10.1016/j.enconman.2019.112050)

[17] Yang, Y., Wang, L., Dong, C., Xu, G., Morosuk, T., & Tsatsaronis, G. (2013). Comprehensive exergy-based evaluation and parametric study of a coal-fired ultra-supercritical power plant. Applied energy, 112, 1087-1099. (doi:10.1016/j.apenergy.2012.12.063)

[18] Mrzljak, V., Prpić-Oršić, J., & Poljak, I. (2018). Energy Power Losses and Efficiency of Low Power Steam Turbine for the Main Feed Water Pump Drive in the Marine Steam Propulsion System. Pomorski zbornik, 54(1), 37-51. (doi:10.18048/2018.54.03)

[19] Škopac, L., Medica-Viola, V., & Mrzljak, V. (2020). Selection Maps of Explicit Colebrook Approximations according to Calculation Time and Precision. Heat Transfer Engineering, 1-15. (doi:10.1080/01457632.2020.1744248)

[20] Tanuma, T. (Ed.). (2017). Advances in Steam Turbines for Modern Power Plants. Woodhead Publishing.

[21] Kostyuk, A., & Frolov, V. (1988). Steam and gas turbines. Mir Publishers.

[22] Kanoğlu, M., Çengel, Y. A. & Dincer, I. (2012). Efficiency Evaluation of Energy Systems. Springer Briefs in Energy. (doi:10.1007/978-1-4614-2242-6)

[23] Mrzljak, V., Poljak, I., & Žarković, B. (2018). Exergy analysis of steam pressure reduction valve in marine propulsion plant on conventional LNG carrier. NAŠE MORE: znanstveni časopis za more i pomorstvo, 65(1), 24-31. (doi:10.17818/NM/2018/1.4)

[24] Aljundi, I. H. (2009). Energy and exergy analysis of a steam power plant in Jordan. Applied thermal engineering, 29(2-3), 324-328. (doi:10.1016/j.applthermaleng.2008.02.029)

[25] Medica-Viola, V., Baressi Šegota, S., Mrzljak, V., & Štifanić, D. (2020). Comparison of conventional and heat balance based energy analyses of steam turbine. Pomorstvo, 34(1), 74-85. (doi:10.31217/p.34.1.9)

[26] Nandini, M., Sekhar, Y. R., & Subramanyam, G. (2021). Energy analysis and water conservation measures by water audit at thermal power stations. Sustainable Water Resources Management, 7(1), 1-24. (doi:10.1007/s40899-020-00487-4)

[27] Mrzljak, V., Blecich, P., Anđelić, N., & Lorencin, I. (2019). Energy and Exergy Analyses of Forced Draft Fan for Marine Steam Propulsion System during Load Change. Journal of Marine Science and Engineering, 7(11), 381. (doi:10.3390/jmse7110381)

[28] Lorencin, I., Anđelić, N., Mrzljak, V., & Car, Z. (2019). Exergy analysis of marine steam turbine labyrinth (gland) seals. Pomorstvo, 33(1), 76-83. (doi:10.31217/p.33.1.8)

[29] Koroglu, T., & Sogut, O. S. (2018). Conventional and advanced exergy analyses of a marine steam power plant. Energy, 163, 392-403. (doi:10.1016/j.energy.2018.08.119)

[30] Mrzljak, V., Poljak, I., & Medica-Viola, V. (2017). Dual fuel consumption and efficiency of marine steam generators for the propulsion of LNG carrier. Applied Thermal Engineering, 119, 331-346. (doi:10.1016/j.applthermaleng.2017.03.078)

[31] Lemmon, E. W., Huber, M. L., & McLinden, M. O. (2010). NIST Standard Reference Database 23, Reference Fluid Thermodynamic and Transport Properties (REFPROP), version 9.0, National Institute of Standards and Technology. R1234yf. fld file dated December, 22, 2010.

[32] Lorencin, I., Anđelić, N., Mrzljak, V., & Car, Z. (2019). Multilayer Perceptron approach to Condition-Based Maintenance of Marine CODLAG Propulsion System Components. Pomorstvo, 33(2), 181-190. (doi:10.31217/p.33.2.8)

[33] Baressi Šegota, S., Lorencin, I., Ohkura, K., & Car, Z. (2019). On the Traveling Salesman Problem in Nautical Environments: an Evolutionary Computing Approach to Optimization of Tourist Route Paths in Medulin, Croatia. Pomorski zbornik, 57(1), 71-87. (doi:10.18048/2019.57.05)

[34] Anđelić, N., Baressi Šegota, S., Lorencin, I., Mrzljak, V., & Car, Z. (2021). Estimation of COVID-19 epidemic curves using genetic programming algorithm. Health Informatics Journal, 27(1), 1460458220976728. (doi:10.1177/1460458220976728)

Scissor lift dynamic analysis and motion regulation for the case of lifting with maximum load

Ilir Doçi, Shpetim Lajqi, Shkumbin Makolli, Burim Bibaj
Faculty of Mechanical Engineering –University of Prishtina "Hasan Prishtina", Kosovo
*Corresponding author: shkumbin.makolli@uni-pr.edu

Abstract: *This paper deals with Dynamic analysis of Scissor Lifts during the Load Lifting to determine their dynamic behavior, find the nature of oscillations, and the regulation of lifting to minimize these oscillations and optimize the work process. During the motion processes, the lift and its main parts undergo heavy forces, moments, and oscillations. The method of research is acquiring results through design, modeling, and simulations, comparing them with analytic calculations, and looking for the optimal motion regulation of the Load Lifting. The analysis will be acquired when the Scissor lift is carrying maximum Load. The study will be concentrated in the finding the nature of dynamic forces and stresses that acts on the main parts of the lift and the extent and the form of oscillations. Results will be shown in the form of diagrams and contour views as the solution results of the tested system. Modeling and simulations will be carried using software SimWise 4D, based on the type of the Scissor Lift taken from Standard Manufacturer. Conclusions of these analyses are useful for design considerations, dynamic behavior, and safety of these types of lifts.*

Keywords: SCISSOR LIFT, DYNAMIC ANALYSIS, LOAD LIFTING, OSCILLATIONS, REGULATION, MODELING, SIMULATIONS

1. Introduction

Scissor Lifts are Material Handling Machines, mainly used in warehouses and industrial facilities. Their primary use is lifting and lowering loads, and short horizontal traveling with or without load. The Scissor Lift taken for study is a type of Hydraulic Lift. The name comes from the form of bar's (Fig.1). It is an elevated work platform that consists of many parts used to lift people and other loads. Working with Scissor Lifts can lead to problems with load lifting due to the occurring oscillations, which can result in safety issues. It is important to find optimal scenario of lifting to minimize the oscillations. To do this, main kinematic and dynamic parameters of the motion must be found, which is difficult with instrumentation. The model of the Scissor Lift is designed and modeled with software SimWise 4D [2] (Fig.2). In Fig.1 is shown the Scissor Lift in the working environment.

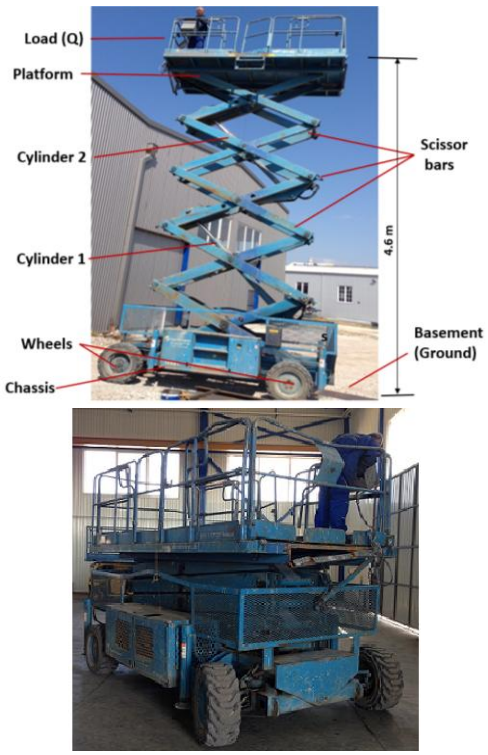


Fig.1. *Scissor Lift at highest position and lowest position [1],[13]*

Until now, authors have studied scissor lifts, with suggestions about design [4], [6], [7], dynamic stability [5], [13], [14], motion control and regulation [3], [11], [12], multibody dynamics [9],[10], oscillations [8], and simulations [3], [13], [14].

Scissor Lift is modeled based on the Lift *Type Genie® GS™-4390 RT* (Fig.1) [1]. It is used in one Local Factory near Prishtina City. Main parts of the Lift are: Chassis on 4 wheels, scissors bars, joints, hydraulic cylinders, and at the top is platform. Dimension of the Chassis are 4 m Length x 2.2 m Width. Total mass of the Lift is $m_L = 5849\ kg$. Max lifting capacity is $Q_{max} = 6670.8\ N \approx 680\ kg$. Max lifting Height: $H_{max} = 13.1\ m$. Lifting velocity: $v = 0.35\ m/s$. Diameter of the wheels $D_w = 380\ mm$. Other dimensions are given in Fig.3 & Fig.4. Type of the Motor: Ford MSG 425 4-cylinder gas/LPG 75hp (56 kW) [1]. There are 2 hydraulic cylinders that lifts the load, mounted between the scissor bars. During this process, the lift is not moving horizontally. (Fig.2)

2. Modelling and simulations of Scissor Lift

Lift is modelled based on the Data from manufacturer [1] and then assembled to make the functional model. In Fig.2 is shown the model of the Scissor Lift created with software [2]. For the simulation purposes, flat ground is also modelled, where lift stands [3].

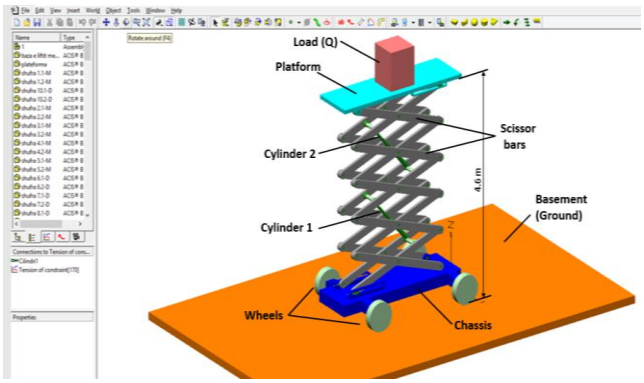


Fig.2. *Model of Scissor Lift in the software environment, at the highest position, created in the software SimWise 4d [2]*

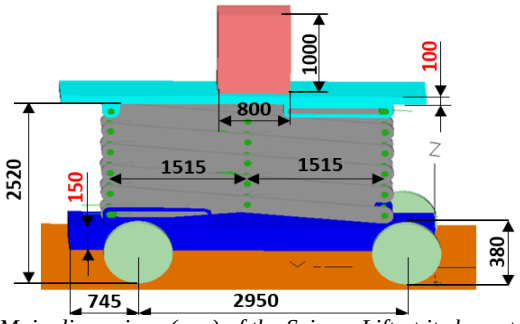


Fig.3. *Main dimensions (mm) of the Scissor Lift at its lowest and initial position (Left View)*

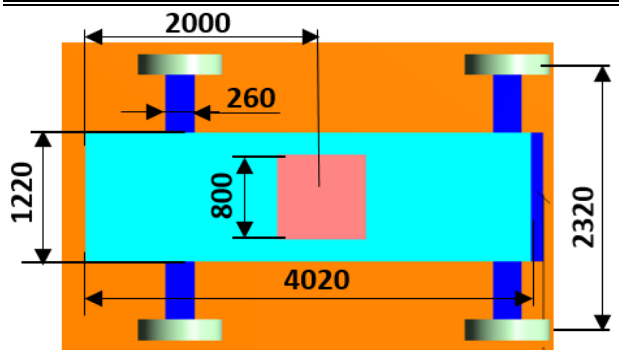


Fig.4. *Main dimensions (mm) of the Scissor Lift at its lowest and initial position (Top View)*

Load Q has prismatic form with dimensions 0.8m x 0.8m x 1m, laying on the platform. We consider that the best results will be achieved if the study is done with maximum loading capacity Q_{max} *= 680 kg* = 6670.8 N [14].

Before starting the simulations, lift stands in the position of relative rest, where platform and scissors are at initial lowest position (Fig.3 & Fig.4).

Simulation scenario of lifting is programmed close to real motion, which is important for achievement of reliable results. Platform (with Load Q) will start lifting from its initial lowest position (stowed) $H_1 = 1.8$ *m* up to the height $H_2 = 4.6$ *m*. This means that platform will lift for $\Delta H = H_2 - H_1 = 2.8$ *m*. Simulation has three phases [3],[13] (Fig.5):

First phase – initial position of relative rest with no lifting of Scissor Lift. Starts at time $0\ s < t < 0.5\ s$. Used to identify startup occurrences with no lifting.

Second phase – The process of lifting with the speed $v_l = 0.35$ *m/s* up to max height $H_2 = 4.6$ *m*. Starts after first phase and occurs between time $0.5\ s < t < 8.5\ s$. Time of lifting is $t = 8\ s$.

Third phase - motion stoppage. Lifting will stop, but load Q, platform, bars, and other parts will continue to oscillate. Starts after second phase, between time sequence $8.5\ s < t < 9.5\ s$. Important for evaluation of the results after motion stoppage.

Only one kinematic data of lifting we have from manufacturer for the lifting purpose, and that is the speed of lifting $v_l = 0.35$ *m/s* [1]. Regulation of lifting is done with the adjustment of hydraulic power given from two cylinders to have the required lifting speed $v_l = 0.35$ *m/s*. For this purpose, a step function is implemented to represent a real scenario of lifting simulation (Fig.5). The value of piston speed in cylinders that accurately represents required lifting speed of platform is $v_{cyl} = 0.077$ *m/s*. This is determined through numerous simulations (iterations). Definition of this function and its form was done to enable 'smooth' lifting and minimize oscillations in the lift. This is the most important process of motion regulation of scissor lifting in this paper [3],[13].

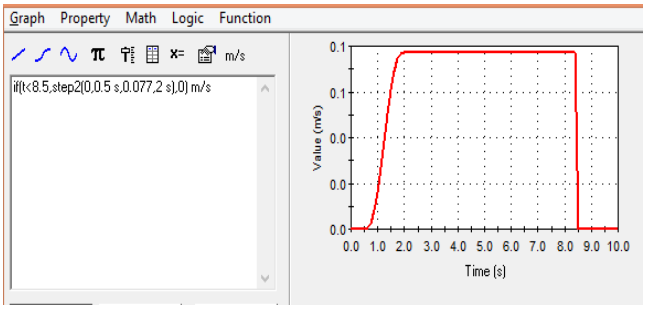


Fig.5*. Step function of the lifting speed*

Dynamic and kinematic parameters investigated for results are: forces, oscillations as part of acceleration, motion length, stresses that act in main parts of the lift. Results will be achieved using Numerical methods (Kutta-Merson) and Finite Elements Method (FEM), supported by software, in order to achieve accurate results [2], [13].

3. Results on the lifting cylinders

Hydraulic cylinder (actuator) is the device that lifts and lowers the load using hydraulic power of fluid. There are 2 cylinders mounted inside Scissors. Main parameter for analysis is finding the Force F_{cyl} acting on cylinder while it lifts the Load and upper parts of the lift. The force on cylinders depends on the dimensional and positional parameters of scissor bars and pistons (Fig.6|).

3.1. Calculation of Forces acting on the cylinders

Weight of parts lifted by cylinders is:

$Q_u = 20 \cdot Q_b + 2 \cdot Q_{cyl} + Q_{pl} + Q = 20 \cdot 100 + 2 \cdot 100 + 750 + 860 = 3710$ [kg] = 36395.1 [N]

Where:

Q_u – Weight of upper parts of the lift,

$Q_b = 100$ kg = 981 [N] – Weight of one scissor bar, out of twenty,

$Q_{pl} = 750$ kg = 7357.5 [N] – weight of the platform,

$Q_{cyl} = 100$ kg = 981 [N] – weight of one cylinder, out of two,

$Q = 860$ kg = 8436.6 [N] – maximal carrying load.

Force acting on the cylinder is based on the position of cylinder as in Fig.6 and referred to the literature [6], [7], and will be calculated considering the forces and reactions in two bars, where in the *Bar1* is connected (mounted) the cylinder.

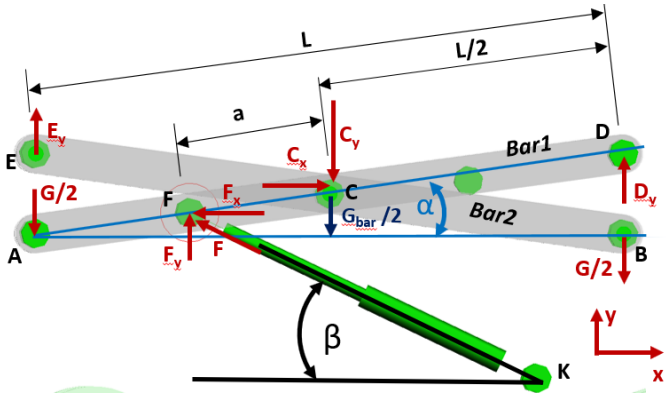


Fig.6. *Parameters of force acting on cylinders*

According to the diagram (Fig.6), we have [6], [7]:

$$D_y = E_y = \frac{G + G_{bars}}{2} \qquad [1]$$

$G = Q_{pl} + Q$; $G_{bars} = 20 \cdot Q_b + 2 \cdot Q_{cyl}$ [2]

$F_x = F \cdot \cos\beta$; $F_y = F \cdot \cos\beta$ - Force components in cylinder

α – Angle between the scissor bar and chassis,

β - Angle between the cylinder(s) and chassis.

C - Reaction force in the center of the bar's connections,

Equations of equilibrium in ***Bar1*****:**

$\sum X_i = 0$; $C_x - F_x = 0 \rightarrow C_x = F_x = F \cdot \cos\beta$

$\sum Y_i = 0$; $-G/2 + F_y - C_y - G_{bars}/2 + D_y = 0$

$-G/2 + F_y - C_y - G_{bars}/2 + (G+G_{bars})/2 = 0 \rightarrow C_y = F_y = F \cdot \sin\beta$

$\sum M_D = 0$; $G/2 \cdot L \cdot \cos\alpha + G_{bars}/2 \cdot (L/2) \cdot \cos\alpha - F_y \cdot \cos\alpha \cdot (L/2+a) + C_y \cdot L/2 \cdot \cos\alpha + F_x \cdot \sin\alpha \cdot (L/2+a) - C_x \cdot L/2 \cdot \sin\alpha = 0$

Using factorization and trigonometry identities, we get:

$G/2 \cdot L \cdot \cos\alpha + G_{bars}/2 \cdot (L/2) \cdot \cos\alpha - F \cdot \sin\beta \cdot \cos\alpha \cdot (L/2+a) + C_y \cdot L/2 \cdot \cos\alpha + F \cdot \cos\beta \cdot \sin\alpha \cdot (L/2+a) - C_x \cdot L/2 \cdot \sin\alpha = \mathbf{0}$

$\rightarrow \quad L \cdot \cos\alpha \cdot (G/2 + G_{bars}/4) - F \cdot \sin\beta \cdot \cos\alpha \cdot (L/2+a) + F \cdot \sin\beta \cdot L/2 \cdot \cos\alpha + F \cdot \cos\beta \cdot \sin\alpha \cdot (L/2+a) - F \cdot \cos\beta \cdot L/2 \cdot \sin\alpha = \mathbf{0}$

→ $L\cdot\cos\alpha\cdot(G/2+G_{bars}/4)+F\cdot[\sin\beta\cdot\cos\alpha\cdot(-L/2-a+L/2)+$

$+\cos\beta\cdot\sin\alpha\cdot(L/2+a-L/2)]=\mathbf{0}$

→ $L\cdot\cos\alpha\cdot(G/2+G_{bars}/4)+F\cdot[-a\cdot\sin\beta\cdot\cos\alpha+a\cdot\cos\beta\cdot\sin\alpha]=\mathbf{0}$

→ $L\cdot\cos\alpha\cdot(G/2+G_{bars}/4)-F\cdot a\cdot[\sin\beta\cdot\cos\alpha-\sin\alpha\cdot\cos\beta]=\mathbf{0}$

→ $L\cdot\cos\alpha\cdot(G/2+G_{bars}/4)-F\cdot a\cdot\sin(\beta-\alpha)=\mathbf{0}$

→

$$F=\frac{L\cdot\cos\alpha\cdot\left(\frac{G}{2}+\frac{G_{bars}}{4}\right)}{a\cdot\sin(\beta-\alpha)}=\frac{L\cdot\cos\alpha\cdot\left(\frac{Q_{pl}+Q}{2}+\frac{20\cdot Q_b+2\cdot Q_{cyl}}{4}\right)}{a\cdot\sin(\beta-\alpha)}$$

For our task, the parameters are:

L = 1.515 [m] – Length of one scissor bar (Fig.3 & Fig.6),

a = 0.745 [m] – Distance between the center of scissor bars joint (C) and restraint point of the cylinder (F) (Fig.6)

n = 2 – Number of cylinders. We assume that power is distributed equally between two cylinders.

Finally, force in the cylinder(s) is calculated by the formula:

$$F_{cyl}=\frac{L\cdot\cos\alpha\cdot\left(\frac{w}{2}+\frac{w_{bars}}{4}\right)}{n\cdot a\cdot\sin(\beta-\alpha)}=\frac{L\cdot\cos\alpha\cdot\left(\frac{Q_{pl}+Q}{2}+\frac{20\cdot Q_b+2\cdot Q_{cyl}}{4}\right)}{2\cdot a\cdot\sin(\beta-\alpha)}$$

Calculations of the Force are done for three positions of lifting height:

Position 1 – Lowest position of the platform. Height is H_1 = 1.8 m. Parameters, as in Fig.6, are: α= 4.42° , β = 14.896° , a = 0.745 m , L = 3.03 m. Time t = 0.2 s. Value of the Force in the cylinders is:

$$F_{cyl1}=\frac{3.03\cdot\cos(4.42^\circ)\cdot\left(\frac{750+860}{2}+\frac{20\cdot100+2\cdot100}{4}\right)}{2\cdot0.745\cdot\sin(14.896^\circ-4.42^\circ)}=15177.92$$

[kg] = **148895.38 [N]**

Position 2 - Middle height of the platform. Height is H_2 = 3.36 m. Parameters are (Fig.6): α= 10.367° , β = 32.827° , a = 0.745 m , L = 3.03 m. Height of platform H_2 = 3.36 m. Time t = 4.5 s. Value of the Force in the cylinders is:

$$F_{cyl2}=\frac{3.03\cdot\cos(10.367^\circ)\cdot\left(\frac{750+860}{2}+\frac{20\cdot100+2\cdot100}{4}\right)}{2\cdot0.745\cdot\sin(32.827^\circ-10.367^\circ)}=7094.97$$

[kg] = **69601.7 [N]**

Position 3 - Highest position of the platform. Height is H_3 = 4.6 m. Parameters are: α= 15.258°, β = 44.04°, a = 0.745 m, L = 3.03 m. Time t = 8.4 s. Value of the Force in the cylinders is:

$$F_{cyl3}=\frac{3.03\cdot\cos(15.258^\circ)\cdot\left(\frac{750+860}{2}+\frac{20\cdot100+2\cdot100}{4}\right)}{2\cdot0.745\cdot\sin(44.04^\circ-15.258^\circ)}=5526.4$$

[kg] = **54214.05 [N]**

Results of these calculations will be compared with graphical result for accuracy and validity of results.

3.2. Graphical results of the Force acting on cylinders

In Fig. 7 is given the graph of acting Force F_{cyl1} in the Hydraulic Cylinder 1. The process of lifting ends in time t = 8.5 s.

Based on the graph in Fig.7, we can conclude that force in the cylinder is close to the calculated values from the paragraph 3.1, which are shown with red dots. This validates the graphical results with simulations. Force F_{cyl} is dynamic in nature. At the start of the lifting process, in the interval $0.2\ s< t <1\ s$, it shows high frequencies up to $\upsilon \approx 11\ Hz$ and amplitudes $\lambda \approx 78000\ [N]$. Maximum value of force is achieved in time $t = 0.3\ s$, with the value $F_{cyl1} = -149000\ [N]$. Negative values denote pressure. After time $t=1\ s$, oscillations are low, until the start of phase 3, when there are more oscillations after stoppage, but with lower amplitudes.

This is important part of regulation, where oscillations are high at the beginning of the lifting, but later they decrease significantly.

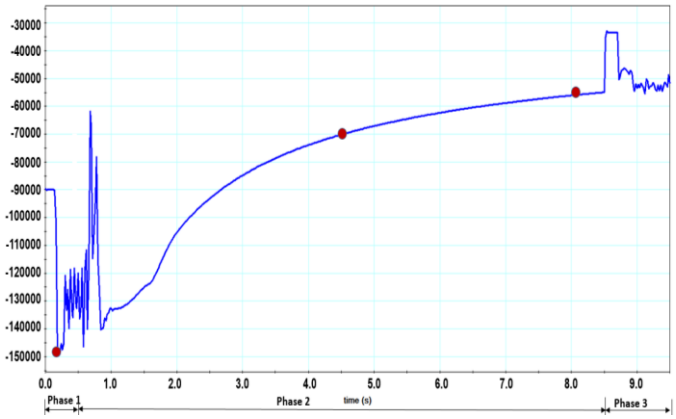


Fig. 7. *Force F_{cyl1} in the hydraulic Cylinder 1*

In Fig. 8 is the graph of the linear incerasing length of the cylinder's piston during the process of lifting. Cylinder will extend from 1.84 m to 2.4 m.

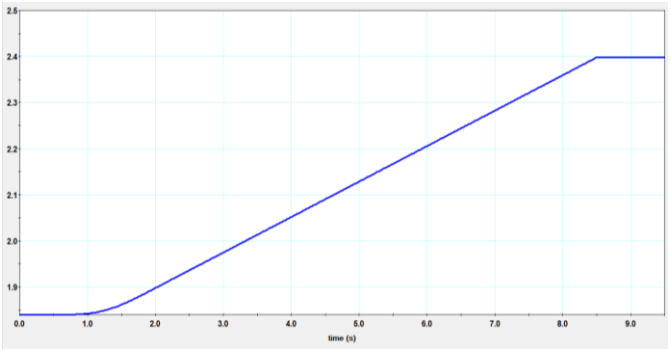


Fig. 8. *Length of hydraulic piston in Cylinder 1 during lifting*

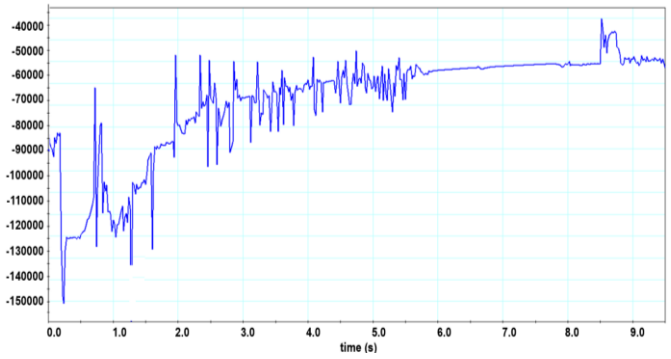


Fig. 9. *Force F_{cyl2} in the hydraulic Cylinder 2*

In Fig. 9 is given the graph of the Force F_{cyl2} in the Hydraulic Cylinder 2. The values are similar that of Cylinder 1, but the dynamic occurrences are intense, with more oscillations and frequencies than in Cylinder1, particularly in the time period 2.5 s <t< 6 s.

4. Oscillations in the Lifts Platform and Chassis

In the Fig. 10 is given the graph of acceleration ***a*** (m/s^2) in the platform of the lift. This is the parameter used to define the oscillations during the lifting.

Based on Fig. 10, we can conclude that platform undergoes heavy oscillations with high amplitudes up to $\lambda \approx 3.3\ (m/s^2)$ and frequencies up to $\upsilon \approx 13\ Hz$ at the start of the lifting to time $t = 2\ s$.

After time $t = 5.7$ s, amplitudes and frequencies tend to decrease. Based on the graph, medium value of acceleration is a ≈ 2.5 (m/s^2). Maximal value is $a_{max} \approx 6.5$ (m/s^2) at time t = 5.7 s.

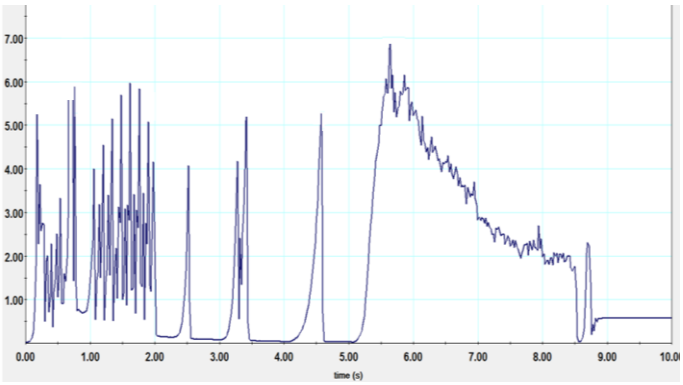


Fig. 10. *Oscillations on the platform, measured through acceleration* (m/s^2)

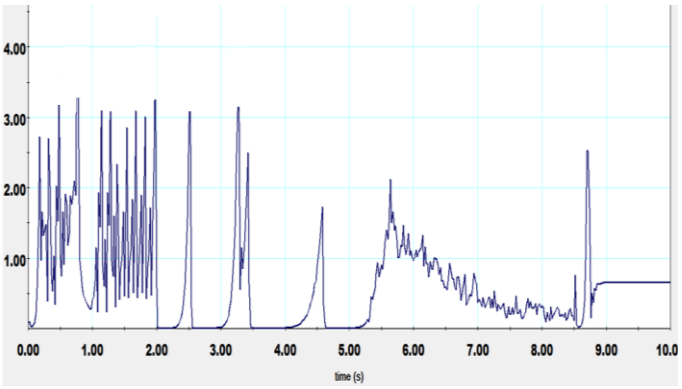


Fig. 11. *Oscillations on the chassis, measured through acceleration* (m/s^2)

In Fig. 11 is given the graph of acceleration $\boldsymbol{a}$ (m/s^2) in the chassis of the lift. We can conclude that chassis undergoes heavy oscillations, similarly to the platform, but intensity of accelerations is lower. Based on the graph, medium value of acceleration is a $\approx$ 1.2 (m/s^2) and maximal value is $a_{max} \approx 3.3$ (m/s^2) at time $t = 0.8$ s.

5. Results of the Scissor bars

Scissor bars are the part of the lift that passes the force from cylinders to the raise of the platform. They are one of the heaviest loaded parts. We will present the forces that act on their joints, and stresses. For this case, we will take one Scissor bar (Fig.14), considering that other bars will undergo similar forces and stress.

In the Fig.12 is shown the joint of Scissor bar: *Bar1*, taken for analysis, which is a revolute joint. In Fig.13 is given the result of Resultant Force in this joint. Medium value of resultant force (close to static) in the *Bar1* is $R_{b1} \approx 140000$ *[N]*, and maximal force (dynamic force) is $R_{b1max} \approx 250000$ *[N] (t = 1.5 s).* Value of dynamic Force is for 78% higher, which is a matter of concern. Based on the curve of Resultant Force, we can conclude that Scissor bars undergo heavy dynamic loads, with high amplitudes and frequencies until time $t \approx 7$ s. After that, dynamic occurrences decrease significantly.

In Fig.14 is shown the Contour spread of Stresses in Scissor *Bar1*. In this figure we can see the discretization of *Bar1* in FEM volume Elements. Based on the contour colors, we can conclude that highest value of stress is in the right joint of the bar.

In the Fig.15 is given the graph of stresses in the *Bar1*. Stress result is the type of Von Misses Stress. Stress curve changes in high dynamic oscillations, with high frequencies and amplitudes. Dynamic occurrences are intense at the start of the process, and after $t=3$ s start to decrease. Maximal value of stress is $\sigma \approx 476$ *MPa* $= 4.76 \cdot 10^8$ at time $t \approx 1.4$ s.

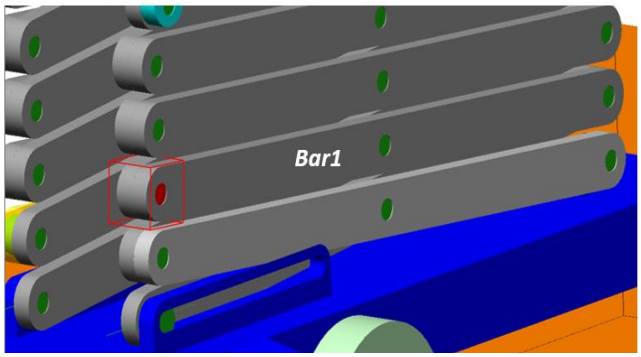


Fig.12. *Scissor Bar Joint taken for force calculation.*

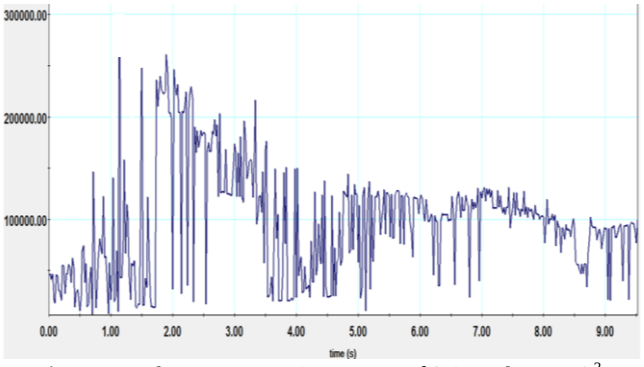


Fig.13. *Resultant Force acting on one of Scissor bars,* m/s^2

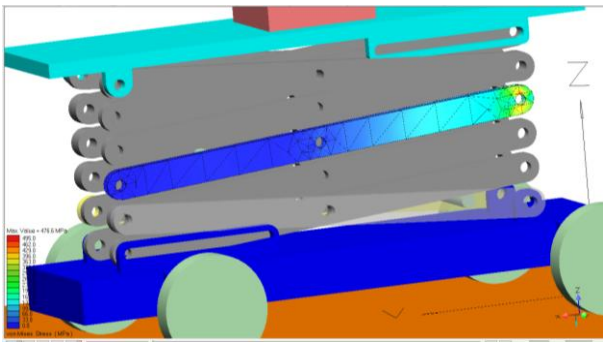


Fig.14. *Contour spread of Stresses in one of Scissor Bars - Bar 1*

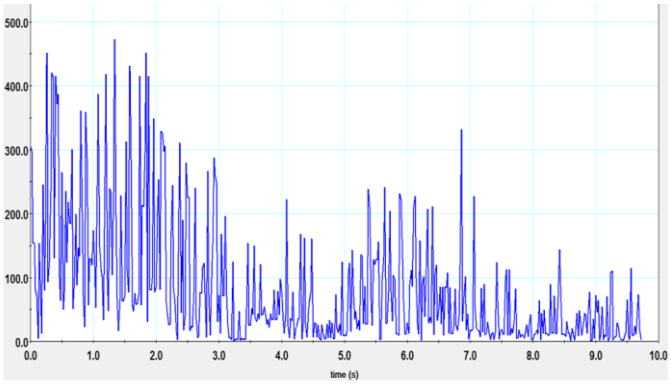


Fig.15. *Stress in one of Scissor Bars - Bar 1, MPa*

6. Forces in the Wheels

Wheels of the lift are connected in chassis and enables travel of the lift. In Fig.16 is given the graph of the Resultant Force R_w in the joint of front-left wheel. Based on the curve of Resultant Force, we can conclude that forces on the wheels are heavy dynamic in nature, with changes in amplitudes and frequencies until time t $\approx$ 5 s. After that, dynamic occurrences decrease significantly. Medium value of the resultant force (static force) after time $t=1$ s is $R_w \approx 31000$ *[N]* s, and maximal value of the dynamic force is $R_{wmax} \approx 42000$ *[N] (t = 1.5 s).* This is a difference of 35%, which is a matter of concern. As

a conclusion, during the lifting there should be additional outriggers from the chassis to the basement to increase the stability of the lift.

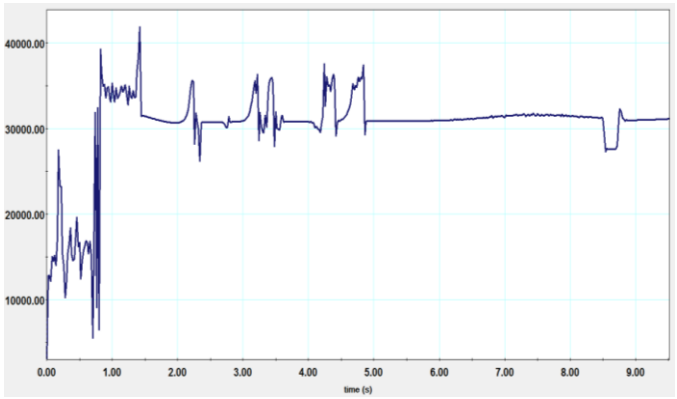


Fig.16. *Resultant Force acting on one of the Wheels.*

7. Conclusions

In this paper we have analyzed a Scissor Lift in the process of lifting to determine its dynamic behavior during load lifting, and the methodology to implement motion regulation through modeling and simulations with software. Modelling and simulations helps determining lift's behavior and its main parts. For the proper analysis and motion regulation it is important to develop accurate models to describe the lift dynamics [10], [12]. This can help also in further analysis for lifts regulation and optimization.

Dynamic analysis was carried after modelling and simulation of the scissor lift. The analysis proved the dynamic nature of the process and showed importance for the regulation to have less oscillations. Results of the forces in cylinder(s) are calculated analytically to determine the acting forces, then presented graphically using simulations, and then compared. Other results of kinematic and dynamic parameters in other parts of lift are presented graphically, analyzed, and commented.

Main issues in the lifting process are oscillations that are intensive in some parts of the lift. Their occurrence is irregular, with high amplitudes and frequencies. The form and influence of oscillations in the scissor lift can explain causes of parts failures, materials fatigue, and stability problems [8], [10]. These oscillations are difficult to be measured with actual instruments, so the methodology of analysis with simulations and comparison with analytical calculations helps to identify the dynamic occurrences in the scissor lift during the load lifting and leads to actions to be taken to minimize them and increase the safety of working with such a device.

Conclusions in this paper are important for safety and design considerations of these types of hydraulic lifts [3] and similar ones. They can be used also for analysis of other work processes, like lift travel in stowed or raised position.

8. References

[1] Scissor Lift manual Genie® GS™-4390 RT , https://www.genielift.com/en/aerial-lifts/rough-terrain-scissor-lifts/gs4390rt

[2] *SimWise 4D*, Design Simulation, Technologies, https://www.design-simulation.com/SimWise4D/.

[3] I. Doçi, M. Bruqi, N. Qehaja, *Dynamic analysis and motion control of hydraulic crane for men lifting using modeling and simulations*, 27TH DAAAM International Symposium on Intelligent Manufacturing and Automation, 2016.

[4] C. G. Dengiz, M. . Şenel, K. Yıldızlı, E.Koç, *Design and Analysis of Scissor Lifting System by Using Finite Elements Method*, Universal Journal of Materials Science 6(2): 58-63, 2018.

[5] Ren G. Dong, et al., *An Investigation on the Dynamic Stability of Scissor Lift*, Open Journal of Safety Science and Technology, 2012, 2, 8-15/

[6] Georgy Olenin, *Design of hydraulic scissors lifting platform, Saimaa University of Applied Sciences*, Thesis 2016.

[7] https://www.engineersedge.com/mechanics_machines/scissor-lift.htm

[8] Dresig, Hans, *Shwingungen mechanischer Antriebssysteme, Modellbildung, berechnung, analyse, synthese*, Springer Verlag, Berlin, 2001.

[9] Garcíaorden, J. Carlos, Goicolea, José M., Cuadrado Javier, *Multibody Dynamics, Computational methods and app*lications, p.91, 2007 Springer.

[10] La Hera, P. M., *Dynamics modeling of an electro-hydraulically-actuated system, 2011*, Umea University.

[11] Jon Danielson. *Mobile boom cranes and advanced input shaping control*. 2008. Georgia Institute of Technology.

[12] Vaughan J., *Dynamics and control of mobile cranes*, Georgia Institute of Technology, 2008.

[13] Burim Bibaj, *Analiza dinamike e liftit gërshërë me kapacitet bartës prej 750 kg*, Punim Masteri, FIM, Prishtinë, 2017.

[14] Doçi Ilir, Lajqi Naser, *Truck Mounted Cranes During Load Lifting – Dynamic Analysis and Regulation Using Modelling And Simulations*, International Journal for science, technics and innovations for the industry-MTM 2016.

Experimental Results of the Hybrid Electric Vehicle Energy Efficiency in Urban Transportation

Slavcho Bozhkov[1], Georgi Tonkov[2], Vladislav Boinovski[3], Petar Chernev[4]

[1]Department of Transport Equipment, [2,3]PhD student, Todor Kableshkov University of Transport, Bulgaria
[4]Sofia University Kliment Ohridski, Bulgaria
E-mail: stbozhkov@vtu.bg, tonkov.smolyan@gmail.com, V.boynovski@gmail.com, prchernev@gmail.com

Abstract: *The development of internal combustion engine vehicles, especially automobiles, is one of the greatest achievements of modern technology. Automobiles have made great contributions to the growth of modern society by satisfying many of its needs for mobility in everyday life. The automotive industry and the other industries that serve it constitute the backbone of the word's economy and employ the greatest share of the working population. However, the large number of automobiles in use around the world has caused and continues to cause serious problems for the environment and human life. Air pollution, global warming, and the rapid depletion of the Earth's petroleum resources are now problems of paramount concern [1]. A hybrid vehicle combines any type of two power (energy) sources. Possible combinations include diesel/electric, gasoline/fly wheel, and fuel cell (FC)/battery. Typically, one energy source is storage, and the other is conversion of a fuel to energy. The most modern hybrids are powered by a combination of traditional gasoline power and the addition of an electric motor. However, hybrid still use the petroleum-based engine while driving so they are not completely clean, just cleaner than petroleum only cars. This enables hybrid cars to have the potential to segue into new technologies that rely strictly on alternate fuel sources [2,3].*

This paper considers the experimental result obtained from HEV energy efficiency researching in urban transportation in the town of Sofia.

Keywords*: HEV, FUEL FLOW, METERING, METHODOLOGY*

1.Introduction

The hybrid electric vehicles (HEV) are equipped both with internal combustion engine (ICE) and electric motor (EM) which is powered by energy storage unit i.e., battery (B). The ICE used in a HEV is, of course, downsized compared to an equivalent vehicle engine. The ICE in combination with the EM provide an extended range for HEV and bring down pollution. The HEV energy efficiency is the main factor for its advantage and evaluating and depends directly on the HEV both fuel consumption and electricity consumption. Moreover, the city traffic conditions determine the quantity of the energy consumed by the HEV, so it is very important to measure the fuel consumption in accurate manner and with suitable equipment to obtain the correct results.

2.Object

As object of experimental researching of the hybrid electric vehicle energy efficiency (HEVEE) can be selected various HEV models which can be researched and evaluated. At this paper is selected Honda CR-Z [4] which common view is shown on figure 1.



Fig.1 *Researched HEV (Honda CR-Z)*

The selected HEV is of the mild class hybrid. The HEV propulsion system is known as Integrated Motor Assistance [4]. The EM is linked rigidly with the ICE and serve as assistant motor as well as the starter motor. The HEV technical data are shown in table 1.

Table 1: HEV technical data

Quantity	Designation	Dimension	Value
Engine	1.5 SOHC i-VTEC		
Max. Power (Engine)		kW/PS/rpm	84/114/6100
Max. Torque (Engine)		Nm/rpm	145/4800
Max. Power (Electric Motor)		kW/PS/rpm	10/14/1500
Max. Torque (Electric Motor)		Nm/rpm	78.4/1000
Max. Power (Combined)		kW/PS/rpm	91/124/6100
Max Torque (Combined)		Nm/rpm	174/1000-1500
Fuel system	Honda PGM-FI Electronic Injection		
Fuel rating	Unleaded		95 RON
Maximum design total mass	m_{HEV}	kg	1520
Frontal area	A	m^2	2,43
Drag coefficient	C_d		0,30
Gear ratios	i_n	1^{st} 2^{nd} 3^{rd} 4^{th} 5^{th} 6^{th}	3.142 1.869 1.303 1.054 0.853 0.688
Final drive ratio	i_o		4.111
Transmission efficiency	η_t		0,9 [6]
Tyres	195/55R16		
Rim diameter	D	mm	406,4mm (16in)
Tyre aspect ratio	H/B	%	55
Coefficient of the wheel inertia	δ_1		0,04
Coefficient of the powertrain inertia	δ_2		0,0025
Air density	ρ_a	kg/m^3	1,25
Fuel density	ρ_f	kg/m^3	710

The metering equipment is Bosch KTS 560 interface [5] which is shown on the figure 2. The test-bench can be programmed and managed by the Flowcode 7 software [6], which ensures adjustment to the real work mode of the fuel injectors in the modern automobiles and HEVs.



***Fig. 2** Common view of the metering interface [5]*

The selected interface is connected to the HEV OBD-2 diagnostic plug and receive the data from the HEV electronic control unit (ECU) via ISO 15765-4 protocol [6]. The measuring quantities are as following:

- Discharging current I_{disch}, A;
- HEV required power P_{HEV}, W;
- EM speed n_{EM}, min^{-1};
- Battery voltage under load U_B, V;
- Driving speed υ_d, km/h;
- Electric motor phase current, A.

The fuel consumed is determined by the difference in the HEV fueling volume before and after researching test. The initial fuel volume is equal to the full HEV fuel tank volume. The difference is metered by the fuel equipment in the gas station in accuracy 0.5% according to the OIML R 117-1 [7].

The researching is carried on in the town of Sofia according to the route which is tracked and measured by the GPS navigation system NMEA Monitor for windows Ver 3.79 [8]. The recorded route is shown on the figure 3. The total travelled distance is 53 km.

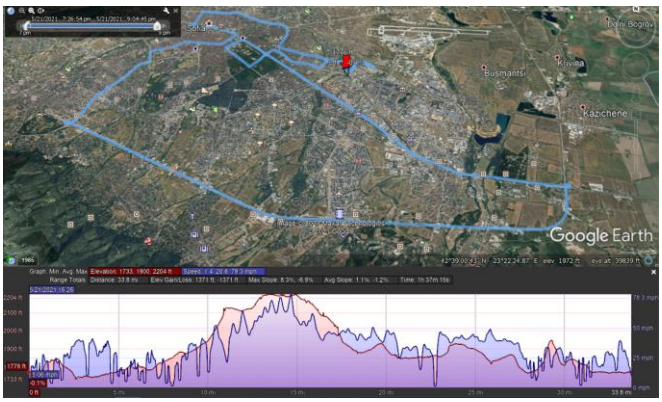


***Fig. 3** The travelled route*

The fig.3 contains the map of the route, the elevation characteristic of the route and the driving speed characteristic. These data correspond to the Bosch KTS 560 clock and are used to experimental determining the parameters of HEVEE. The average road inclination is 1%.

During the experiments, the HEV driving modes are selected as follows:

0-1700 s – Normal mode

1700-3200 s – Sport mode

3200-3800 s – Eco mode.

These modes are determined by the IMA system and cannot be modified. The specific energy efficiency during these modes is evaluated in point 4.

3.Results

After the performed experiments is obtained the following results, which are displayed in graphic diagrams. A fig.4 to fig.7 displays the energy characteristic of the Normal mode. Fig.4 presents the discharging current I_{disch} and the battery voltage under load U_B. The maximum value of the I_{disch} is 98,63 A. The maximum value of the driving speed υ_d is 70 km/h.

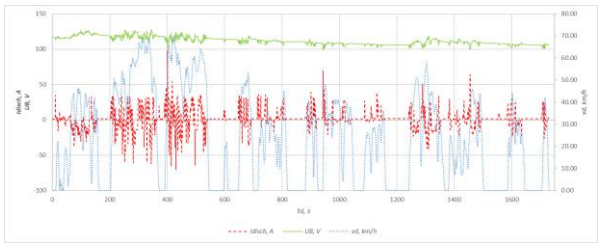


***Fig.4 Normal mode:** Characteristic of the discharging current I_{disch} and battery voltage under load U_B*

At the next fig.5 is displayed the electric motor phase current. The maximum value of the EM phase current is 98,9 A.

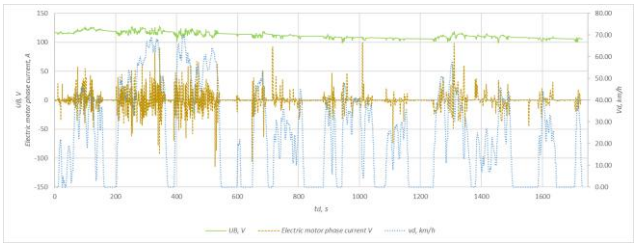


***Fig.5 Normal mode:** Characteristic of the electric motor phase current and battery voltage under load U_B*

The HEV required electrical power P_E is displayed on the fig.6. The required power P_E is determined by the IMA system and is part of the whole required driving power. The maximum P_E = 9773 W. The maximum n_{EM} = 3048 min^{-1}.

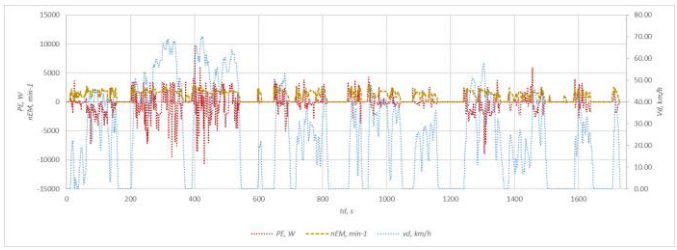


***Fig.6 Normal mode:** Characteristic of the HEV required electrical power P_E*

The electricity consumed Q_{disch} and electricity regenerated Q_{reaen} is shown on fig.7. The electricity consumed Q_{disch} = 0,183 kWh. The electricity regenerated Q_{regen} = 0,235 kWh.

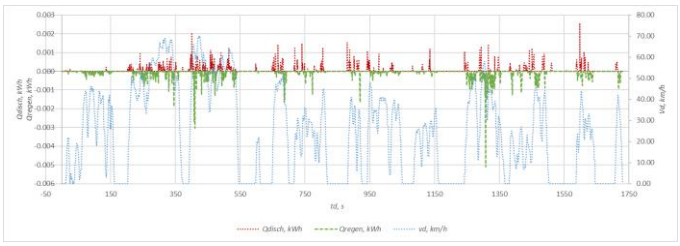


***Fig.7 Normal mode:** Characteristic of the HEV electricity consumed Q_{disch} and electricity regenerated Q_{regen}*

A fig.7 to fig.10 displays the energy characteristic of the Sport mode. Maximum I_{disch} = 109,37 A. Maximum driving speed v_d = 135 km/h.

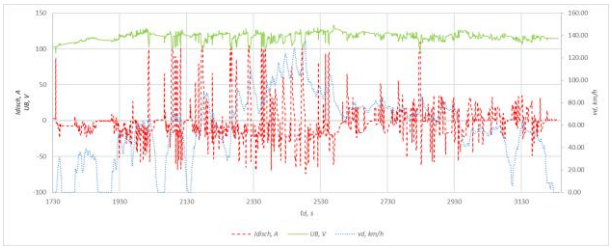


Fig.7 Sport mode: *Characteristic of the discharging current I_{disch} and battery voltage under load U_B*

Maximum EM phase current is 116,3 A.

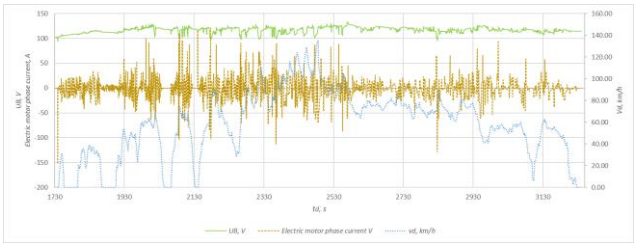


Fig.8 Sport mode: *Characteristic of the electric motor phase current and battery voltage under load U_B*

Maximum P_E = 10262 W. Maximum n_{EM} = 4015 min^{-1}.

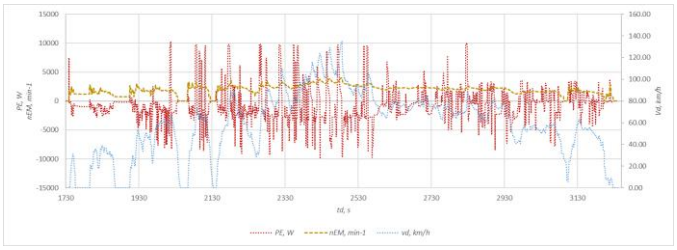


Fig.9 Sport mode: *Characteristic of the HEV required electrical power P_E*

The electricity consumed Q_{disch} = 0,316 kWh. The electricity regenerated Q_{regen} = 0,566 kWh.

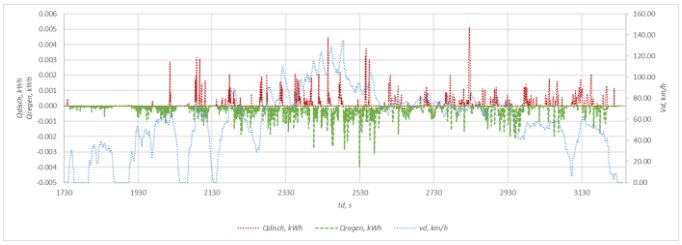


Fig.10 Sport mode: *Characteristic of the HEV electricity consumed Q_{disch} and electricity regenerated Q_{regen}*

A fig.11 to fig.14 displays the energy characteristic of the Eco mode. Maximum I_{disch} = 100,09 A. Maximum driving speed v_d = 68 km/h.

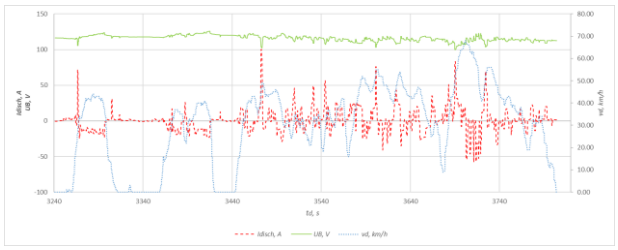


Fig.11 Eco mode: *Characteristic of the discharging current I_{disch} and battery voltage under load U_B*

Maximum EM phase current is 91,75 A.

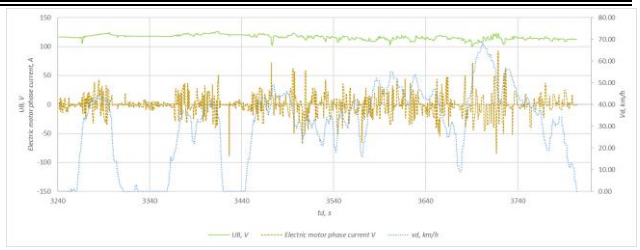


Fig.12 Eco mode: *Characteristic of the electric motor phase current and battery voltage under load U_B*

Maximum P_E = 9858 W. Maximum n_{EM} = 2996 min^{-1}.

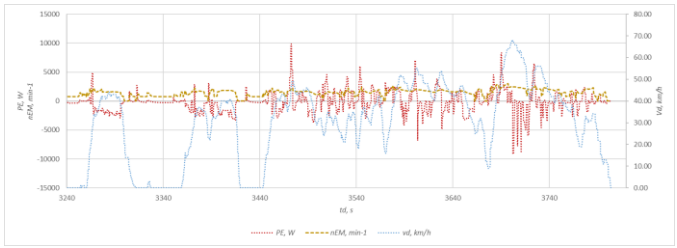


Fig.13 Eco mode: *Characteristic of the HEV required electrical power P_E*

The electricity consumed Q_{disch} = 0,082 kWh. The electricity regenerated Q_{regen} = 0,107 kWh.

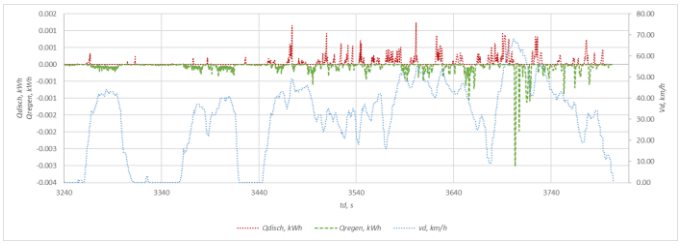


Fig.14 Eco mode: *Characteristic of the HEV electricity consumed Q_{disch} and electricity regenerated Q_{regen}*

On all characteristics the battery has stable voltage with maximum value 132,89 V and minimum value 93,99 V.

The subtotal electricity consumed Q_{disch} = 0,58 kWh. The subtotal electricity regenerated Q_{regen} = 0,91 kWh.

Because of the state of charge of the HEV battery and recharging limitation by the IMA system $Q_{regen} > Q_{disch}$, i.e. this is the case with recharged HEV battery, which has decreased lifetime.

The total fuel consumed Q_f = 3,73 l.

4.Evaluation

According to the evaluation criteria [2,9] is obtained data which is represented in table 3. The selected HEV is not rechargeable and in this case the Q_{rech} = 0.

Table 2: *Evaluation data.*

Mode	Distance criterion		Mass criterion		Combined criterion	
	Fuel consumed $Q_{D,f}$, l/100km,	Electricity consumed $Q_{D,e}$, kWh/100km	Fuel consumed $Q_{M,f}$, l/kg	Electricity consumed $Q_{M,e}$, kWh/kg	Fuel consumed $Q_{DM,f}$, l/kgkm	Electricity consumed $Q_{DM,e}$, kWh/kg.km
Normal	6.22896	-0.46989	0.00046	0.00003	0.00518	-0.00039
Sport	8.16227	-1.02218	0.00132	-0.00016	0.03224	-0.00404
Eco	5.65222	-0.13823	0.00068	-0.00002	0.01235	-0.00030

The official data for the researched HEV [4] are as follows: Urban 6.1 l/100km; Extra Urban 4.4 l/100km; Combined 5.0 l/100km. The obtained data in the table 2 include official data and give the detailed HEV energy efficiency evaluation. The outreaching of the data is because of the decrease battery resource.

Conclusion

The experimental researching of the hybrid electric vehicle is carried on and the real data according to traffic condition in town of Sofia and selected hybrid model are obtained.

The evaluation of the obtained data make clear the real energy efficiency of the selected HEV and estimate its real technical condition.

Acknowledgment

The article is related to the implementation of the project "Modelling and design of position sensors based on multiferroic layered structures" under Contract № КП-06-Русия/20 28.09.2019, Todor Kableshkov University of Transport – Sofia, of the Bulgarian side. For the Russian side, the reported study was funded by RFBR project number № 19-58-18001. The article also related to the implementation of the project "Experimental researching of the hybrid electric vehicle energy efficiency in the city of Sofia traffic conditions" under Contract №66/21.04.2021, Todor Kableshkov University of Transport - Sofia.

Literature

[1] Ehsani M Y Gao S Longo K Ebrahimi 2019 Modern Electric, Hybrid Electric, and Fuel Cell Vehicles Third edition (Nee York: CRC Press LLC)

[2] Iqbal Husain 2018 Electric and Hybrid Vehicles Design Fundamentals 2nd ed (New York: CRC Press Taylor & Francis Group)

[3] Slavcho Bozhkov, Marian Mutafchiev, Ivan Milenov, Penko Bozhkov, M.I. Bichurin, R.V. Petrov. Method for determination of the hybrid electric vehicle energy efficiency in urban transportation // Вестн. Новг. гос. ун-та. Сер.: Технические науки. 2019. УДК 681.586.785, 2019, DOI: https://doi.org/10.34680/2076-8052.2019.4(116).4-8 http://www.novsu.ru/file/1575020

[4]https://hondanews.eu/eu/lv/cars/media/pressreleases/1343/honda-cr-z

[5] https://ESItronic.com

[6] https://www.iso.org/standard/67245.html

[7] https://www.oiml.org/en/files/pdf_r/r117-1-e07.pdf

[8] http://4river.a.la9.jp/gps/file/NmeaMon.htm

[9] Slavcho Bozhkov, Marian Mutafchiev, Ivan Milenov, Roman Petrov, Viktor Leontiev, Penko T. Bozhkov. Method for Determination of the Hybrid Electric Vehicle Energy Efficiency in Urban Transportation, International Scientific Conference „MACHINERY AND CONSTRUCTION TECHNOLOGIES IN TRANSPORT" - 2020", Velingrad, 09th -11th September 2020, Academic journal "Mechanics Transport Communication", ISSN 1312-3823 (print), ISSN 2367-6620 (online), volume 18, issue 3/3, 2020, article No 1943, pp.VI-24-VI-29, Todor Kableshkov University of Transport, Sofia, 2020 https://mtc-aj.com/library/1943_EN.pdf

Design of a sailplane based on modern computational methods

Ivo Angelov, Simeon Simeonov
Technical University – Sofia, Bulgaria
E-mail: ivvoangelov@gmail.com simaeronov@gmail.com

Abstract:*The purpose of the current study is to evaluate and apply a new approach to the design process of an aircraft with a high aspect ratio wing, based on modern understandings and development in the fields of aerodynamics and computational fluid dynamics. Conventional methods rely on semi-analytical models for describing different flow characteristics and interactions with bodies. The classical approach requires numerous coefficients to account for unknown effects, what is more, such workarounds are derived for well-defined cases and are not easily applicable for complex problems which could be dangerously misleading. CFD analysis, based on new developments in computational machines, give the possibility of analyzing complex aerodynamic interactions such as shading, downwash, ground effect and vortex shedding. Such use of innovative technology has already proven itself to have beneficial effect on reduction of cost and human error by being able to simplify and speedup many of the calculations without the need of coefficient adjustments.*
Keywords*: SAILPLANE, AEROSPACE ENGINEERING, CFD, FLIGHT DYNAMICS, AIRCRAFT DESIGN.*

1. Introduction

The world of engineering has changed for the better. Nowadays engineers are able to solve complex fluid and structural analysis without drawing a single line on a sheet of paper [1], [2]. Technology has advanced faster than our ability to adapt to use new methods for solving existent problems. The field of design in aeronautics in many cases is an example of industry that falls behind the most modern development methods. The goal of this work is not to prove current methods wrong, but to improve on them the same way Wright brothers improved on the work of previous inventors before them. For the purpose of the research sailplane is designed. The process of developing heavier-than-air machine that is able to stay aloft for prolonged amount of time without the need of an engine is a task that requires approach that differs from the conventional one [3].

Methods in use nowadays rely heavily on semi-analytical equations derived from the experience of previous concepts [4], [5]. The goal of our work is to present and test new way of thinking. The carried process of designing a sailplane is shown in the following paragraphs. Note; the information given is compressed extensively due to paper volume requirements.

2. Defining aircraft mission

One of the most important phases of an aircraft design is the definition of all the requirements that the aircraft will have to meet. Generally those are split into two categories. Ones that depend on the designers' choices such as maximum takeoff weight (MTOW) and ones that depend on legal regulations, such as certification requirements [6]. Skipping a point in the very beginning of the design process will lead to expensive workarounds and costly delays. On (table 1) are shown just some of the requirements that depend both on the designers' choice and legal requirements. It should be noted that filling up this table is iterative processes many of the characteristics of an aircraft depend on each other. Example is the relation between MTOW, Stall speed and Aspect ratio where the stall speed depends on the MTWO and the area of the wing. Data about existing aircraft is also gathered in this phase of the project.

Table 1. *Mission requirements*

No	Factor	Requirement
1	Aircraft Type	Sailplane – Standard class
2	Certification	CS - 22
3	Crew	1 pilor
4	MTOW	300 - 400 kg
5	Stall Speed	17 - 19 m/s
6	Max Speed	50-56 m/s
7	Glide Ration	Above 21
8	Aspect Ratio	Above 12
9	Max Altitude	5000 m
10	Landing Gear	Monowheel
11	Tail Configuration	T – Tail
12	Wing Configuration	High Wing
13	Wing Platform	Tapered

3. Preliminary Design

This is the part of the design process where the team could benefit from existing machines of similar mission. Characteristic features of successful aircraft could be incorporated as a stepping stone in the development of a better design. In the preliminary design more specific layout and sizes of the future aircraft comes to light. Type of control surfaces, means of propulsion, construction materials and more accurate areas for the tail and mail lifting surfaces are only part of all the factors that are considered in phase. In the case of the sailplane that is being designed, the team of engineers has chosen the following characteristics as most adequate for the mission requirements.

3.1 Main Lifting Surface

Top Wing mounting is chosen due to the requirement that the aircraft is intended for field landings. Higher wing means more clearance from the ground and therefore reducing the risk of collision with obstacles. High wing also means more stable aircraft and better characteristics during landing (ground effect is reduced and thus the stopping distance).

Tapered wing planform is preferable due to high aerodynamic efficiency without the need of complex manufacturing process [7]. Aerodynamic and geometrical twist will be present with the goal of increasing efficiency and controllability during stall. 3.2 Tail surfaces

3.2 Tail surfaces

T-tail is considered to be most suitable for the purposes of this project as this configuration provides high aerodynamic efficiency and better clearance of the ground.

3.3 Fuselage

The fuselage does not provide any significant amount of lifting force and its' main purpose is only to carry the crew and provide structural support for the lifting surfaces. This is why the main concern regarding the body of the aircraft is drag reduction.

(Fig. 1) shows the conceptual design on this stage of the design process.

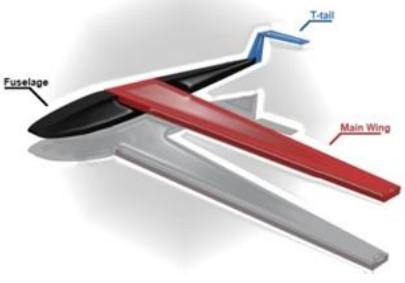


Fig. 1 *Preliminary design*

4. Main Lifting Surface

The actual design of the main lifting surface starts by calibrating the CFD software. For that purpose results are compared with experimental data of a wing tested in a wind tunnel until adequate match is obtained [8]. After evaluation the k-ω SST model is proven to be most accurate. A series of CFD analysis is run in order to find the best matching root and tip airfoil. Tested are combinations of airfoils; NACA43018, NACA43012, NACA633-618, NACA4412, Wort FX-61-163, Wor FX-61-126, GOE533 (at root) and GOE532 (at tip) of which the last two have proven to have greatest efficiency and stall characteristics. Angle of incidence and geometrical twist are also evaluated and corresponding incidence of $+2^o$ at the root and -1^o tip is found to be beneficial (Fig. 2).

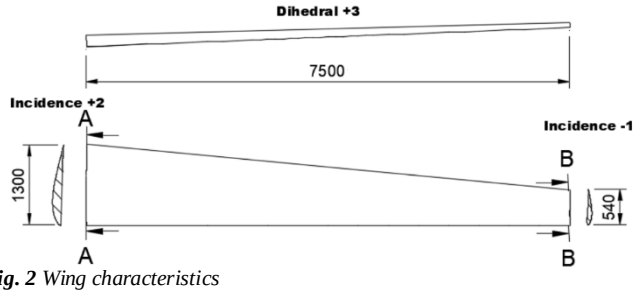


Fig. 2 *Wing characteristics*

5. Fuselage

When designing the fuselage of an aircraft of such type it is important to note the trajectory of the flight. For a sailplane it is specific that the air flow will be hitting the body at an angle coming from beneath the longitudinal axis of the machine. That said the design team has chosen to apply biomimicry and the shapes of several forms found in nature are evaluated in a CFD environment. After careful analysis of the obtained results the final shape of the fuselage is a complex morph between a drop and a whale's body. It is important to note that ergonomics was also taken into consideration as sailplanes are known for long duration missions and safety regarding ground strike (Fig. 3). [9].



Fig. 3 *Pilot ergonomics*

6. Tail surfaces

The main purpose of the tail surfaces of a fixed-wing aircraft is to balance the moments generated by the main wing and to provide aid with the dynamic and static stability of the aircraft in flight. First step is to analyze separate cases for horizontal and vertical surfaces and then combined model is tested to inspect the aerodynamic interferences (Fig. 4). After selecting the best shape and size for the tail surfaces the whole model of the aircraft is ran through CFD analysis for high angle of attack cases. This is done in order to evaluate deep stall characteristics of the aircraft. It is important to note that all the sizes derived from the CFD analysis up to this moment might be updated due to dependencies down the line of the design process.

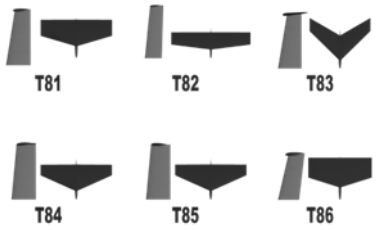


Fig. 4 *Tested Tail Planforms*

7. Static and Dynamic stability of the aircraft

Flight stability is easily considered one of the most important characteristics of an aircraft. Static stability dictates how the machine responds to disturbances and control deviations. The dynamic stability on the other hand is all about how the aircraft returns to its neutral attitude.

7.1 Requirements for evaluating aircraft stability

In order for the static and dynamic stability of the aircraft to be evaluated some additional information is required. Data from the precious CFD analysis is used to estimate all moments acting on the aircraft about its axis. The frame of reference of the aircraft along with the angular velocities and the acting moments is shown in (Fig. 5).

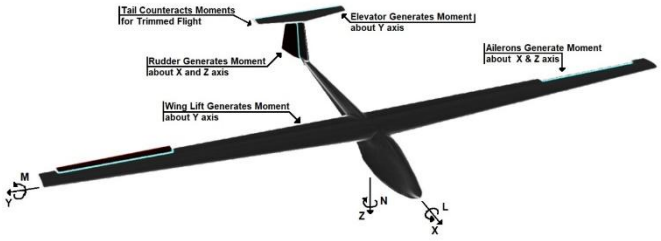


Fig. 5 *Moments acting on the aircraft*

Another very important characteristic of the aircraft is its moment of inertia along the three main axes. In order to obtain this data a full preliminary design of the structure of the aircraft is required (Fig. 6). After finishing this step, new more precise information about the aircraft weight can be obtained. This enables the design team to choose the type and the best location for the landing gear. A fixed monowheel landing gear is selected due to weight requirements.

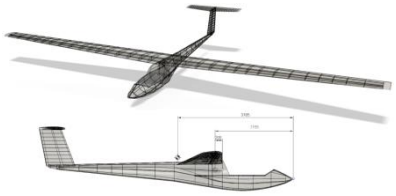


Fig. 6 Aircraft preliminary structure.

7.2 Static stability

Since and aircraft inflight has six degrees of freedom there are three stabilities that need to be established; Longitudinal, lateral and directional. It is important to note that lateral and directional stabilities are related to each other and thus one can be evaluated from the other. Estimation of the static stability is done by running a CFD analysis of the aircraft at various angles of attack and slip. Pitching, Yawing and Rolling moments for every case are studied (Fig. 7).

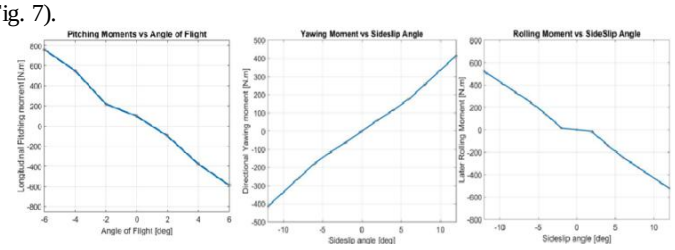


Fig. 7 *Pitching, Yawing and Rolling moment vs angle of deviation*

7.3 Dynamic stability

Evaluation of the dynamic stability of the aircraft is done by running transient simulations in CFD. A dynamic mesh method is used for setting angular velocities of 0.5; 1.0; 1.5; 2 [rad/sec]. After the required data is obtained the equations of motion are solved in Matlab Simulink [10]. Dutch roll and spiral mode cases are analyzed. All results from the study are compatible with the certification requirements (Fig. 8), [6].

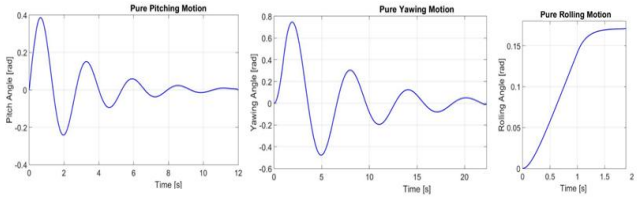


Fig. 8 *Pitching, Yawing and Rolling motion vs time elapsed*

Evaluation of the accuracy is done by comparison with similar existing aircraft such as B-4 [11], LET L-13 Blanik [12] and Schleicher K-8 [13]. (Fig. 10) shows the design of aircraft after the modifications done due to the requirements of static and dynamic stability.

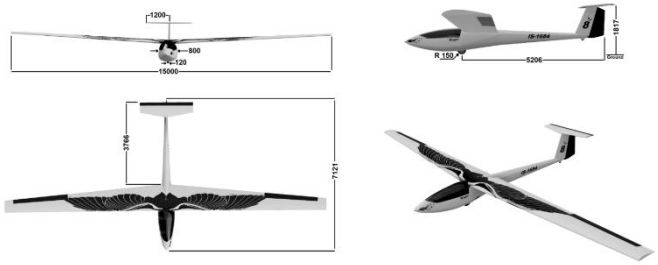


Fig. 10 *Aircraft dimensions after flight stability analysis*

8. Control surfaces sizing

Conventional aircrafts are controlled in the air by means of three moving surfaces; Ailerons (on both sides of the wing) are responsible for roll, Rudder (on the vertical tail) for directional control and Elevator (on the horizontal tail) for pitch motion control. The process of sizing the control surfaces is an iterative process and might lead to major changes to other parts of the aircraft.

8.1 Aileron sizing

It is important to note that a yawing moment is generated due to the drag induced by aileron deflection. In the same manner the rudder generates rolling motion due to its location. Control surfaces are designed by using the requirements for certification of the aircraft [6]. In the case of roll maneuverability it should be possible for the aircraft to achieve a change of direction of 45° for a time equal to the wing span divided by three at a speed equal to 1.3 stall speed. Other requirements include; required maximum force input and stall recovery characteristics. The best location for the ailerons is derived using data from the previous analysis for pressure distribution along the span. (Fig. 11) shows the pressure distribution over the aircraft, used for the sizing of the ailerons. This results are obtained by numerical simulations

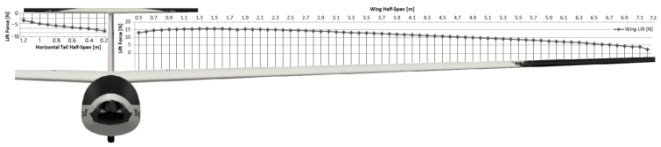


Fig. 11 *Pressure destitution along the wing and tail span*

After choosing the best location for the ailerons next step is to run numerous CFD analysis for different angle of deflection and aileron sized in order to evaluate the characteristics and pick the best configuration (Fig. 12). All results are put into plots for better analysis.

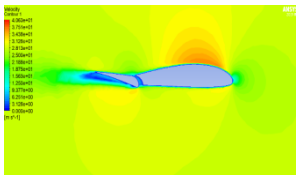


Fig. 12 *CFD of an Aileron*

8.2 Rudder sizing

The rudder of a sailplane is even more important compared to other types of aircraft due to the high aspect ratio of the wing and its use for flying with a sideslip. The rudder needs to be large enough to provide the required force to correct side gusts as well, shown in (Fig. 13).

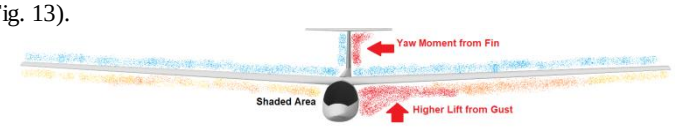


Fig. 13 *Cross wind effects*

The requirements for the rudder are as follows; Aircraft should be able to sustain straight flight during 12 [kn] cross winds coming at 30° to the side at speeds of 1.3 stall speed. Other requirements include that full rudder deflection should not stall the vertical tail and other [6]. After numerically evaluating the aerodynamic parameters of several rudder configurations the following design was chosen (Fig. 14).

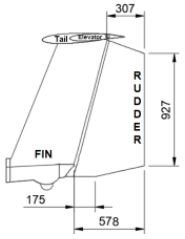


Fig. 14 *Tail Sizing*

8.3 Elevator sizing

The design process for the elevator is carried out the same was as it was for the other two types of control surfaces. The requirements for the elevator are written in the regulations as; For any speed below 1.3 stall speed there should be sufficient elevator input so that the aircraft is able to increase its speed back to 1.3 stall speed. For a tail-dragger configuration the pilot should be able to lift the tail with an angular acceleration of 8-10 [m/s^2] about the main landing gear at speed of 0.5 take off speed. This is required so that the pilot has control over when the aircraft lifts off the ground. Same stall requirements are required here as well. CFD simulations are ran to gather the required data for evaluating the characteristics of the elevator in all expected cases (Fig. 15).

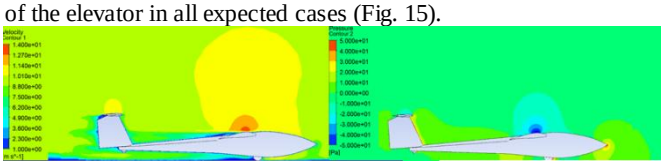


Fig. 15 *Velocity (left) and pressure (right) distribution at takeoff*

9. Cruise flight and trajectory analysis

By analyzing the actual flight characteristics of the aircraft the design team is able to get a better understanding of the quality of their work. The glide ratio is one of the most important factors describing the efficiency of an aircraft. It represents the horizontal distance the aircraft can travel for a unit of vertical distance lost. The differential equations describing the motion of a sailplane are as follows:

$$\begin{cases} m\ddot{x} = -\frac{1}{2}C_D\rho S\frac{\dot{x}}{\sqrt{\dot{x}^2+\dot{y}^2}} + \frac{1}{2}C_L\rho S\frac{\dot{y}}{\sqrt{\dot{x}^2+\dot{y}^2}} \\ m\ddot{y} = G - \frac{1}{2}C_D\rho S\frac{\dot{y}}{\sqrt{\dot{x}^2+\dot{y}^2}} - \frac{1}{2}C_D\rho S\frac{\dot{x}}{\sqrt{\dot{x}^2+\dot{y}^2}} \end{cases} \quad (1)$$

The derived equations are solved numerically in Matlab using ode45. As a starting point when solving the equations is taken initial speed of 40[m/s] as this is the speed at which the tug cable is released. All results are put in plots in (Fig. 16).

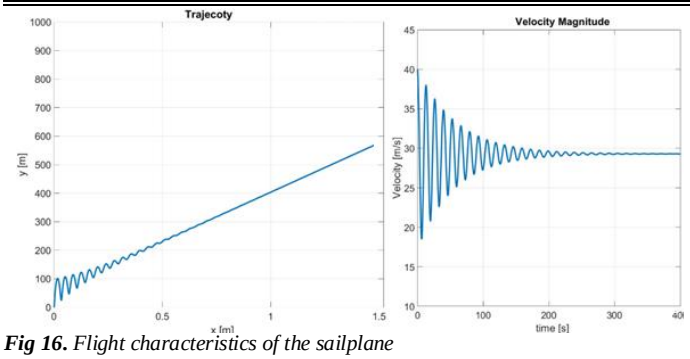


Fig 16. *Flight characteristics of the sailplane*

The calculated glide ratio is 25. The calculated cruise velocity is 29.3 m/s.

9. Conclusion

In the present work, an innovative method based on computational fluid dynamics for determining the aerodynamic characteristics of an aircraft and in particular a non-powered aircraft is proposed. The described method has been successfully applied in the design of a prototype sailplane Magpie (Magpie) IS-1684. The proposed method is proven accurate by means of comparison with other aircraft. Using CFD as a tool for designing aircraft has proven cost and time efficient compared to conventional methods. In the process of our work many 3d computer models have been developed instead of actual models. Based on simulations data from the 3d models is extracted and put in use for evaluation of aircraft characteristics. The steps performed for the overall modeling of the aircraft are described. Numerous numerical simulations have been performed in order to size the wing, tail surfaces, and control surfaces. The static and dynamic stability of the aircraft has been determined. A mathematical model for studying the cruise phase of flight has been developed and applied.

10. References

1. M. Mahdi, *„Prediction of wing downwash using CFD“*, 3rd International Workshop on Numerical Modelling in Aerospace Sciences, (2015)
2. J.Genov, I.Angelov,,,Numerical investigation on the effects of the aerodynamic shading between the tower and the blade of wind turbine generator with horizontal axis Numerical investigation on the effects of the aerodynamic shading between the tower and the blade of wind turbine generator with horizontal axis“, IOP Conference Series Materials Science and Engineering, (2020)
3. S. Frati, The Glider, (2007)
4. A.Ortiz, L. Quiroz, R.Köck, *„Aerodynamicperformance analysis of a low-speed acrobatic airplane by numerical simulation“*, Mechanica Computacional, Vol. XXI, p.378 – 391, (2002)
5. D.Coiro, F.Marulo, F.Nicolosi, F.Ricci, *„Numerical wind tunnel and flight tests for P92J and P96 light aircraft“*, 21st ICAS Congress, (1998)
6. European Union Aviation Safety Agency, *„Certification Specifications for Sailplanes and Powered Sailplanes CS-22*,“, (2008)
7. https://www.quora.com/What-is-the-advantage-of-elliptical-wings-over-trapezoidal-wings (04.2021)
8. Bak, C. Fuglsang, P. Johansen, J. Antoniou, I. *„Wind tunnel tests of the NACA 63-415 and a modified NACA 63-415 airfoil“* - Risø National Laboratory, Roskilde, Denmark, (2000)
9. Snorri Gudmundsson, *„General Aviation Aircraft Design Applied Methods and procedures“*, APPENDIX C4: Design of Sailplanes, Basic Mathematical Relations for Glide Performance
10. R. Herman, *„Solving differential equations using Simulink“*, p.20-23, (2017)
11. Pilatus Aircraft LTD. STANS (Switzerland), *„Approved Flight manual and operating manual for sailplane model: Pilatus B4-PC11“*, (1972)
12. Aero Letnany, *„Pilot's notes for the Blanik L-13 Saolplane, 2nd revised edition Czechoslavak Aeronautical Works“* , (1972)
13. Alexander Schleicher GmbH & Co. Ka8 and Ka8 B/C, "Rhonsegler" Operating Instructions. (2010)

Characteristics and state of road traffic safety in Montenegro

Marko Lučić[1,]
Faculty of Mechanical Engineering, University of Montenegro, Podgorica, Montenegro[1]
E-mail: markol@ucg.ac.me

Abstract: *The subject of research in this paper is the analysis of road traffic safety in Montenegro. Road traffic safety in Montenegro is not at an enviable level. The number of traffic accidents on the territory of Montenegro has been constantly increasing in the last few years. The state of traffic safety in Montenegro differs significantly from most EU countries. In the last few years, Montenegro has made great efforts to improve road safety. Infrastructure is being improved, technical inspections of road vehicles are being tightened, and a large number of campaigns have been done to improve road traffic safety.*
Keywords*: ROAD TRANSPORT, ROAD TRAFFIC, ROAD TRAFFIC SAFETY*

1. Introduction

Traffic is an independent human activity whose goal is to change the position of people, things or statements. It can be said about the traffic that the movement of traffic units on the traffic roads is organized. Traffic has made a great contribution to the development of civilization. Road traffic has its positive but negative effects. Road safety deals with the negative effects of road traffic. The most significant harmful consequences of traffic are:

- injured in traffic accidents
- pollution of the environment with noise, exhaust gases but also waste materials,
- depletion of natural resources,
- material damages of traffic accidents,
- losses and costs of traffic accidents

The safety of road traffic can be said to be a scientific discipline that deals with the study of harmful consequences of traffic and methods of reducing them.

Two aspects of traffic safety are active and passive traffic safety. Active traffic safety deals with the prevention of traffic accidents. This refers to reducing the likelihood that an accident will occur. Passive traffic safety refers to reducing the harmful consequences of traffic accidents that have occurred. [1]

2. Road traffic

In road traffic, there are higher frictional resistances in relation to water and rail traffic. Road traffic takes place on a very diverse network of roads. Various road vehicles travel on this network of roads. The car can be said to best meet the needs of individual transportation. One of the important positive effects is that road traffic is simply combined with other branches of traffic. This traffic has the simplest organization in relation to other branches of traffic. One of the most significant negative effects of road traffic is that it is the least safe. The negative effects of road traffic are: high dependence on the weather climate, the impact of the current configuration on costs, passability and safety. Road traffic is more expensive than rail and water. It also pollutes the environment more. [1]

3. The importance of road safety

Traffic safety belongs to traffic science. It does not represent an independent and isolated scientific discipline, but relies on social, technical and natural sciences. Duma traffic safety is of great importance globally. As is the road traffic, the traffic with the most participants has the largest number of potential victims. Enormous efforts are needed to improve traffic safety, especially road traffic as the most dominant.

4. Road traffic safety in Montenegro

Road traffic safety in Montenegro is not at an enviable level. Traffic safety statistics are conducted in accordance with Regulation (EC) No 93/704. These statistics are shown in Table 1.

Table 1: *Statistical overview of traffic accidents in Montenegro for the period from 2013 to 2019*

	2013	2014	2015	2016	2017	2018	2019
Number of traffic accidents	5264	5531	4944	5229	5678	5872	6210
Total number of casualties	1886	1900	2224	2423	2711	2611	2801
Number of injured persons	1812	1835	2173	2358	2648	2563	2754
Number of dead	74	65	51	65	63	48	47

4.1 Total number of traffic accidents in Montenegro

The total number of traffic accidents is the sum of all accidents that have occurred. The total number of traffic accidents consists of the sum of the number of total casualties (the number of injured and As for the total number of traffic accidents in Montenegro, it can be seen that from 2015 to 2019 is constantly increasing as shown in Table 1 but also in Figure 1.

4.2.1 Number of injured persons

An injured person is any person who is not killed but who has sustained injuries in a traffic accident with an injured person and who usually requires medical care. The number of injured persons in traffic accidents in Montenegro for the period from 2013 to 2019 is shown in Table 1 and Figure 3.

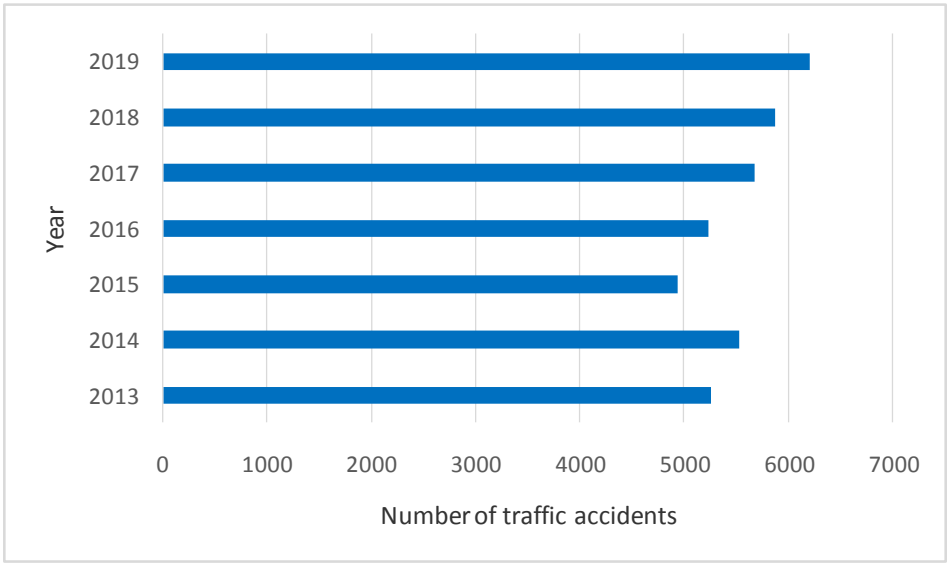


Fig. 1 *The total number of traffic accidents in Montenegro for the period from 2013 to 2019*

The total number of casualties is the sum of injured people and people killed in traffic accidents. The total number of casualties is shown in Table 1 but also in Figure 2.

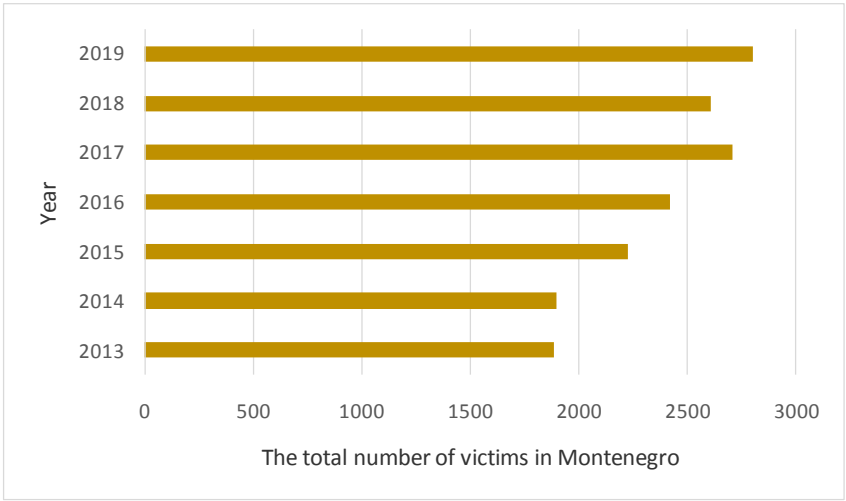


Fig. 2 *The total number of victims in Montenegro*

From Figure 2 and Table 1 it can be clearly seen that from 2013 to 2019 we have a constant increase in the number of casualties in traffic accidents except for 2018 when there was a decline compared to 2017.

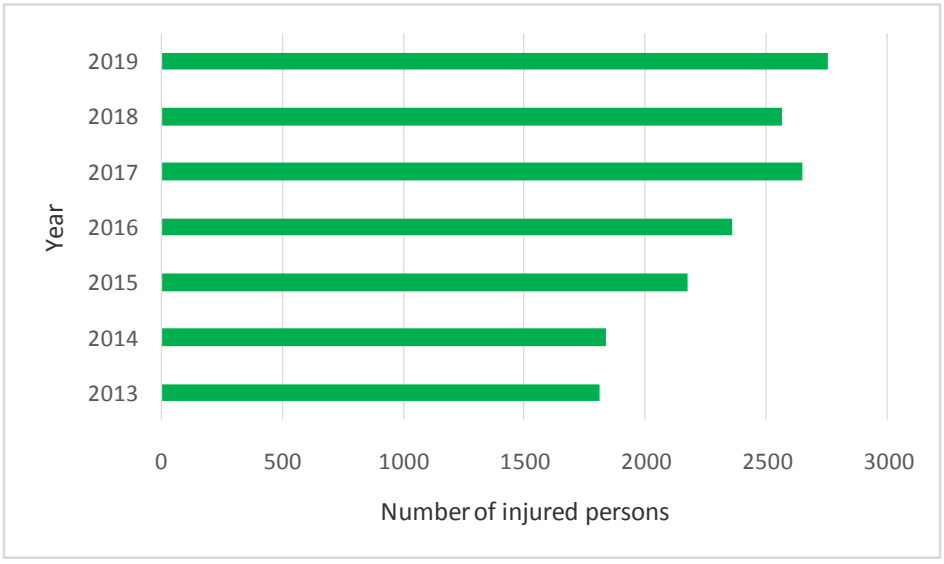


Fig. 3 *The total number of injured persons in traffic accidents in Montenegro for the period from 2013 to 2019*

From Figure 3 and Table 1 it can be seen that the number of injured persons in traffic accidents is constantly increasing from 2013 to 2017. In 2018, there was a decline in the number of injured persons in traffic accidents, but in 2019 the maximum number of injured persons for the period from 2013 to 2019 was reached.

4.2.2 Number of dead

A dead person is any person who lost his life immediately or within a period of 30 days from the consequences of a traffic accident with an injured person. The number of dead persons is shown in Table 1, but also in Figure 4.

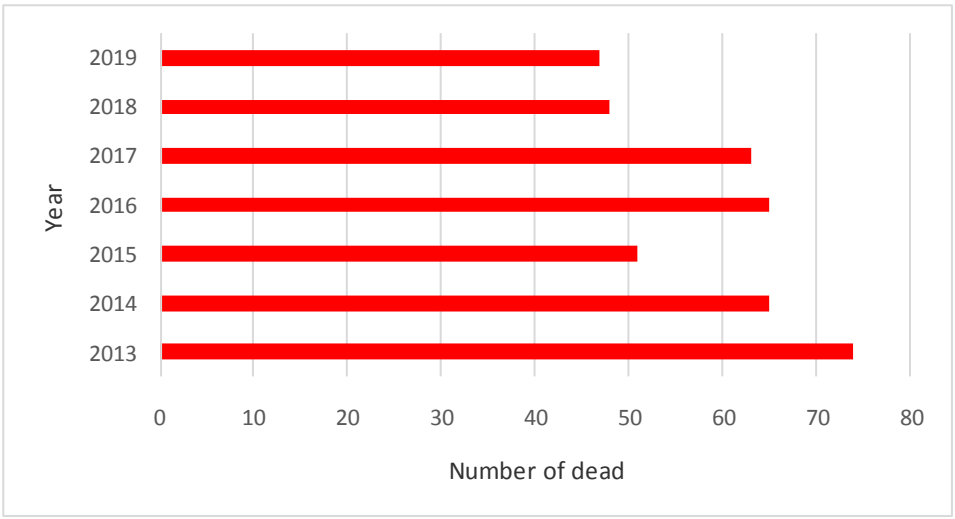


Fig. 4 *The total number of injured persons in traffic accidents in Montenegro for the period from 2013 to 2019*

In the observed period (2013 to 2019), the maximum number of fatalities was in 2013. Over the next two years, there was a constant decline in the number of people killed in traffic accidents. In 2016, we have an increase in the number of fatalities, and then a constant decline in the number of fatalities in traffic accidents.5. Conclusion

Traffic safety is a very important discipline. Road traffic safety in Montenegro is not at an enviable level. As the dominant mode of transport in Montenegro is road safety, it has additional significance. As there is a general increase in the number of traffic accidents from year to year, it is necessary to take a number of measures to improve road safety. Road traffic safety in Montenegro needs to be improved with the improvement and modernization of road infrastructure. It is also necessary to provide more rigorous technical inspections of vehicles. Great attention needs to be paid to education on road safety. Montenegro, as a candidate for EU membership, should opt for an effective strategy for reducing traffic accidents.

6. References

1. Krsto Lipovac, Traffic Safety, Beograd, 2008
2. MONSTAT, Annual statistics of traffic, storage and connections 2014, Podgorica, 2015
3. MONSTAT, Annual statistics of traffic, storage and connections 2015, Podgorica, 2016
4. MONSTAT, Annual statistics of traffic, storage and connections 2016, Podgorica, 2017
5. MONSTAT, Annual statistics of traffic, storage and connections 2017, Podgorica, 2018
6. MONSTAT, Annual statistics of traffic, storage and connections 2018, Podgorica, 2019
7. MONSTAT, Annual statistics of traffic, storage and connections 2019, Podgorica, 2020
8. MONTENEGRO STATISTICAL OFFICE, STATISTICAL YEARBOOK 2020, Podgorica 2020

Common dimensions of European transport policy and the "Belt-Road" initiative

Antoaneta Kirova, Dimitar Todorov
Transport University "Todor Kableshkov", Sofia, Bulgaria
akirova@vtu.bg, dimitar_todorov@mail.bg

Abstract: *China's stated objectives for the Belt and Road Initiative (BRI) refer to a broad intention to foster international collaboration with the countries involved, which focus on capacity building, liberalisation and facilitation of trade and investment, financial cooperation and people-to-people exchange. All of them are closely related to policies. According to our opinion, the most outstanding are the logistics objectives for the BRI, in order to support Chinese exports of products and equipment, as well as its engineering and construction capabilities and technologies and controlling logistics chains with Europe. Among the other not less important objectives is the necessity of balanced development across China.*
Keywords*: BRI, INTENATIONAL TRANSPORT AND LOGISTICS, EUROPEAN TRANSPORT POLICY*

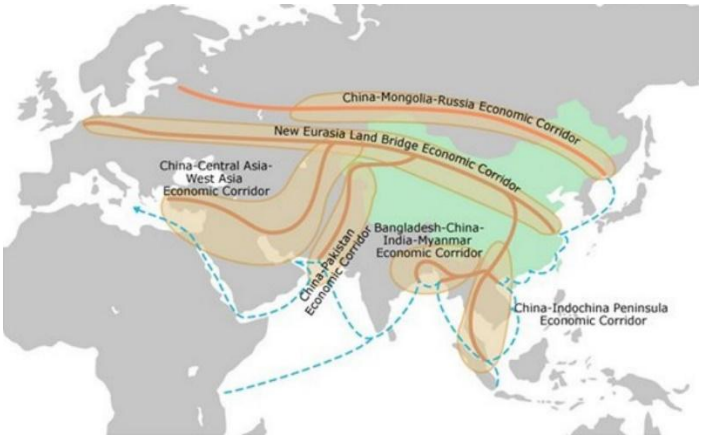
Introduction

China's engagement with the EU on the BRI is on individual basis. Since 2014, EU Member States and non-EU countries (mainly in Central and Eastern Europe), have signed Memoranda of Understanding (MoUs) with China within the framework of the BRI. In addition, a specific framework for cooperation between China and Central and Eastern European countries (the "16+1 Format[1]") has been implemented as a means to enhance the development of the BRI in these regions of Europe. The general impression is that there is a lack of coordinated and pan-European approach, still the key areas of EU-China cooperation in the field of logistics in order to secure liberalized market access and promote mutually acceptable international standards are concerning coordination of infrastructure investments and transport services.
The EU-China "Connectivity Platform" is intended to be a forum to coordinate the infrastructure policies of the EU and China.

1. *The mutual relation "European Transport Policy – Belt-Road Initiative"*

The EC's studies on the effect of BRI on traffic are hampered by the inability to determine the extent to which existing trade volumes will be affected by the initiative, given the levels of international trade between the Far East and Europe. In support of this, the volume of sea freight transport between the Far East and the EU in 2016 is just over 16 million TEU, with a tendency to increase more than twice, to about 40 million TEU by 2040. For the same period, in the air transport, the total two-way freight volume between Europe and the Far East was 3.3 million tons, with forecasts reaching 5 million tons by 2040 [1].
An interesting fact is the promotion of the movement of goods currently transported by sea and air between Europe and the Far East to rail, as a result of improved services, which is achieved through BRI. The results of the analysis show that around 2.5 million TEU can be transferred to rail by sea and 0.5 million by air by 2040. It is estimated that this equates to 50 to 60 additional trains per day or 2 up to 3 trains per day hour, in each direction. Rail services can be expected to be targeted at higher value goods and more time sensitive than current maritime transport. This comes as a further support to the efforts of European transport policy to revive and further develop railway freight transport.
Also, within the EU it is planned to make significant investments in the development of transport infrastructure, which will be made by infrastructure managers. The conclusion is that the One Belt One Road initiative for Eurasia partially overlaps the envisaged measures of the European transport policy with regard to logistics infrastructure.
Seven transport corridors are defined within BRI, among which the most important for the EU is the **New Eurasian Land Bridge Economic Corridor**: based on a railway line that connects Western China with Rotterdam (Netherlands) through Kazakhstan, Russia, Belarus and Poland. It is obvious, that the logistic land connection between China and European Union crossed intermediary countries.

Map of the Belt and Road Initiative's economic corridors



Source: Hong Kong Trade Development Council (HKTDC) Research

The goals focus on improving transport connectivity through investment in infrastructure, but also include measures to streamline processes to further improve connectivity, such as customs clearance procedures. They cover all modes of transport across the geographical scope of BRI.

Table 1

Transport related goals in BRI[2]

Area	Goal
Transport infrastructure construction	Focus on key passageways, junctions and linking up unconnected road sections, removing bottlenecks; road safety and traffic management facilities and equipment
Coordination and custom clearance	Building a unified coordination mechanism for whole-course transportation, increase connectivity of customs clearance, multimodal transport between countries, application of compatible and standard transport rules. Support for inland cities in building airports and international land ports, strengthen customs clearance cooperation between inland ports and ports in the coastal and border regions

[1] "16+1 Format" includes China, 11 EU Member States (Bulgaria, Croatia, the Czech Republic, Estonia, Hungary, Latvia, Lithuania, Poland, Romania, Slovakia, Slovenia) and five Balkan countries (Albania, Bosnia and Herzegovina, Macedonia, Montenegro, Serbia).

[2] **Source:** National Development and Reform Commission of Republic of China (2015), https://en.ndrc.gov.cn/ , cited in [1]

1

Land transport	Focus on jointly building a new Eurasian Land Bridge and developing the corridors along international transport routes, relying on core cities along the Belt and Road; using key economic industrial parks as cooperation platforms. Setting up coordination mechanisms for railway transport and port customs clearance for the China-Europe corridor, cultivate the brand of "China-Europe freight trains", and construct a cross border transport corridor connecting the eastern, central and western regions."
Maritime transport	Focus on jointly building smooth, secure and efficient transport routes connecting major sea ports. Focus on port infrastructure construction, smooth land-water transportation channels, port cooperation; increase sea routes and the number of voyages, and enhance information technology cooperation in maritime logistics.
Air transport	Expand platforms for civil aviation cooperation; improving aviation infrastructure

Further analysis of the transport related goals in BRI and European transport policy indicates, that infrastructure problems, digitalization and ITS are considered in both cases.

2. Degree of compliance between EU transport system and the requirements of BRI

Increasing the opportunities for improvement of transport and logistics connections between EU and China requires synergies to be achieved in the process of mutual efforts in this field. The European Commission (DG MOVE) and the National Development and Reform Commission of China (NDRC) established a Connectivity Platform in 2015[3], accepting a common approach to connectivity, including the Trans-European Transport Network (TEN-T), and BRI. The cooperation includes information sharing to promote seamless traffic flows and transport facilitation, and between their relevant initiatives and projects; seeking co-operation opportunities between TEN-T and BRI, including establishment of a favourable environment for sustainable and inter-operable cross-border infrastructure networks in countries and regions between the EU and China; promotion of business and investment opportunities open to both China and the European side. Still, responsibilities between China and EU are not clearly distributed and future work is needed in order to co-ordinate TEN-T and BRT development.

7 of the 9 TEN-T corridors have a real east-west dimension: the Baltic-Adriatic, the North Sea - the Baltic Sea, the Mediterranean, the East /Eastern Mediterranean, the Atlantic, the North Sea - the Mediterranean and the Rhine-Danube. In practice, in the future, corridors with multimodal connections will extend from east to west and from peripheral geographical areas to the center of the EU.

The review of the European Commission's North Sea – Baltic Core Network Corridor Study [4] found that that rail infrastructure capacity in 2030 should be capable of meeting the current and forecast demand to that date. While bottlenecks may still emerge in the EU's transport network, specific changes to the TEN-T programme are not justified at the moment and are classified as premature and inadequate, depending on the future evolution of the BRI. One of the issues for TEN-T is whether there is a necessity for project modification in response to the effects expected from BRI, in order to avoid duplication or to be expanded according to the requirements of BRI-related traffic.

[3] Source: https://ec.europa.eu/transport/themes/international/eu-china-connectivity-platform_en

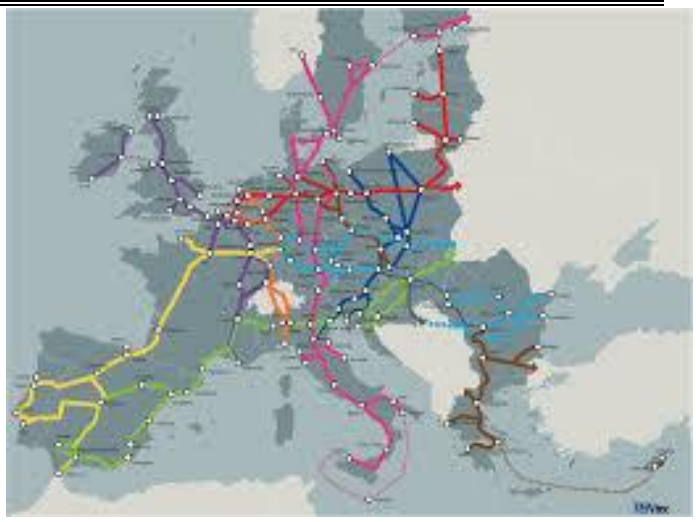


Fig. 1. ***Map of TEN-T in Europe affected by BRI*** [2].

The new European mobility strategy [3], together with an Action Plan of 82 initiatives[4] will guide the directions EC has to implement for a reduction of 90% in emissions by 2050, delivered by a smart, competitive, safe, accessible and affordable transport system. It will shift the way people and goods move across Europe and make it easy to combine different modes of transport in a single journey. All the transport modes need to become more sustainable, with green alternatives widely available and the right incentives will lead to zero-emission mobility while making the European transport system efficient and resilient.

On **sustainable** area, the strategy highlights five main actions involving the introduction of zero-emission vehicles, vessels and aeroplanes, renewable and low-carbon fuels by 2030; creating zero-emission airports and ports; making interurban and urban mobility healthy and sustainable; greening freight transport; and pricing carbon and providing better incentives for users. The European Commission initiative highlights the benefits of rail as a sustainable, smart and safe means of transport and placing rail in the spotlight throughout 2021 across the continent means to further encourage the use of rail in order to contribute to the EU Green Deal goal of becoming climate-neutral by 2050.

On **smart** area, which includes the innovation and digitalisation of the transport sector, the actions must lead to a more connected and automated multimodal mobility system and the innovation is encouraged through the use of data and artificial intelligence.

To become a **resilient** transport, the European Commission is committed to reinforce the single market, to make mobility fair and just for all and to step up transport safety and security across all modes.

3. Conclusions

The investigation shows continuous mutual influence between European transport policy and BRI. There are also suggestions of the routes most likely to be used in the future for the shift of container traffic to rail, i. e. the route north of the Alps, towards EU Member States bordering the North Sea and the Baltic Sea[5]..

Due to the Covid-19 crisis, the completion of the EU-China Comprehensive Agreement on Investment (CAI) has been postponed until the end of 2020. It is an extremely ambitious

[4] The action plan boosting long-distance and cross-border rail passenger transport will be proposed in 2021, involving all interested stakeholders are expected to test different models for new connections and services by 2030

[5] The containers carried by rail would primarily be those previously shipped to North Sea ports, and would mainly travel along the route from Moscow (Russia) through Brest (Belarus) and Warsaw (Poland) to Berlin (Germany), including part of the TEN-T North Sea – Baltic Core Network Corridor [4]

agreement on which China and the European Union have been negotiating since 2013. When it is signed, the agreement will foster trade between Europe and China and will facilitate investment in the two regions. This agreement has the potential to make the Sino-European relationship one of the main cornerstones of world trade [5].

This CAI will replace the various existing bilateral investment treaties between China and most of the EU members. With this new agreement, European companies will have wider access to the Chinese market, and will no longer be required to create joint ventures with local Chinese partners. Despite the current health crisis, several BRI projects in Europe are still making progress; in particular the Budapest-Belgrade rail line.

3. References

[1] Research for TRAN Committee: the new Silk Route – opportunities and challenges for EU Transport, Study, 2018, https://www.europarl.europa.eu/thinktank/en/document.html?reference=IPOL_STU(2018)585907

[2] Dick Dunmore, D., Al. Preti, C. Routaboul, The "Belt and Road Initiative": impacts on TEN-T and on the European transport system, p. 6, https://jshippingandtrade.springeropen.com/track/pdf/10.1186/s41072-019-0048-3.pdf

[3] Sustainable and Smart Mobility Strategy – European transport on track for the future, Source: https://egvi.eu/mediaroom/sustainable-and-smart-mobility-strategy-european-transport-on-track-for-the-future/

[4] North Sea – Baltic Core Network Corridor Study, Final Report December 2014, p. 19, https://ec.europa.eu/transport/sites/transport/files/north_sea-baltic_study_0.pdf

[5] Dr. Goulard, Sebastien, BRI in Europe during the Covid-19 crisis, OBOREurope, https://www.oboreurope.com/en/bri-europe-covid/

Modeling travel behavior onboard of privately autonomous vehicle and shared autonomous vehicle

Jamil Hamadneh and Domokos Esztergár-Kiss
Department of Transport Technology and Economics
Budapest University of Technology and Economics
Budapest, Hungary
jamil.hamadneh@kjk.bme.hu

***Abstract**: The impact of travel time, travel cost, and multitasking availability on the selection of privately use AV (PAV) and shared AV (SAV) are examined. The main daily trip is only studied, where all trips are within urban areas. A stated preference (SP) survey which includes a discrete choice experiment, was designed and distributed in Budapest, Hungary to collect the preferences of people towards PAV and SAV. As a result, a sample size of 2056 observations was obtained from the survey. A discrete choice modeling approach was applied to the data using a conditional logit (CL) model, where the characteristics of the alternatives are considered. The analysis results show that the value of travel time (VOT) of SAV is lower than AV, and the probability of choosing a transport mode is increased when multitasking is available in a transport mode. Moreover, the impact of travel cost on transport mode choice is higher than the impact of travel time. In conclusion, people are more likely to select SAV over PAV when the multitasking availability is considered as one criterion in the transport mode selection.*

***Keywords:** MULTITASKING, SHARED AUTONOMOUS VEHICLE, TRAVEL BEHAVIOR, VALUE OF TRAVEL TIME*

1. Introduction

The continuous advancement in the technology of vehicle manufacturing will lead to having fully automated vehicles in the market in the coming few years [1]. A fully automated vehicle is characterized as no intervention by humans is needed to control the driving, where the machine can drive a car instead of a human driver as in conventional cars. The impacts of Autonomous Vehicles (AVs) on the mobility of people need further studies. Travelers generally assign an indirect money for travel time based on the importance of travel time, for example, traveling for work is more important than traveling for leisure activity [2]. The value of travel time (VOT) is a measure that describes the amount of money a traveler pays in traveling [3]. Some factors that impact VOT negatively are waiting time and crowding, or in other words, those factors increase the VOT [4]. The travelers' willingness to pay money to overcome the unwanted factors is high because they want to maximize their utility; they can choose better transport modes or shorter routes to minimize the travel time [4]. The VOT is affected by the experience of a traveler onboard of a transport mode, for instance, finding a good environment to multitask during travel decreases the VOT. Moreover, the carried tools onboard also determine the multitasking onboard, such carried tools are internet bundle, and such multitasking is using social media [5-7]. In the conventional transport modes, the travel is divided into three parts, walking time, in-vehicle time, and waiting time [8]. In the AV era, the walking time is minimized and the waiting time is done in the closest street of passenger location where a passenger can track the vehicle and minimize the waiting time. In this study, the in-vehicle time is studied, where AV is used as a transport mode. It is found that the AV will have different characteristics than a conventional car, for example, no human driver, no driving license, higher safety, and door-to-door service [9, 10]. Berliner et al. [11] define travel-based multitasking as people select a transport mode based on the potential of conducting onboard activities. The attribute multitasking availability is well defined in this paper. Several scholars study the impact of multitasking on travel behavior, such as Varghese and Jana [5] and Ettema and Verschuren [12] who study the impact of onboard activities in conventional transport modes on the VOT. Keseru et al. [13] show that information and communication technology (ICT) are associated with the trip purpose. While Malokin et al. [14] show a change in the mode share based on multitasking and the availability of ICT. Litman [15] shows that travelers are willing to switch to different transport modes in order to find a better environment to multitask (e.g. studying, working, and relaxing) to have a productive travel time. Banerjee and Kanafani [16] find that ICT motivates people to multitask onboard during their travel, which consequently decreases the VOT (i.e. positive impact). Singleton [17] says that transport mode characteristics impact the type of onboard activity.

The focus of this study is two models of AV, the privately-used autonomous vehicle (PAV), and the shared autonomous vehicle (SAV). The in-vehicle time is studied when travelers travel to their main destinations in urban areas. A stated choice experiment considering multitasking availability is scarce in literature, especially, about PAV and SAV, as pointed by [10]. The travelers are asked to choose PAV or SAV based on travel time, travel cost, and multitasking availability. This study adds a new contribution to the literature, where multitasking onboard of autonomous vehicle is modeled using a discrete choice modeling approach. It is obvious from the literature that previous studies focus on the CTMs, while this research studies the PAV, SAV. The contributions of this research are (1) developing a transport choice model for PAV and SAV, and (2) finding the impacts of changes on travel time, travel cost, and multitasking availability on the selection of transport choice.

2. Literature Review

The rapid advancement of the vehicle manufacturing industry due to the advanced technology will emerge fully autonomous vehicles (AVs) [18]. The people's acceptability to AV which a machine takes the role of driving instead of a human driver is a challenge that will change the travel behavior of people [17, 18]. Travelers are willing to change a transport mode based on the importance of in-vehicle time for them, for example, traveling of high value includes onboard activities, minimum travel time, and minimum travel cost [19]. Travelers pay money to remove the unwanted travel time by changing a transport mode, route, time of conducting activities [2]. The saved time from using faster transport mode or using shorter route is considered an opportunity for other activities (positive utility) [20, 21].

The qualitative improvements on the transportation system (e.g., safety, service, comfort, and conveniences) is more attractive than infrastructure actions (i.e., less costly with varied positive impacts), as stated by Litman [15]. He demonstrates that VOT is improved when qualitative measures are enhanced and not only when travel time is reduced. The advancement of technology that enables people to carry and use ICT and the changes in the design of new vehicles as well as the future promising technology AV, all participate in enhancing the qualitative measures of transportation system. The utilization of the travel time by involving travelers in onboard activities makes the perceived travel time smaller than actual, as stated by Belenky [4]. Cirillo and Axhausen [22] find that having a pleasant journey affect the preferences of people, such as the authors find that people do not mind choosing longer travel

distance if they experience pleasant journey. It is found that travelers try to enhance their perceived travel time by conducting onboard activities during their travel [23]. Xumei et al. [24] finds that the VOT of work trips is larger than the VOT of leisure trips, while the waiting time has the largest VOT. Based on the characteristics of AV and SAV, travelers will have less stress than conventional cars because the task of driving is removed, and the provided service is door to door [21, 25, 26].

The VOT is estimated based on the random utility theory, where a discrete choice modeling approach is applied [27]. Several studies are conducted on conventional transport modes using a discrete choice modeling approach where VOT is estimated and the travel behavior is assessed, while studies on the AV are limited. The study of Simoni et al. [28] shows AV will have lower VOT than conventional cars. Others show the factors that impact using AVs, such as Gurumurthy and Kockelman [29] say the long travel commuters are more willing to use AVs, Lavieri and Bhat [30] show that using SAV is influenced by companion's type and the number of picked up passenger along the travel (i.e., additional time), and the group of people impacts using AV. The high-income group has smaller VOT when they use AVs, as stated by Bozorg and Ali [31], Steck et al. [6] show that the commuters can reduce their VOT when AV and SAV are used. Steck et al. [6] show that AV is more attractive than SAV. Kolarova et al. [32] find that the VOT of AV is less than conventional cars, and the VOT of SAV is higher than conventional cars. Studies such as [17, 33] show that multitasking can reduce the VOT and when drivers get rid of their tedious driving task. The reduction in VOT is high when travelers involve in multitasking in long distances as stated by Singleton [17]. The VOT is affected by trip purpose as also multitasking is influenced by the trip purpose [33].

The acceptability of people to ridesharing determines the use of SAV. Bansal et al. [34] find that the acceptability of people to the SAV depends on the level of fear regarding the system failure which is considered the strongest reason to not use SAV. Burghout et al. [35] show that people can use SAVs if the average waiting time in ridesharing is acceptable to them. Krueger et al. [36] show that waiting time determines the use of SAVs, in addition to the cost and travel time factors. Stoiber et al. [37] use choice experiments that SAVs are more likely to be used in pooled mode where multiple riders can join through a trip and the travel time can be used more efficiently through SAVs compared to regular cars. Lavieri and Bhat [30] finds that people are likely to use SAVs with strangers on commute trips, and the waiting time is a negative impact on the use of SAVs during picking up and dropping passengers off.

In this research, the travelers' behavior onboard of PAV and SAV is discussed using discrete choice modeling. A new definition for multitasking is proposed where a traveler chooses a transport mode based on multitasking availability, travel time, and travel cost.

3. Methodology

The section presents the methodological approach of this study. Travelers choose a transport mode based on their preferences, where each traveler seeks to maximize his/her utility. The travel time is considered unproductive time (i.e., negative utility) based on the random utility theory while conducting activities is considered productive (i.e., positive utility) [38]. The reduction in the travel negative utility is obtained when travelers experience pleasant journeys or conduct onboard activities during their travel. The possibility to conduct onboard activities is influenced by several factors, such as transport mode. Moreover, the perceived travel time is affected by the environment onboard of transport mode, where the perceived travel time is improved when travelers experience pleasant journey. This section will present the methods that are used in analyzing the impacts of conducting onboard activities in PAV and SAV, where the changes in the travel time and travel cost are also examined. A stated choice experiment survey is conducted where other factors are collected, such as sociodemographic, economic, and trip variables. The stated choice experiment includes two alternatives (AV and SAV), travel time, travel cost, and multitasking availability. The power of the stated choice experiment method is its efficiency to obtain responses from respondents based on their preferences, associated with characteristics of transport modes [27]. The aim of the analysis is to develop mode choice models for AV, and SAV.

Fig. 1 shows the structure of the survey and the used methods. The discrete choice experiment includes travel time, travel cost, and multitasking availability. Multitasking availability means that a traveler has the possibility to conduct one or more of the following activities: reading, writing, talking, listening, using social media, eating-drinking, while multitasking unavailability means doing other activities such as thinking, window gazing, and sleeping that do not need contact with ICT and passengers (e.g., talking). Three levels of each travel time and travel costs are used, and two levels for multitasking are used. The alternatives are PAV and SAV. Some descriptive statistics are presented to characterize the sample. Moreover, other variables are used and examined to see their impacts on the transport mode choice, such as gender, income, age, education, job, car ownership, trip purpose, and transport mode, Finally, the VOT is calculated which describes the importance of traveling using monetary values per hour.

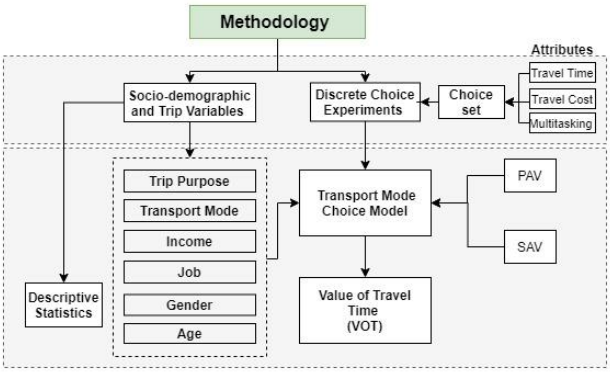


Fig. 1 *The methodological approach*

A stated preference (SP) survey is distributed in Budapest, Hungary, during the period from March to April 2020. The respondents are asked to report their existing conditions and their preferences towards PAV and SAV considering normal conditions away from the impact of COVID-19.

In the random utility theory, every person is a rational decision-maker, where each individual seeks a decision to maximize his/her utility [38]. The probability of a traveler to select one alternative out of certain outcomes is given in Equation 1:

$$P(s_j/S) = \Pr(U_{s_j} > U_k)\ \forall\, k \neq s, K \in S \qquad 1$$

where P (sj/S) is the probability of a person to choose outcome (si) from a choice set (S), Usj is the utility of choosing the outcome (sj) from the choice set S, where the earned utility is larger than the utility of all other outcomes (K) in the choice set S [38]. The utility that a person has when he conducts daily activities contains a deterministic and a stochastic part, as shown in Equation 2:

$$U_j = D_j + \varepsilon_j \qquad 2$$

where D is the deterministic part while the ε stands for the stochastic part. The deterministic part is defined as the average perceived utility of individuals when they choose an outcome [38]. The random part is defined as the unknown deviation of a person's utility from the mean value. The random part is used to capture the uncertainty in the choice modeling [38]. The conditional logit (CL) model which is one of the random utility models is selected.

In CL, all persons are given different situations before they choose an outcome Moreover, the same persons are used in choosing an outcome per situation is taken into account by CL.

Moreover, the characteristics of outcomes are taken into account rather than the characteristics of individuals [39]. Let Z ij is the characteristics of outcome (j), and α is the vector parameter of choosing the outcome (j), the probability that a person (i) will choose outcome j is given in Equation 3.

$$P_{ij} = \exp(Z_{ij}\alpha) / \sum_{k=1}^{J} \exp(Z_{ik}) \quad 3$$

From Equation (3), the likelihood function is calculated.

4. Results and discussion

The results of the survey include 2056 observation, where each observation represent an outcome with its characteristics. For example, each person is subjected to two observations to choose one of them (i.e., 2056/2=1028 answers). The characteristics of the collected sample are presented in Table 1 and Грешка! **Невалидна препратка на показалец към себе си.** presents some trip characteristics of the respondents, where the main trip and the frequent transport mode are recorded in the urban areas.

Table 2.

Table 1 presents descriptive statistics of the sample, such as age, job, income, and gender groups.

Table 1. *Sociodemographic variables, age, job, and income*

Age	%	Job	%	Income	%	Gender	%
15-24	18.44%	Workers	50.00%	High	34.43%	Male	64.75%
25-54	75.41%	Student	40.16%	Middle	26.64%	Female	35.25%
55-65	4.51%	Unemployed	6.15%	Low	38.93%		
>65	1.64%	Retired	3.69%				

Грешка! Невалидна препратка на показалец към себе си. presents some trip characteristics of the respondents, where the main trip and the frequent transport mode are recorded in the urban areas.

Table 2. *Trip Characteristics variables, transport mode, and trip purpose*

Transport mode	%	Trip purpose	%
Bike	5.74%	Education	41.39%
Car as driver	21.31%	Work	43.85%
Cas as passenger	5.74%	Leisure and others	6.56%
Public transport	53.69%	Shopping	4.10%
Taxi	3.69%	Home	4.10%
Walking	9.84%		

Table 3 presents the estimates of the model, where CL is applied. The results show the marginal utilities of travel time and travel cost are negative (-0.0161, and -0.0027, respectively), which means traveling is disutility (i.e., negative utility) where travelers pay money instead of gaining money from travel. Multitasking availability increases the probability of choosing a transport mode by 0.25 points more than the probability of choosing a transport mode without multitasking availability. All variables are significant at confidence interval 95% except travel time which is significant at confidence level 90%. The result of the model shows that the model without considering the variables; travelers are more likely to choose SAV over PAV, as shown in the PAV-β0. Moreover, the VOT is 358 Ft/hr.

Table 3. *Conditional logit-model estimates*

Alt.	Estimates	Value	Std.	z	P>|z| a
	Time	-0.0161	0.011	-1.31	0.095*
	Cost	-0.0027	0.001	-4.98	0.000***
	ML=1	0.25	0.09	2.78	0.005***
	ML=0	base	-	-	-
PAV	β0	-0.212	0.064	-3.31	0.001***
SAV	base	-	-	-	-
Number of observations=2056					
Chi2(2) = 34.73					
Log simulated-likelihood = -688.381					
Prob > chi2 =0.000					
AIC= 1384.764					
BIC= 1404.505					

*** p<0.01, ** p<0.05, * p<0.1

Table 4 present the predictive margins across multitasking options. The model demonstrates that the predictive probability (i.e., margin) of using SAV when multitasking is available is 58.1% while it is 52.13% when multitasking is unavailable. Similarly, the predictive margin of using PAV when multitasking is available onboard is 47.84%, while it is 41.85% when multitasking is unavailable. Thus, having multitasking onboard of PAV and SAV impacts the choice of travelers.

Table 4. *Predictive margins across multitasking*

Delta method					
Alt.	Attribute	Margin	Std.	z	P>|z|
SAV	Multitasking availability = no	0.5213	0.0189	27.47	0.0***
	Multitasking availability = yes	0.581	0.0186	31.18	0.0***
PAV	Multitasking availability = no	0.4185	0.0187	22.32	0.0***
	Multitasking availability = yes	0.4784	0.0189	25.22	0.0***

*** p<0.01, ** p<0.05, * p<0.1

Table 5 present the predictive margins across travel time. In this table, three values are used to estimate the margins, bottom value, middle value, and upper value. In the case of SAV, the probability of choosing SAV is decreased when travel time is increased. For example, at the travel time of 20 minutes; the margin of SAV is 56.9%. While at the travel time of 25 minutes; the margin of SAV is 55.2%. Moreover, the margin of SAV is examined, when a change in the travel time of PAV is occurred rather than SAV. It is found that the margin of SAV is increased when the travel time in PAV (i.e., the opponent alternative) is increased. For example, the margin of SAV is 53.5% when the travel time in PAV is 20 minutes, and the margin of SAV is 55.3% when the travel time in PAV is 25 minutes. In the case of PAV, the probability of choosing PAV is decreased when travel time is increased. For example, at the travel time of 20 minutes; the margin of PAV is 46.5%. While at the travel time of 25 minutes; the margin of PAV is 44.7%. Moreover, the margin of PAV is examined when in the travel time of SAV a change is occurred rather than PAV. It is found that the margin of PAV is increased when the travel time in SAV (i.e., the opponent alternative) is increased. For example, the margin of PAV is 43.1% when the travel time in SAV is 20 minutes, and the margin of PAV is 44.7% when the travel time in SAV is 25 minutes. It is found that the change on the margins in the case of PAV is higher than SAV, for example, changing the travel time from 20 minutes to 25 minutes the margin is decreased by 1.9% in the case of PAV, while it is 1.7% in cased of SAV, for the same travel time interval. Fig. 2 illustrates the probability of choosing PAV and SAV when travel time is varied. It is shown that travelers are more willing to use SAV over PAV.

Table 5. *Predictive margins across travel time*

Delta method					
Alt. (x)	At alt. (x) at travel time (i)	Margin	Std. Error	z	P>|z|
SAV	SAV @ 20min	0.569	0.019	29.6	0.0***
	SAV @ 25min	0.552	0.015	35.76	0.0***
	SAV @ 30min	0.534	0.022	24.41	0.0***
	PAV @ 20min	0.535	0.021	25.23	0.0***
	PAV @ 25min	0.553	0.015	36.03	0.0***
	PAV @ 30min	0.571	0.02	28.81	0.0***
PAV	SAV @ 20min	0.431	0.019	22.38	0.0***

	SAV @ 25min	0.448	0.015	29.06	0.0***
	SAV @ 30min	0.466	0.022	21.33	0.0***
	PAV @ 20min	0.465	0.021	21.94	0.0***
	PAV @ 25min	0.447	0.015	29.15	0.0***
	PAV @ 30min	0.429	0.02	21.68	0.0***

*** p<0.01, ** p<0.05, * p<0.1

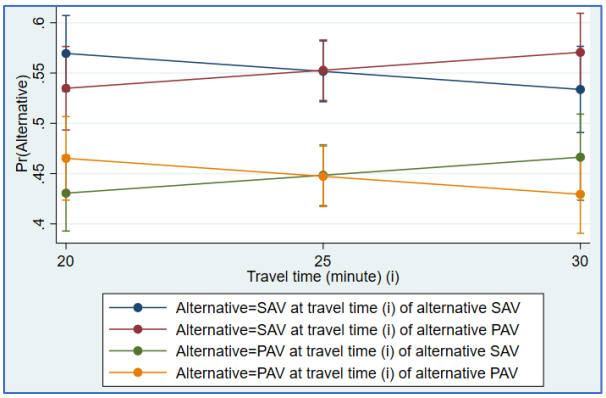


Fig. 2 *Prediction margin based on the changes in travel time*

Table 6 present the predictive margins across travel costs. Three values are used to estimate the margins, bottom value, middle value, and upper value. In the case of SAV, the probability of choosing SAV is decreased when travel cost is increased. For example, at the travel cost of 175 Ft; the margin of SAV is 61.9%. While at travel cost 250 Ft; the margin of SAV is 55.3%. Moreover, the margin of SAV is examined when a change in the travel cost of PAV is occurred rather than SAV. It is found that the margin of SAV is increased when the travel cost of AV (i.e., the opponent alternative) is increased. For example, the margin of SAV is 44.8% when the travel cost of PAV is 175 Ft, and the margin of SAV is 55.5% when the travel cost of PAV is 250 Ft In the case of PAV, the probability of choosing PAV is decreased when travel cost is increased. For example, at the travel cost of 175 Ft; the margin of PAV is 51.2%. While at travel cost 175 Ft; the margin of PAV is 44.5%. Moreover, the margin of PAV is examined when a change in the travel cost of SAV is occurred rather than PAV. It is found that the margin of PAV is increased when the travel cost of SAV (i.e., the opponent alternative) is increased. For example, the margin of PAV is 38.1% when the travel cost of SAV is 175 Ft, and the margin of PAV is 44.7% when the travel cost of SAV is 250 Ft

Table 6. Predictive margins across travel cost

Delta method					
Alt. (x)	At alt. (x) at travel time (i)	Margin	Std. Error	z	P>|z|
SAV	SAV @ 175 Ft	0.619	0.019	32.11	0.0***
	SAV @ 250 Ft	0.553	0.016	35.62	0.0***
	SAV @ 300 Ft	0.485	0.021	23.54	0.0***
	PAV @ 175 Ft	0.488	0.02	24.02	0.0***
	PAV @ 250 Ft	0.555	0.015	35.85	0.0***
	PAV @ 300 Ft	0.621	0.019	31.91	0.0***
PAV	SAV @ 175 Ft	0.381	0.019	19.75	0.0***
	SAV @ 250 Ft	0.447	0.016	28.78	0.0***
	SAV @ 300 Ft	0.515	0.021	24.98	0.0***
	PAV @ 175 Ft	0.512	0.02	25.25	0.0***
	PAV @ 250 Ft	0.445	0.015	28.7	0.0***
	PAV @ 300 Ft	0.379	0.019	19.45	0.0***

*** p<0.01, ** p<0.05, * p<0.1

Fig. 3 illustrates the probability of choosing PAV and SAV when travel cost is varied.

As a result, it is found that the change in the travel cost impacts the margins more than the changes in the travel time, and multitasking availability increases the probability of choosing a transport mode. However, in almost all situations, travelers demonstrate choosing SAV over PV based on the three attributes: time, cost, and multitasking.

It is worth mentioning that the sociodemographic, economic and trip characteristics show insignificant results at a confidence level of 95%. Therefore, they are removed from the model.

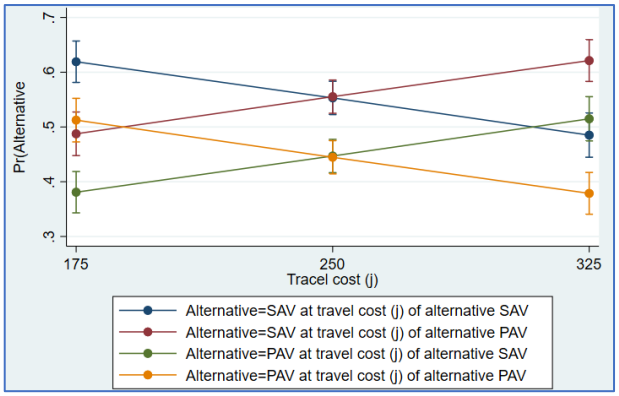


Fig. 3 *Prediction margin based on the changes in travel cost*

5. Conclusion

The travel behavior of people towards two types of automated vehicles is discussed through a discrete choice modeling approach. An SP survey is conducted where a discrete choice experiment (DCE) is designed. Two alternatives (PAV and SAV) are included in the DCE, where CL is used to study the behavior of travelers toward these two alternatives considering the characteristics of each alternative. The included characteristics are called attributes, and they are travel time, travel cost, and multitasking availability. The SP is distributed in Hungary, and the collected observations are analyzed. The results of the analysis show that the availability of multitasking onboard increases the opportunity to use a transport mode (i.e., travel-based multitasking). In conclusion, people are more willing to use SAV over PAV considering travel time, travel cost, and multitasking availability when they travel to their main destination within the urban area. Moreover, the travel time influences the use of PAV and SAV, while more influence is obtained when travel cost is changed.

6. Acknowledgment

The research reported in this paper and carried out at the Budapest University of Technology and Economics has been supported by the National Research Development and Innovation Fund (TKP2020 Institution Excellence Subprogram, Grant No. BME-IE-MISC) based on the charter of bolster issued by the National Research Development and Innovation Office under the auspices of the Ministry for Innovation and Technology.

References

1. Hamadneh, J. and D. Esztergár-Kiss, *Potential Travel Time Reduction with Autonomous Vehicles for Different Types of Travellers.* Promet - Traffic&Transportation, 2021. **33**(1): p. 61-76. DOI:10.7307/ptt.v33i1.3585
2. Becker, G. S., *A Theory of the Allocation of Time.* The economic journal, 1965: p. 493-517. DOI:10.2307/2228949
3. Mackie, P. J., S. Jara-Dıaz, and A. Fowkes, *The value of travel time savings in evaluation.* Transportation Research Part E: Logistics Transportation Review, 2001. **37**(2-3): p. 91-106. DOI:10.1016/S1366-5545(00)00013-2
4. Belenky, P., *The value of travel time savings: departmental guidance for conducting economic evaluations, revision 2.* Department of Transportation, 2011.
5. Varghese, V. and A. Jana, *Impact of ICT on multitasking during travel and the value of travel time savings: Empirical*

evidences from Mumbai, India. Travel Behaviour, 2018. **12**: p. 11-22. DOI:10.1016/j.jtrangeo.2012.02.007
6. Steck, F., et al., *How autonomous driving may affect the value of travel time savings for commuting.* Transportation Research Record: Journal of the Transportation Research Board, 2018. **2672**(46): p. 10. DOI:10.1177/0361198118757980
7. Kouwenhoven, M. and G. de Jong, *Value of travel time as a function of comfort.* Journal of choice modelling, 2018. **28**: p. 97-107. DOI:10.1016/j.jocm.2018.04.002
8. Cherlow, J. R., *Measuring values of travel time savings.* Journal of Consumer Research, 1981. **7**(4): p. 360-371. DOI:10.1086/208826
9. Coppola, P. and D. Esztergár-Kiss, *Autonomous Vehicles and Future Mobility*. 2019: Elsevier.
10. Etzioni, S., et al., *Modeling cross-national differences in automated vehicle acceptance.* Sustainability, 2020. **12**(22): p. 9765. DOI:10.3390/su12229765
11. Berliner, R. M., et al., *Travel-based multitasking: modeling the propensity to conduct activities while commuting*, in *Transportation Research Board 94th Annual Meeting*. 2015: Washington DC, United States.
12. Ettema, D. and L. Verschuren, *Multitasking and value of travel time savings.* Transportation Research Record: Journal of the Transportation Research Board, 2007. **2010**(1): p. 19-25. DOI:10.3141%2F2010-03
13. Keseru, I., et al., *Multitasking on the go: An observation study on local public transport in Brussels.* Travel Behaviour Society, 2020. **18**: p. 106-116. DOI:10.1016/j.tbs.2019.10.003
14. Malokin, A., G. Circella, and P. L. Mokhtarian, *How do activities conducted while commuting influence mode choice? Using revealed preference models to inform public transportation advantage and autonomous vehicle scenarios.* Transportation Research Part A: Policy and Practice, 2019. **124**: p. 82-114. DOI:10.1016/j.tra.2018.12.015
15. Litman, T., *Valuing transit service quality improvements.* Journal of Public transportation, 2008. **11**(2): p. 3. DOI:10.5038/2375-0901.11.2.3
16. Banerjee, I. and A. Kanafani, *The value of wireless internet connection on trains: Implications for mode-choice models*, in *UC Berkeley*, U.o.C.T. Center, Editor. 2008: Berkeley.
17. Singleton, P. A., *Discussing the "positive utilities" of autonomous vehicles: will travellers really use their time productively?* Transport reviews, 2019. **39**(1): p. 50-65. DOI:10.1080/01441647.2018.1470584
18. Khaloei, M., A. Ranjbari, and D. Mackenzie, *Analyzing the Shift in Travel Modes' Market Shares with the Deployment of Autonomous Vehicle Technology.* 2019.
19. Zhong, H., et al., *Will autonomous vehicles change auto commuters' value of travel time?* Transportation Research Part D: Transport and Environment 2020. **83**: p. 102303. DOI:10.1016/j.trd.2020.102303
20. Horni, A., K. Nagel, and K. W. Axhausen, *The multi-agent transport simulation MATSim*. 2016: Ubiquity Press London. 620.
21. Hamadneh, J. and D. Esztergár-Kiss. *Impacts of Shared Autonomous Vehicles on the Travelers' Mobility*. in *2019 6th International Conference on Models and Technologies for Intelligent Transportation Systems (MT-ITS)*. 2019. Poland: IEEE. DOI:10.1109/MTITS.2019.8883392
22. Cirillo, C. and K. W. Axhausen, *Evidence on the distribution of values of travel time savings from a six-week diary.* Transportation Research Part A: Policy and Practice, 2006. **40**(5): p. 444-457. DOI:10.1016/j.tra.2005.06.007
23. DeSerpa, A. C., *A theory of the economics of time.* The Economic Journal, 1971. **81**(324): p. 828-846. DOI:10.2307/2230320
24. Xumei, C., L. Qiaoxian, and D. Guang, *Estimation of travel time values for urban public transport passengers based on SP survey.* Journal of Transportation Systems Engineering Information Technology, 2011. **11**(4): p. 77-84. DOI:10.1016/S1570-6672(10)60132-8
25. Janssen, C. P. and J. L. Kenemans. *Multitasking in autonomous vehicles: Ready to go?* in *3rd Workshop on User Experience of Autonomous Vehicles at AutoUI'15*. 2015. Nottingham, UK: ACM Press.
26. Ortega, J., et al., *Simulation of the Daily Activity Plans of Travelers Using the Park-and-Ride System and Autonomous Vehicles: Work and Shopping Trip Purposes.* Applied Sciences, 2020. **10**(8): p. 2912. DOI:10.3390/app10082912
27. Hauber, A. B., et al., *Statistical methods for the analysis of discrete choice experiments: a report of the ISPOR Conjoint Analysis Good Research Practices Task Force.* Value in health, 2016. **19**(4): p. 300-315. DOI:10.1016/j.jval.2016.04.004
28. Simoni, M. D., et al., *Congestion Pricing in a World of Self-driving vehicles: an Analysis of Different Strategies in Alternative Future Scenarios.* Transportation Research Part C: Emerging Technologies, 2018. **98**: p. 167-185. DOI:10.1016/j.trc.2018.11.002
29. Gurumurthy, K. M. and K. M. Kockelman, *Modeling Americans' autonomous vehicle preferences: A focus on dynamic ride-sharing, privacy & long-distance mode choices.* Technological Forecasting Social Change, 2020. **150**: p. 119792. DOI:10.1016/j.techfore.2019.119792
30. Lavieri, P. S. and C. R. Bhat, *Modeling individuals' willingness to share trips with strangers in an autonomous vehicle future.* Transportation research part A: Policy and Practice, 2019. **124**: p. 242-261. DOI:10.1016/j.tra.2019.03.009
31. Bozorg, S. L. and S. M. Ali, *Potential Implication of Automated Vehicle Technologies on Travel Behavior and System Modeling*. 2016.
32. Kolarova, V., F. Steck, and F. J. Bahamonde-Birke, *Assessing the effect of autonomous driving on value of travel time savings: A comparison between current and future preferences.* Transportation Research Part A: Policy Practice, 2019. **129**: p. 155-169. DOI:10.1016/j.tra.2019.08.011
33. Wadud, Z. and F. Y. Huda, *The potential use and usefulness of travel time in fully automated vehicles*, in *Transportation Research Board 97th Annual Meeting*. 2018: Washington DC, United States.
34. Bansal, P., K. M. Kockelman, and A. Singh, *Assessing public opinions of and interest in new vehicle technologies: An Austin perspective.* Transportation Research Part C: Emerging Technologies, 2016. **67**: p. 1-14. DOI:10.1016/j.trc.2016.01.019
35. Burghout, W., P. J. Rigole, and I. Andreasson. *Impacts of shared autonomous taxis in a metropolitan area*. in *Proceedings of the 94th annual meeting of the Transportation Research Board, Washington DC, 2015*. 2015.
36. Krueger, R., T. H. Rashidi, and J. M. Rose, *Preferences for shared autonomous vehicles.* Transportation Research Part C: Emerging Technologies, 2016. **69**: p. 343-355. DOI:10.1016/j.trc.2016.06.015
37. Stoiber, T., et al., *Will consumers prefer shared and pooled-use autonomous vehicles? A stated choice experiment with Swiss households.* Transportation Research Part D: Transport and Environment, 2019. **71**: p. 265-282. DOI:10.1016/j.trd.2018.12.019
38. Cascetta, E., *Random utility theory*, in *Transportation systems analysis*. 2009, Springer. p. 89-167.
39. Hoffman, S. D. and G. J. Duncan, *Multinomial and conditional logit discrete-choice models in demography.* Demography, 1988. **25**(3): p. 415-427. DOI:10.2307/2061541

Determination of pre-collision travel speed in the event of a frontal collision between a vehicle and a fixed obstacle, using video recordings

Irina Duma[1], Nicolae Burnete[1], Adrian Todoruț[1], Daniel Trușcă[2]
Technical University of Cluj-Napoca, Romania[1],
"Transilvania" University of Brașov, Romania[2]
dumairina.d@gmail.com

Abstract: *The present paper evaluates the pre-collision travel speed of a road vehicle, in the event of a frontal collision with a fixed object such as a pole. In this regard, the method of video recordings and image processing using Tracker software program is used. In order to validate the proposed method, the obtained results are compared to the ones acquired with the use of accelerometers mounted on the inferior surface of the vehicle's body. These accelerometers provide a series of real data during the time of the crash, which are then processed in order to reduce the anomalies that appear as a consequence of external factors such as vibrations or signal interferences.*
Keywords*: Accident reconstruction, Video recording, Vehicle velocity, Pre-collision speed, Road vehicle, Frontal collision*

1. Introduction

Statistical data gathered globally show that frontal collisions, especially those between vehicles and fixed objects cause more deaths than any other type of road crashes [1]. In the case of a frontal collision with a tree or a pole, the probability for it to penetrate the vehicle's cabin, causing deadly head injuries to the occupants [2, 3].

According to data provided by IIHS (Insurance Institute for Highway Safety), only in the United States of America (USA), 20% of the deaths caused by road traffic accidents occur from leaving the vehicle's trajectory and hitting fixed obstacles from the proximity of the road [4]. It is noticed, though, a descendent trend in mortality rate, so that in 2018 have been 6% less people killed from road accidents, compared to 2017 and 30% less than in 1979. Out of these deaths, the main majority came from frontal collisions with trees (48%) and poles (12%), respectively [4].

When it comes to data provided from the European Union (EU), collisions with fixed obstacles from nearby public roads cause between 18-50% of the deaths of vehicles' occupants [5].

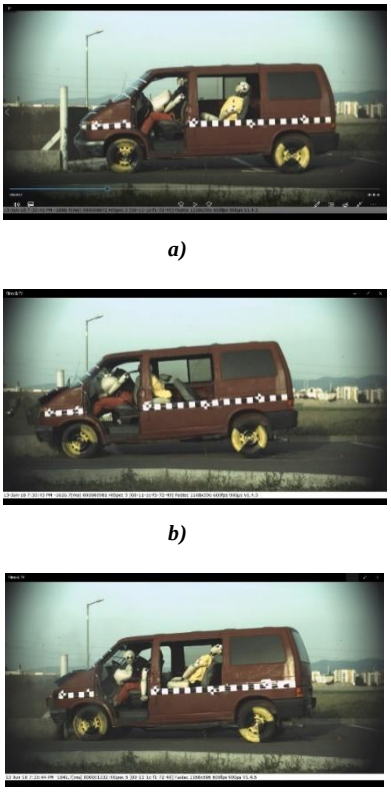
Despite the relatively high incidence of frontal collisions between road vehicles and fixed objects such as poles or trees, European normative in the field of road safety [5] only regulate the testing of vehicle's resistance structure and safety systems for the frontal impact with a fixed barrier and, respectively, for the lateral impact with a pole at a traveling speed of 29 km/h (*NCAP - New Car Assessment Programme*), the latter being considered a secondary impact caused by projecting the vehicle from a primarily frontal collision with another fixed object (barrier) or another vehicle.

Hence, this paper proposes a methodology of reconstructing the frontal impact between road vehicles and fixed objects such as poles, this being a less tackled issue by the current legal frameworks. It is aimed to validate a method for determining the pre-collision vehicle's velocity, by using a video recording of the impact, in order to facilitate the road accidents reconstruction process.

The analysis of video recordings of a given collision represents one of the road vehicle accidents reconstruction means [6, 7], thus being able to find, after calibrating the obtained images, the dynamic parameters of the collision. The specialty literature in the field also approaches this research direction from the perspective of data analysis acquired from traffic surveillance cameras [8, 9].

2. Experimental testing

The experimental testing has the aim of real data acquisition during the timeframe of the frontal impact between the tested vehicle and the pole. The main data to be acquired are the accelerations the decelerations levels to which the vehicle is subjected during the collision and its travel velocity at the time of the impact, respectively. Thus, the data obtained from the accelerometers represent a starting point for the validation of the proposed video processing method in order to determine the pre-collision vehicle's speed. The experimental tests have been conducted within the testing area of the *Research and Development Institute of Transilvania University of Brașov*, Romania [10].



a)

b)

c)

Fig. 1. *Collision phases during the experimental testing [10]: a) pre-collision phase; b) the proper collision; c) post-collision phase.*

From the experimental test (Fig. 1), there have been obtained a series of data regarding the accelerations to which the tested vehicle and its two occupants, through the anthropometric testing devices, are subjected during the impact. This data has been processed using the software programme *Accel.exe*. The obtained results show an unfiltered image of the vehicle's acceleration values during its movement, whereas the accelerometers mounted inside the vehicle are highly susceptible to shock and vibrations caused by the noisy and uneven operation of the powertrain subassemblies.

The obtained values in terms of vehicle speed, decelerations and the total distance traveled during the testing are depicted in Figures 2, 3 and 4.

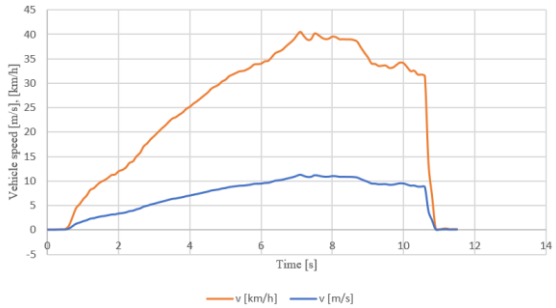


Fig. 2. *The overall vehicle speed during the experimental test.*

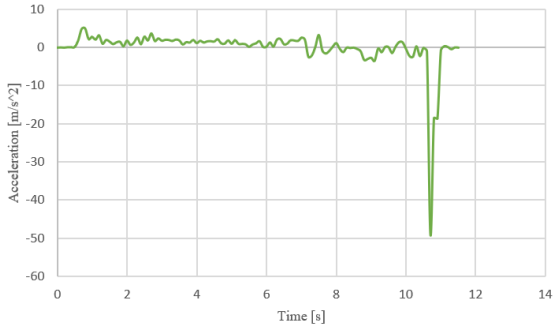


Fig. 3. *The overall vehicle's decelerations during the experimental testing.*

Figure 3 shows a maximum value of the travel speed reached by the vehicle of 11.26 m/s and 40.54 km/h, respectively, recorded at the starting point of the loss of speed due to the inertia of the vehicle and a maximum deceleration of 49.18 m/s^2, recorded at the time of impact.

As the GPS device operates with an error of ±1 m, and from the moment of impact until the moment of the total stopping of the vehicle, the latter is printed a rotational movement around the pole, there is registered a series of abnormal data in the timeframe 9÷11 s.

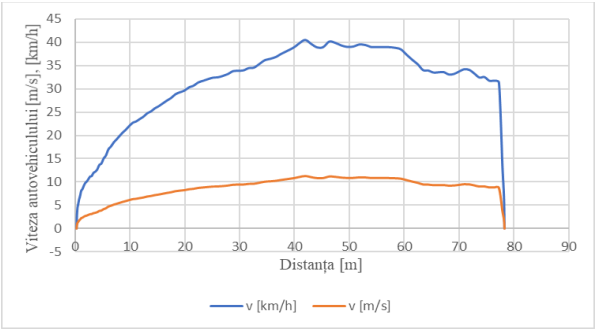


Fig. 4. *The total distance traveled by the vehicle during the experimental test.*

The results depicted in Figure 4 show a total vehicle displacement of 78.31 m, which includes both the service sector and the measurement sector. Also, Figures 2 and 4 show that the vehicle's travel velocity, registered in the impact point, varies between 10.93÷10.07 m/s and, respectively 39.35÷36.26 km/h.

Therefore, it can be ascertained that the experimental frontal impact testing between a road vehicle and a fixed obstacle provides a series of indicative data for a number of parameters, such as vehicle velocity, acceleration and movement, throughout the whole process. This data further represents a starting point for the validation of methods for determining the behaviour of a vehicle in the event of such a collision.

In the following, the value of the pre-collision travel velocity measured by the GPS device will be used as a reference, in order to verify the accuracy of the proposed method which implies the processing of the video recording.

3. Video processing of the collision

The processing of the video recording was realized, in the initial stage, using the software program *Tracker* (Fig. 5), which involves tracking the vehicle's center of mass that was previously chosen throughout the proper collision phase.

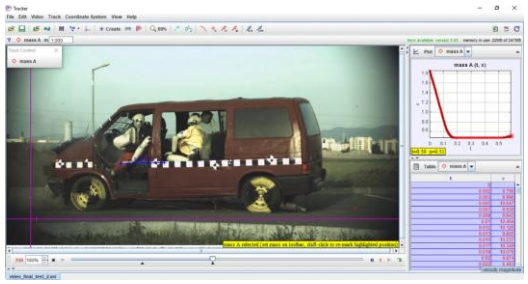


Fig. 5. *Video recording analysis, using the Tracker software program.*

The data thus obtained are then introduced, for further processing, in the *OriginPro* software program (Fig. 6), in order to obtain a graphical interpretation of the results for the variation of the vehicle's acceleration as a function of time and the distance traveled during the testing (in this case, the immediate pre-collision phase, the actual collision and the post-collision phase were included, the latter representing the rotation of the vehicle around the pole).

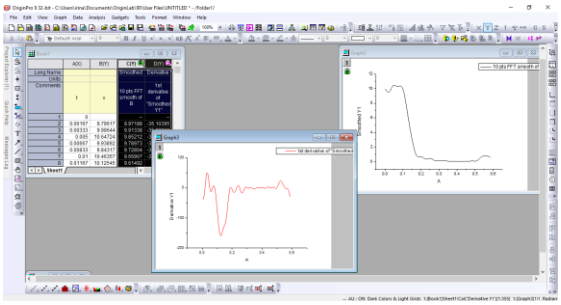


Fig. 6. *Data processing using OriginPro.*

4. Results and conclusions

Following the processing of the results obtained in the previous stage of the study (see Fig. 2, 3 and 4), there is a time-dependent variation of the travel speed and, respectively, accelerations printed on the vehicle, if the moment of impact is chosen as the time interval to be more closely analysed (Fig. 7 and 8).

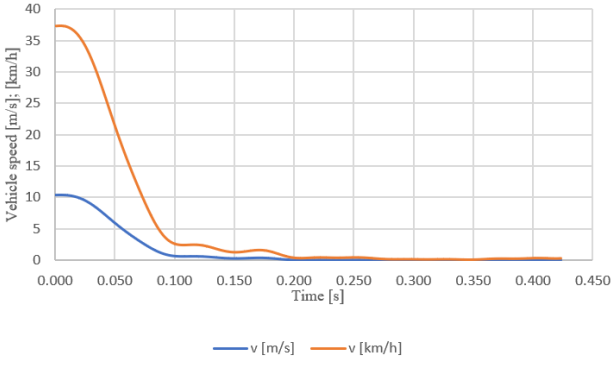


Fig. 7. *Vehicle speed as a function of time, during the moment of the actual collision, according to the video recording processing.*

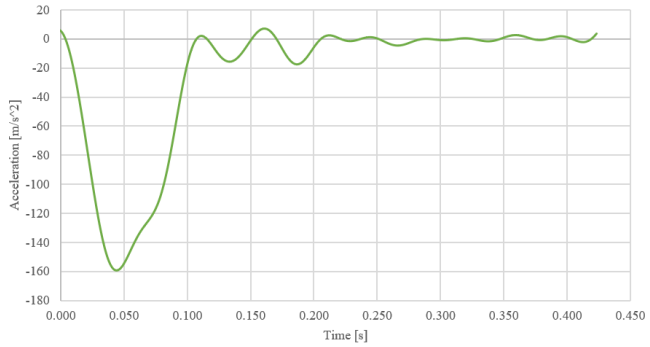


Fig. 8. *Vehicle acceleration as a function of time, during the moment of the actual collision, according to the video recording processing.*

Thus, it is found that the vehicle's impact velocity (37.3 km/h, according to the video recording data processing) falls within the range of 36.26÷39.36 km/h, obtained previously through the GPS data sampling. Therefore, it can be concluded that the proposed working methodology used to evaluate the kinematic and dynamic parameters of the vehicle during its collision with a fixed obstacle such as a pole, can be a true account of the reality.

5. References

[1] **** Offset deformable barrier - OBD, New Car Assessment Programs (NCAP),* https://www.euroncap.com/en/vehicle-safety/the-ratings-explained/adult-occupantprotection/ offset-deformable-barrier/, (accessed at 27/05/2018).
[2] Cordoș, N., Burnete, N., Todoruț, A., *Coliziunea automobilelor,* (Editura Todesco, Cluj-Napoca, 2003).
[3] Todoruț, I.-A., Barabas, I., Burnete, N., *Siguranța autovehiculelor și securitatea în transporturi rutiere,* (U.T.Press Publishing, Cluj-Napoca, 2012).
[4] **** Fatality Facts 2018. Collisions with fixed objects and animals,* Insurance Institute for Highway Safety (IIHS), https://www.iihs.org/topics/fatality-statistics/detail/collisions-with-fixed-objects-and-animals, (accessed at la 04/04/2020).
[5] **** Vehicle Safety 2018,* European Road Safety Observatory, https://ec.europa.eu/transport/road_safety/sites/roadsafety/files/pdf/ ersosynthesis2018-vehiclesafety.pdf, (accessed at 04/04/2020).
[6] Dima, D.S., *Cercetări privind dezvoltarea unor metode de analiză și reconstrucție a accidentelor rutiere,* PhD thesis, Transilvania University of Brașov, (2018).
[7] Neale, W., Fenton, S., McFadden., S., Rose, N., *A video tracking photogrammetry technique to survey roadways for accident reconstruction,* SAE Technical Paper, (2004).
[8] Crouch, M., Cash, S., *Video analysis in collision reconstruction,* (Independent Publishing Network Ltd, London, 2017).
[9] Kolla, E., Ondrus, J., Vertal, P., *Reconstruction of traffic situations from digital video-recording using method of volumetric kinetic mapping,* (2019).
[10] Duma, I., *Analysis of frontal collision between a road vehicle and a fixed obstacle, using numerical modelling and computational simulations methods,* Bachelor's degree thesis, Technical University of Cluj-Napoca, (2018).

Ride comfort in road vehicles: a literature review

Diana Dacova
Technical University of Sofia, Bulgaria
ddacova@tu-sofia.bg

Abstract: *Passengers and the driver in vehicles are subjected to vibrations, noise, acceleration, etc., which affect the comfort, activity and health of people. The effect of vibrations on the human body depends on their frequency, amplitude, duration and direction of impact. Prolonged exposure to vibration causes fatigue in the driver and passengers, which reduces their performance and worsens their functional condition. This can affect traffic safety, so one of the main requirements for modern vehicles is to increase ride comfort. The ride comfort is a set of conditions, impacts and sensations of the driver and passengers when traveling in vehicles. Over the years, there have been many studies and scientific developments aimed at measuring, evaluating and analysing the various factors that affect ride comfort. This paper presents a review on the research studies that have been done on dynamic factors that affect the ride comfort in road vehicles and methods used for measurement and its evaluation were discussed. Finally, some existing suggestions for improving the ride comfort in road vehicle are presented.*

Keywords*: RIDE COMFORT, ROAD VEHICLES, MOTION SICKNESS, VEHICLE VIBRATION, ACCELERATION*

1. Introduction

Nowadays, people spend most of their time traveling by private or public transport. Passengers and the driver in vehicles are exposed to vibrations, noise, acceleration, etc., which affect the comfort, activity and health of people. The effect of vibrations on the human body depends on their frequency, amplitude, duration and direction of impact. Prolonged exposure to vibration causes fatigue in the driver and passengers, which reduces performance and worsens their functional condition. This can affect traffic safety, so one of the main requirements for modern vehicles is to increase the ride comfort. Over the years, there have been numerous studies and scientific developments aimed at measuring, evaluating and analysing the various factors that affect ride comfort.

The comfort is subjective state of well-being or absence of mechanical disturbance in relation to the induced environment (concerning mechanical vibration or repetitive shock) [1]. The car passenger comfort is determined by the complex impact of many factors, which can be separated in the following areas [2, 3]:

- **dynamic factors** influencing the ride comfort (mechanical comfort - vibrations with low and very low frequency, shocks and accelerations) and the levels of vibrations with high frequency and noise (vibroacoustic comfort);
- **the microclimate** in the passenger compartment (cabin) of the vehicle (thermal comfort, air quality, atmospheric pressure, etc.);
- and factors depending on the **ergonomic position** of the passengers.

The driver and passengers assess the ride comfort subjectively based on their own feelings.

This paper reviews research on the dynamic factors that influence the vehicles ride comfort, methods for its evaluation and suggestions for its improvement.

2. Impact of Vibrations in Vehicles on Passengers

The ride comfort depends on the characteristics of the forces that cause oscillations and vibrations, on the design of the car, the parameters of the suspension, the driving conditions etc. The forces that cause low-frequency vibration (oscillations) and high-frequency vibrations of the car arise because of internal (unbalanced rotating masses of the engine and transmission, uneven engine operation) and external causes (uneven roads).

The unpleasant and harmful effects of vibrations on human being depend primarily on the way they are transmitted to the human body and on the transmission of vibrations in the body, on the physical nature of vibrations, on the time a person is exposed to vibrations and from the individual characteristics, etc.

The vibrations of the car in real road conditions are varied, and the sprung mass can receive low-frequency 1–3 Hz, high-frequency 7–15 Hz, vibration 15–30 Hz and complex shocks. The human driver or passenger is also a system with a fundamental frequency of free vibrations, which is in the range of 3.5-5 Hz. The human being is adapted to exposure with a frequency of about 1 to 2 Hz corresponding to the frequency of the everyday walking [2, 4].

In [5] is noted that when humans exposed to interference with certain frequencies, resonant phenomena occur, which must be considered in the vibrations of the driver, operator and passengers. The resonant frequencies of the human body are eyes 12–27 Hz; throat 6–27 Hz; chest 2–12 Hz; legs, arms 2–8 Hz; head 8–27 Hz; face-jaw 4–27 Hz; lumbar part of the back 4–14 Hz; stomach 4–12 Hz. At significant vibration values in the frequency range 4–10 Hz, the person may feel painful sensation and discomfort due to resonant oscillations of the "breast-stomach" system. According to the authors of [4, 5] vibrations with a frequency of 3–5 Hz cause reactions of the vestibular apparatus and can cause motion sickness.

It is important to study the effects of vibrations on the human body and their consequences is to study the mode of head vibrations. Regardless of the direction of disturbance (vertically or horizontally), the head always makes movements in space with an elliptical trajectory. In [6] the author notes that nodding head movements have a resonant frequency of 2 Hz and vertical ones 8–27 Hz. According to the author, the human vestibular apparatus also responds to low-frequency vibrations and the symptoms of motion sickness appear at a frequency of 0.5–1.3 Hz.

There are many international standards for assessing the vibrations to which a person may be exposed. The international standard ISO 5349-1:2001 "Mechanical vibration – Measurement and evaluation of human exposure to hand-transmitted vibration – Part 1: General requirements" refers to the measurement and assessment of the impact of vibrations transmitted to the human hand [7]. The second part of this standard is a practical guide for measuring human hand vibration in the workplace: ISO 5349-2: 2001/Amd 1:2015 "Mechanical vibration – Measurement and evaluation of human exposure to hand-transmitted vibration – Part 2: Practical guidance for measurement at the workplace – Amendment 1" [8]. Another international standard for the assessment of mechanical vibration is ISO 10326-1:2016 "Mechanical vibration – Laboratory method for evaluating vehicle seat vibration – Part 1: Basic requirements". ISO 10326-1:2016 applies to specific laboratory tests on seats that assess the transmission of vibration to passengers in any type of seat used in vehicles and mobile off-road vehicles. It shall specify the test method, the instrumentation requirements, the measurement evaluation method and the method of reporting the test result [9]. The second part of the international standard ISO 10326 is ISO 10326-2:2001 "Mechanical vibration – Laboratory method for evaluating vehicle seat vibration – Part 2: Application to railway vehicles". It concerns tri-axial rectilinear vibration within the frequency range 0.5 Hz to 50 Hz [10]. Another standard for comfort assessment is the standard BS EN 12299:2009 "Railway applications. Ride comfort for passengers. Measurement and evaluation". This standard specifies methods for quantifying the effects of vehicle body motions on ride comfort for passengers and vehicle assessment with respect to ride comfort [11].

The main document for vibration assessment is the international standard ISO 2631:1997 "Mechanical vibration and shock - Evaluation of human exposure to whole-body vibration". It consists

of five parts: Part 1: General requirements [ISO 2631-1:1997/Amd 1:2010]; Part 2: Vibration in buildings (1 Hz to 80 Hz) [ISO 2631-2:2003]; Part 3: Evaluation of exposure to whole-body z-axis vertical vibration in the frequency range 0.1 to 0.63 Hz [canceled and replaced with International Standard ISO 2631-1:2010]; Part 4: Guidelines for the evaluation of the effects of vibration and rotational motion on passenger and crew comfort in fixed-guideway transport systems [ISO 2631-4:2001/Amd 1:2010]; Part 5: Method for evaluation of vibration containing multiple shocks [ISO 2631-5: 2018]. The international standard ISO 2631-1 repeals and replaces the first edition ISO 2631-1:1985, as well as ISO 2631-3: 1985. The revised edition of this part of ISO 2631 combines the new experience and research results published in the literature. In this revised edition, the frequency range is extended below 1 Hz. The main objective of ISO 2631-1 Part 1: General requirements is to define methods for the quantification of whole-body vibrations in relation to human health and comfort; the probability of perception of vibrations; manifestation of motion sickness (travel disorders). ISO 2631-1 defines methods for measuring periodic, random and transient vibrations of the whole body. This section identifies the main factors that are combined to determine the extent to which the impact of vibration is acceptable. The frequency ranges considered are from 0.5 Hz to 80 Hz for health, comfort and perception and from 0.1 Hz to 0.5 Hz for motion sickness [12]. Low frequency acceleration can cause discomfort, instability and motion sickness, leading to impaired travel comfort.

3. Motion Sickness

The term "motion sickness" was first introduced by Irwin in the publication [13]. He suggests that the term motion sickness is more correct than sea-sickness because "not only does it occur on lakes and even on rivers, but as is well known, a sickness identical in kind may be induced by various other motions than that of turbulent water,…". Motion sickness is a response to real or apparent movement to which human being is not adapted. According to [14] motion sickness is a misnomer for this response, the symptoms can be caused both by the absence of expected movement and by the presence of unexpected movement (examples of this are sickness associated with wide-screen movies and simulators).

Motion sickness occurs when there is a contradiction between the perceptions of movement coming from the eyes and the vestibular apparatus, i.e., a person sees that he is moving but does not feel it, or vice versa – he feels that he is moving but does not see it. The vestibular apparatus consists of two main parts – an organ responsible for the perception and reflection of angular accelerations and an organ responsible for the perception and reflection of rectilinear accelerations and gravity. The assessment of the change in the position of the human body in space also depends on the change in the position of the eyeball, the musculoskeletal system, the skin tissue, the constituent ligaments, etc. (Fig. 1). An example of a contradiction between the perceptions of movement coming from the eyes and the vestibular apparatus is when reading in a car when it is dark outside; the vestibular system then gives signals for movement, but the visual system does not confirm this movement and these contradictory factors can cause motion sickness [15]. Another example of a conflict between the perceptions of movement and the vestibular apparatus is with a person parking a car in a parking lot and the one next to him left. Another such situation can occur when a driver/passenger in a car is waiting at a traffic light and the stopped bus in the next lane set off.

Motion sickness occurs when traveling by car, bus, train, plane (mismatch between visual and vestibular irritation), sailing (unusual complexes of linear and angular acceleration with a slow frequency – less than 1 Hz), use of a simulator, when flying in weightlessness, as well as when using virtual reality, computer games, etc. [16–18]. According to [17] motion sickness is a general term for many symptoms and signs, generally unfavourable due to exposure to abrupt, periodic, or unnatural accelerations.

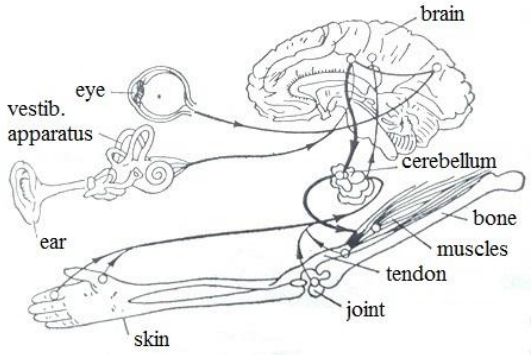


Fig. 1 *Scheme of the relation between the vestibular apparatus and other organs of external influences. Adapted from [4].*

Factors that contribute to the onset of motion sickness symptoms can vary such as air quality, odour, temperature, taste, vibration, visual contribution, oxygen ions, stress, sound, head position, and body posture [19]. The symptoms of motion sickness increase with increased exposure to lateral acceleration at low frequencies (<0.5 Hz) and mainly on predominantly curvy cross-country routes [15]. In [20] the authors conducted a road experiment on a fixed suburban route. During the journey, the spectra of fore-and-aft and lateral acceleration are similar in the frequency range 0.1–0.5 Hz and consequently the motion sickness dose values are similar along these axes. At frequencies less than 0.1 Hz, the fore-and-aft acceleration is slightly greater than the lateral acceleration. According to the authors, the low-frequency fore-and-aft and lateral acceleration in cars are more dependent on the driver's behaviours. After a road experiment, the authors conclude that the dose of the sickness for fore-and-aft and lateral acceleration is significantly higher than motion sickness dose values for vertical acceleration.

The main factors that cause motion sickness are shown in Fig. 2. According to some studies [16, 17, 21] women are more sensitive than men, the most vulnerable to the symptoms of motion sickness are children. However, the age group 4 to 12 years is not included in the standardized dynamic vehicle tests in either regulatory or consumer assessment programs [22].

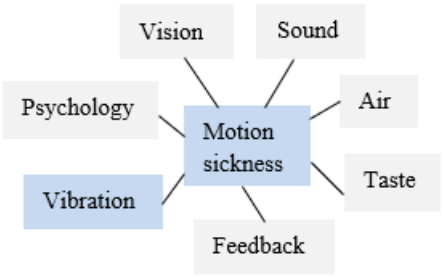


Fig. 2 *The main factors that cause motion sickness. Adapted from [19].*

The vestibular system is what helps us keep our balance. It registers changes in position caused by motion and controls the position of the head through regulation of muscle tension which helps us keep our posture. The vestibular system is affected by vertical and horizontal vibrations and forces of acceleration [19] that results in motion sickness and ride discomfort (Fig. 3).

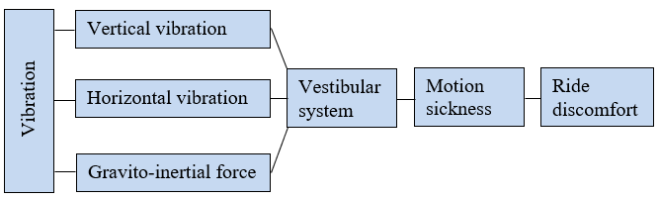


Fig. 3 *Vibrations and forces of acceleration that affect the vestibular system that results in motion sickness and ride discomfort. Adapted from [19].*

Drivers follow the road all the time, do not keep their eyes on stationary objects for a long time and they do not exhibit symptoms of motion sickness. One reason for this may be that the driver can predict the direction of the vehicle and therefore aligns his/her head with the GIF (Gravito Inertial-Force) [19]. The known fact that drivers rarely become motion sick may be due to the driver's prediction of low-frequency horizontal accelerations as they depend on the driver's behaviour [23]. Thus, the conflict between the visual perceptions and the sensations of the vestibular apparatus in the driver is less pronounced than in the passengers. With the advent of autonomous cars, the driver changes his/her role and becomes a passenger. As a passenger, he/she may also at some point show symptoms of motion sickness due to lack of vehicle control in addition to sensory conflicts [24]. In a conflict situation, he/she probably will not be able to take control of the car. In recent years, the possibility of autonomous cars entering has increased, and in this connection, consideration should be given to reducing the mechanical effects that cause the symptoms of motion sickness.

4. Methods for Measurement the Ride Comfort

There are various methods for assessing the ride comfort. In most cases, the acceleration, the frequency of oscillations, the vibrations, the noise to which the passengers in the land vehicles are exposed are measured with the help of equipment. The obtained results are compared with the existing international standards. Various factors can affect a person's response to vibrations such as gender, height, health, driver or passenger etc. Some researchers use methods such as conducting interviews with a lot of participants of different age groups, gender, nationality, etc. The comfort that people feel can be classified as a subjective assessment, as it is possible to detect significant variations in the responses of different people to the same situation [25]. Mathematical models and computer simulations are used to obtain results, which can subsequently be compared with results obtained in road experiments [26–29]. Various vibration measuring test bench are also used in the laboratory [30] and simulators of driving conditions [31]. The main value for the magnitude of the vibration is the acceleration. Accelerometers are used to measure the accelerations to which passengers are exposed when traveling in road vehicles, which record the accelerations on all three axes of movement (Fig. 4). In some cases, the accelerations are measured only in single axis, for example if the researchers work on improving the design of the suspension they are mostly interested in vertical accelerations; if they are working on active transverse stabilizers or tilting systems, they are mostly interested in a change in the lateral accelerations [32]. In [33] the authors explore the possibility of using smartphones to measure comfort when traveling on trains. They conclude that the accelerometers found in modern smartphones are of sufficient quality to be used in assessing ride comfort.



Fig. 4 *Accelerometer and DAQ devise used for data acquisition [32].*

To predict the onset of motion sickness symptoms, the authors of [31], studied the effect of lateral oscillations at frequencies between 0.0315 and 0.2 Hz. The experiment was performed using a simulator capable of a horizontal displacement of 12 m and simulating six motion conditions. After conducting an experiment with 120 people, the authors summarize that there is a very significant effect of the frequency of lateral vibrations on the appearance of mild nausea.

In [34] is studied the effect of vehicle vibration on humans. The calculations are made using a simulation program using a full vehicle model with a driver and the results are evaluated using the international standard ISO 2631. Road irregularities are chosen as the impact. The physical model of the studied system is formed by a full vehicle model and a driver. The conclusions made by the authors after the study: if the driver travels at a speed of 72 km/h from 5 to 6 hours on a smooth road, at frequency ranges from 8 to 10 Hz he/she feels uncomfortable and should not be exposed to vibration more than 5 hours under these conditions.

In the publication of M. Brogioli at all [35] a mechanical model of a seated passenger is presented and through its validation an analysis of the key parameters that affect ride comfort is performed. According to the authors, the size and weight (percentile) of the human object are crucial for assessing ride comfort. Another important component is the seat and its parameters – stiffness, damping and geometric parameters.

In [30] the influence of vibration frequency and pitch motion and roll motion on motion sickness are studied using a vibrating test bench. The conclusions of the experiment are that vertical vibrations and pitch motion at 0.5 Hz or lower affect the frequency of the sickness when the vehicle is moving. The authors present a formula that can be used to assess the level of motion sickness, using differences in vibration levels and coefficients of influence of the direction and frequency of vibrations on motion sickness. Road tests have been carried out with many vehicles to confirm that the level of motion sickness assessed using the developed formula is in good agreement with the result of the subjective assessment. The methods proposed by the authors are applied to verify the effectiveness of an improved suspension system, which is installed in vehicles and suppresses low-frequency vibrations.

5. Suggestions for Improving the Ride Comfort

Most research and development to improve ride comfort relates to ride comfort at frequencies greater than 1 Hz, where movement depends on the dynamic response of the car's suspension and seat.

At these frequencies, in addition to the suspension and the seat that serve as isolation from the road, the characteristics of the tires also influence, as at frequencies up to 30 Hz the comfort depends on the pressure in them and over 30 Hz on the tire design [36, 37]. Other sources of high frequency vibrations are the engine and transmission. Elastic engine mounts and drive shaft bushes are used to dampen their vibrations [38]. Dynamic vibration absorbers and crankshaft dampers is widely used in most vehicle engines [39]. Modern engines with a small number of cylinders and high power often use a dual flywheel [40].

Vehicle movements at frequencies less than about 1 Hz result from the road surface profile (for vertical vibrations), cornering (for lateral acceleration) and acceleration and braking (for fore-and-aft movements). All three are affected by the speed of the vehicle and differently by the behavior of the driver. In newer suspension designs, mainly for high class vehicles, active or semi-active suspensions are used which can reduce roll and pitch angle in this case.

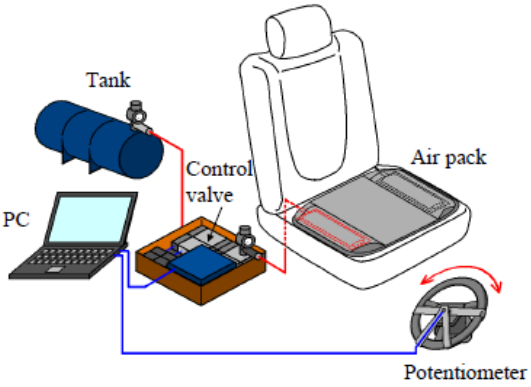


Fig. 5 *Posture Control Device [28].*

Some studies have shown that by tilting the head to the center of the corner, following the example of the driver, the symptoms of motion sickness in car passengers can be significantly reduced, leading to improved ride comfort [28, 41–43]. In [28] is present posture control device when traveling by car (Fig. 5). The proposed device has the effect of increasing the stability of the posture and increasing the comfort of passengers when driving in a corner.

In [44] experimental results performed with a tilting vehicle that was developed by modifying a small electric vehicle are presented. The driver's seat is fixed to the cab, which is attached to the chassis of the vehicle and their relative movement is about the axis of rotation. An electric motor is attached to one end of the axis of rotation to simulate a spring and a shock absorber. The tilting movement of the cab is mainly based on the lateral acceleration of the chassis. The tilt angle is limited to approximately 20º (0.35 rad) with a mechanical stopper. The results show that the tilting function significantly reduces the severity of motion sickness and increases ride comfort.

Tilting the chassis, following the example of railway transport, can compensate lateral accelerations of 1–2 m/s^2. The tilting angle should be approximately 6–12°. This overall tilting angle can be represented by the road bank angle, the vehicle configuration roll angle and the seat angle. To achieve compensation in the specified range, this would only be possible by applying (separately or additionally) tilting the seat [45]. To reduce the vibrations in lateral and vertical direction a seat system is necessary that allows an independent movement in both considered directions. In [46] the design of an active seat suspension is described. As it is difficult to redesign an existing car seat structure, it is possible to make a tilting car child seat [32].

6. Conclusion

This paper introduced a review of scientific papers and standards related to the ride comfort in road vehicles. The methods and the technical equipment for measuring and assessing comfort are considered. Special attention is paid to low-frequency oscillations below 1 Hz and their influence on the occurrence of motion sickness. Some suggestions are given for reducing the lateral inclination or for tilting towards the centre of the corner of the passenger's head, of his body by means of a pad in the seat or of the whole seat, and of the whole body of the car (chassis).

Despite existing research, lateral tilting systems have not been used in road transport, unlike rail transport. The reasons for this are the increase in the cost of construction, reduction of stability in case the whole chassis is tilted, lack of space for tilting the seats, etc. Therefore, the author of the present publication suggests a tilting child seat construction, thus will avoid many of the listed disadvantages and improving the ride comfort of the most vulnerable age group.

Acknowledgments

This work was supported by the research program to support PhD students in Technical University of Sofia internal session 2020 under the project № 202ПД0022-04.

References

1. ISO 5805:1997 *Mechanical vibration and shock – Human exposure – Vocabulary*
2. P. Petkov, *Automotive engineering I*, Todor Kableshkov University of Transport, Sofia, p. 599 (2016) (In Bulgarian)
3. C. Corbridge, *Vibration in vehicles: its effect on comfort*, PhD Thesis, University of Southampton, p. 498 (1987)
4. L. Toshev and P. Tsenkov, *Suspension of buses, trucks and trailers*, Tehnika, p. 214 (1979) (In Bulgarian)
5. I. Angelov and V. Ovcharov, *Vibrations and noise in vehicles*, Tehnika, p. 270 (1985) (In Bulgarian)
6. Yu. I. Chuprakov, *Hydraulic systems to protect the human operator from general vibration*, Mashinostroyeniye, p. 224 (1987) (In Russian)
7. ISO 5349-1:2001 *Mechanical vibration – Measurement and evaluation of human exposure to hand-transmitted vibration – Part 1: General requirements*
8. ISO 5349-2: 2001/Amd 1:2015 *Mechanical vibration – Measurement and evaluation of human exposure to hand-transmitted vibration – Part 2: Practical guidance for measurement at the workplace – Amendment 1*
9. ISO 10326-1:2016 *Mechanical vibration – Laboratory method for evaluating vehicle seat vibration – Part 1: Basic requirements*
10. ISO 10326-2:2001 *Mechanical vibration – Laboratory method for evaluating vehicle seat vibration – Part 2: Application to railway vehicles*
11. BS EN 12299:2009 *Railway applications. Ride comfort for passengers. Measurement and evaluation*
12. ISO 2631-1:1997 *Mechanical vibration and shock – Evaluation of human exposure to whole-body vibration – Part 1: General requirements*
13. J. A. Irwin, M. A. Cantab, M. D. Dub and C., *The pathology of sea-sickness*, The Lancet, **118**(3039), pp. 907–909 (1881)
14. T. G. Dobie, *Motion Sickness. A Motion Adaptation Syndrome*, Springer, p. 302 (2019)
15. M. Turner and M. J. Griffin, *Motion sickness in public road transport: the effect of driver, route and vehicle*, Ergonomics, **42**(12), pp. 1646–1664 (1999)
16. O. Kolev et al, *Otoneurology. Contemporary aspects*, Edited by O. Kolev, Meditsina i fizkultura Publishing, p. 200 (2017) (In Bulgarian)
17. R. S. Kennedy and L. H. Frank, *A review of motion sickness with special reference to simulator sickness*, Technical Report (1985)
18. P. Dunai, *Mozgásbetegség diagnosztizálásának nehézségei, A megelőzés módja a pilótaképzést végző oktatási intézmények speciális földi felkészítésének folyamatában*, RTK, **28**(3), pp. 79–94 (2016) (In Russian)
19. N. Karlsson and H. Tjärnbro, *Motion sickness in cars. Physiological and psychological influences on motion sickness*, Bachelor of Science Thesis on behalf of Volvo Cars, Department of Product and Production Development, Chalmers University of Technology, Gothenburg, Sweden (2012)
20. M. Griffin and M. Newman, *An experimental study of low-frequency motion in cars*, Proc. of the Institution of Mechanical Engineers, Part D: J. of Automobile Engineering, **218**(11), pp. 1231–1238 (2004)
21. D. Huppert, E. Grill and T. Brandt, *Survey of motion sickness susceptibility in children and adolescents aged 3 months to 18 years*, J. of Neurology, **266**, pp. 65–73 (2019)
22. K. Brolin et al., *Safety of children in cars: A review of biomechanical aspects and human body models*, IATSS Research, **38**, pp. 92–102 (2015)
23. G. Bertolini and D. Straumann, *Moving in a Moving World: A Review on Vestibular Motion Sickness*, Front. Neurol. **7:14** (2016)
24. J. Iskander et al, *From car sickness to autonomous car sickness. A review*, Transportation Research Part F, **62**, pp. 716–726 (2019)
25. M. C. Gameiro da Silva, *Measurements of comfort in vehicles*, Measurement Science and Technology, **13**, R41–R60 (2002)
26. L. Jin, Y. Yu, Y. Fu, *Study on the ride comfort of vehicles driven by in-wheel motors*, Advances in Mechanical Engineering, **8**(3), pp. 1–9 (2016)
27. M. K. Mahala, P. Gadkari and A. Deb, *Mathematical models for designing vehicles for ride comfort*, ICORD 09: Proc. of the 2nd Int. Conf. on Research into design, pp. 168–175 (2009)
28. H. Konno, S. Fujisawa, T. Wada, S. Doi, *Analysis of motion sensation of car drivers and its application to posture control device*, SICE Annual Conference, Tokyo, pp. 192–197 (2011)
29. T. Wada, N. Kamiji and S. Doi, *A mathematical model of motion sickness in 6DOF motion and its application to vehicle passengers*, Int. Digital Human Modeling Symposium (2013)
30. B. Atsumi et al., *Evaluation of vehicle motion sickness due to vehicle vibration*, JSAE Review, **23**, pp. 341–346 (2002)
31. B. Donohew and M. Griffin, *Motion sickness: effect of the frequency of lateral oscillation*, Aviat Space Environ Med, **75**(8), pp. 649–656 (2004)
32. N. L. Pavlov and D. I. Dacova, *Solutions for increasing the comfort in road vehicles based on improving the construction of the seats*, IOP Conf. Ser.: Mater. Sci. Eng., **1031**, 012010 (2020)

33. A. Azzoug and S. Kaewunruen, *Ridecomfort: a development of crowdsourcing smartphones in measuring train ride quality*, Front. Built Environ, **3**, article 3, (2017)
34. A. Sezgin and N. Yagiz, *Analysis of passenger ride comfort*, MATEC Web Conf., **1**, 03003 (2012)
35. M. Brogioli, M. Gobbi, G. Mastinu and M. Pennati, *Parameter sensitivity analysis of a passenger/seat model for ride comfort assessment*, Experimental Mechanics, pp. 1237–1249 (2011)
36. Z. Georgiev and L. Kunchev, Study of the vibrational behaviour of the components of a car suspension, MATEC Web Conf., **234**, 02005 (2018)
37. Z. Georgiev, *Model study of the influence of the vibration parameters of the pneumatic tyre on the behaviour of a vehicle*, PhD Thesis, Technical University of Sofia, (2020)
38. F. L. Mrad et al, *Optimization of the vibrational comfort of passenger vehicles through improvement of suspension and engine rubber mounting setups*, Shock and Vibration, **2018**, 9861052 (2018)
39. G. Sheng, *Vehicle noise, vibration, and sound quality*, Society of Automotive Engineers, p. 506 (2012)
40. N. Pavlov, *Numerical simulation on the vibration of a vehicle drivetrain with dual mass flywheel*, MTM, **12**(2), pp. 49–52 (2018)
41. T. Wada, H. Konno, S. Fujisawa and S. Doi, *Can passenger's active head tilt decrease the severity of carsickness? – Effect of head tilt on severity of motion sickness in a lateral acceleration environment*, The Journal of the Human Factors and Ergonomics Society, **54**(2), pp. 226–34 (2012)
42. T. Wada and K. Yoshida, *Effect of passengers' active head tilt and opening/closure of eyes on motion sickness in lateral acceleration environment of cars*, Ergonomics, **59**(8), pp. 1050–1059 (2015)
43. T. Wada, S. Fujisawa and S. Doi, *Analysis of driver's head tilt using a mathematical model of motion sickness*, Int. J. of Industrial Ergonomics, **63**, pp. 89–97 (2018)
44. T. Sugiura, T. Wada, T. Nagata, K. Sakai and Y. Sato, *Analysing effect of vehicle lean using cybernetic model of motion sickness*, IFAC-PapersOnLine, **52**(19), pp. 311–316 (2019)
45. H. Winner, W. Wachenfeld, *Effects of autonomous driving on the vehicle concept*. In: Maurer M., Gerdes J., Lenz B., Winner H. (eds) Autonomous Driving (Springer, Berlin, Heidelberg) (2016)
46. R. Kieneke, C. Graf and J. Maas, *Active seat suspension with two degrees of freedom for military vehicles*, IFAC Proceedings Volumes, **46**(5), pp. 523–529 (2013)

Fuel economy of off-road vehicles in respect to recuperation of vehicle's kinetic energy

Jasna Glišović[1,*], Saša Vasiljević[2], Nenad Miloradović[1], Nadica Stojanović[1], Ivan Grujić[1]
University of Kragujevac, Faculty of Engineering, Kragujevac, Serbia [1]
Academy of Professional Studies Sumadija Department in Kragujevac, Kragujevac, Serbia [2]
E-mail: jaca@kg.ac.rs, vasiljevic.sasa036@gmail.com, mnenad@kg.ac.rs, nadica.stojanovic@kg.ac.rs, ivan.grujic@kg.ac.rs

Abstract: *Since the fuel-saving idea was introduced in the 20th century, energy efficiency has gained attention in the transport industry. Ground vehicles (military, agricultural, and construction) usually operate on unprepared ground and need to overcome very complex and difficult ground obstacles, such as steep grade and very soft ground. The electrification of conventional vehicles, ranging from passenger vehicles and trucks to ground vehicles such as agricultural tractors, construction equipment and military vehicles, can potentially offer improvements in fuel economy and emissions. Applied new systems reduce the amount of mechanical energy needed by the thermal engine by recovering the vehicle kinetic energy during braking and then assisting torque requirements. Energy management strategies for off-road vehicles are studied in this paper. With heavily fluctuating fuel prices, the total cost of ownership of loaders, excavators, and other classes of ground vehicles is nowadays strongly influenced by the fuel costs and there is growing concern about CO_2 emissions as well as about the long-term availability of fossil fuels.*

Keywords*: ENERGY EFFICIENCY, REGENERATIVE BRAKING, ELECTRIFIED, HYDRAULIC, BRAKING SYSTEM*

1. Introduction

The global energy landscape is changing. Traditional centers of demand are being overtaken by fast growing emerging markets. The energy mix is shifting, driven by technological improvements and environmental concerns. A central feature of the energy transition is the continued gradual decarbonization of the fuel mix. Rapid improvements in the competitiveness of renewable energy mean that increases in renewables, together with nuclear and hydro energy, provide around half of the increase in global energy out to 2035. Natural gas is expected to grow faster than oil or coal, helped by the rapid growth of liquefied natural gas increasing the accessibility of gas across the globe. Oil demand continues to increase, although the pace of growth is likely to slow as vehicles become more efficient and technological improvements, such as electric vehicles, autonomous driving and car sharing, potentially herald a mobility revolution.

The Fig. 1 shows the pattern of oil discovery, listing all of the major plays that have dominated oil production. Hybrid vehicles are just one of a number of solutions suggested by the transport industry to reduce dependency on oil and harmful GHG emissions. "Hybrid" has its origin in the Greek language and means: "Mixture or combination of two things." The most common hybrid technologies are electric and hydraulic hybrids. The number of electric cars rises significantly, from 1.2 million in 2015 to around 100 million by 2035 (6% of the global fleet). Around a quarter of these electric vehicles (EVs) are Plug-In Hybrids (PHEVs), which run on a mix of electric power and oil, and three quarters are pure Battery Electric Vehicles (BEVs) [1].

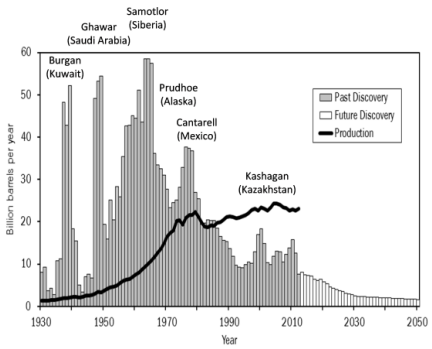


Fig. 1 *Actual and projected worldwide discovery, extraction and demand for conventional oil (From 1930 to 2050 in billions of barrels)[2].*

Hybrid vehicles are called hybrids because they use both an internal combustion engine (ICE) and an electric motor to obtain maximum power and fuel economy with minimum emissions. What all hybrids have in common is the ability to generate electric current, store it in a large battery, and use that current to help drive the car. Hybrids have regenerative braking systems that generate electric power to help keep the batteries charged. When the driver applies the brakes, the electric motor turns into a generator, and the magnetic drag slows the vehicle down. For safety, however, there is also a normal hydraulic braking system that can stop the car when regenerative braking isn't sufficient. There's no difference in maintenance or repair except that the brake pads tend to last much longer because they don't get used as much. The big difference is that regenerative brakes capture energy and turn it into electricity to charge the battery that provides power to an electric motor. Hybrids can also conserve energy by shutting down the ICE when the vehicle is in Park, idling at a light, or stopped in traffic, or when the electric motor's energy is sufficient to drive the vehicle without assistance from the ICE [3].

Regenerative braking has many advantages: emission of carbon dioxide is reduced in the environment; overall performance of the system is increased; during braking most of the heat is converted into useful mechanical energy; engine life enhances; wear of engine is reduced; due to reduction in brake wear, the life span of the friction braking system increases, but has also limitations: regenerative braking system is more complexes; overall weight of the vehicles increases due to the assemble of extra components; higher maintenance is required; for safety purpose friction brake is necessary, in case failure of the regenerative brake system; the size of energy stores mainly depend upon size of vehicles.

It is important to analyze the efficiency of power trains of electric and hybrid electric powered land vehicles to compare them with canonical combustion engines, both in a tank-to-wheels basis and a well-to-wheels basis. One of the question formulations is if an electric or plug-in hybrid electric vehicle charged by public electricity generated by a fossil plant will result in any environmental alleviation at all, in excess of reducing the local tailpipe pollution [4].

An off-road vehicle is any ground vehicle which does not, in general, use normal roads for its operation. Examples of such vehicles include predominantly construction vehicles and equipment, mining vehicles, agricultural vehicles like tractors, and so on. Some military vehicles also fall into this category. Off-road vehicles to be discussed in this section have quite different drive cycles and speed–torque demands, compared to a regular automobile [2].

With heavily fluctuating fuel prices, the total cost of ownership of loaders, excavators, and other classes of ground vehicles is nowadays strongly influenced by the fuel costs. Moreover, there is growing concern about CO_2-emissions caused by the burning of fossil fuels as well as about the long-term availability of these fuels. The fuel economy and efficiencies of the drive train and the hydraulic implements have therefore become extremely important parameters in the design of future ground vehicles. Hybrid transmissions are now considered to be a solution for ground vehicles. Furthermore, hybrid electric vehicles need sophisticated electric transmissions with delicate and expensive inverters,

converters, and batteries. Taking the extreme power transients in mobile machinery and the rough operational conditions of off-road drive trains into account, it is questionable whether the delicate hybrid electric drive trains can be considered a viable, inexpensive, and robust option for ground applications. Yet, there is still the alternative of the hydraulic hybrid drive train-a full series hybrid system with an in-wheel motor in each wheel and hydraulic transformers for efficient power control. For military vehicles, the drivers for hybrid electric vehicles are quite different; although the fuel economy remains a desirable feature for both the commercial and military sectors. The military needs for hybrid electric reside in their ability to generate significant level of electric power onboard the vehicles to meet the demand of the warfighter thus expanding his mission capabilities in terms of mobility, survivability and lethality. However, the fielding of hybrid electric military vehicles has been much slower than the commercial vehicles due to the technical challenges that must be overcome before the hybrid technology can be considered viable for military applications [5].

EVs have penetrated the market of off-road vehicles successfully over the years for clean air as well as for cost advantages. Examples of such applications are airport vehicles for passenger and ground support; recreational vehicles as in golf carts and for theme parks, plant operation vehicles like forklifts and loader trucks; vehicles for disabled persons; utility vehicles for ground transportation in closed but large compounds; etc. There are also EVs that run on tracks for material haulage in mines. There is potential for EV use for construction vehicles. The locomotives that run on tracks with electricity supplied from transmission lines are theoretically no different from other EVs, the major difference being in the way energy is fed for the propulsion motors [6].

This paper presents different configurations of hybrid vehicles to improve the braking energy regenerated potential and engine work efficiency. From the results obtained we try to draw a conclusion on the difference in energy recuperation level in the major strategies with consistent pedal feel in mind.

2. Fuel savings for ground vehicles

Ground vehicles (military, agricultural, and construction) usually operate on unprepared ground and need to overcome very complex and difficult ground obstacles, such as steep grade and very soft ground. Depending on the functional requirements, different criteria are used to evaluate the performance of various types of ground vehicles. For tractors, their main function is to provide adequate draft to pull various types of implement and machinery: drawbar performance is of primary interest. This may be characterized by the ratio of drawbar pull to vehicle weight, drawbar power, and drawbar efficiency. For ground transport vehicles, the transport productivity and efficiency are often used as basic criteria for evaluating their performance. For military vehicles, the maximum feasible operating speed at two specific points in a given area may be employed as a criterion for evaluation of their agility [7].

2.1. Mechanical regenerative braking

Improvements of truck fuel economy are being considered using a flywheel energy storage system concept (KERS-Kinetic Energy Recovery System). This system reduces the amount of mechanical energy needed by the thermal engine by recovering the vehicle kinetic energy during braking and then assisting torque requirements. The benefits of flywheel based KERS are similar to hydraulic regenerative braking but with the advantage of reduced complexity, less space needed and simpler construction and operation. The cost as well as the packaging and weight of a KERS for truck are not an issue as in passenger car applications. Two counter rotating flywheels could possibly solve the stability issue due to the increased rotating mass required for braking vehicles of considerable weight.

The energy boost by KERS may be beneficial more to help trucks climbing hills rather than for engine downsizing, also providing a better road safety. KERS will also collect considerable energy braking down hills reducing the need for engine brakes and thus noise. Boretti [8] summarizes the computed fuel economy benefits of KERS.

2.2. Hybrid-electric ground vehicles

The idea of hybrid-electric drive is based on maximizing the energy efficiency of fuel. In the classical drive the energy disappears by transforming into the heat in all drive components from the fuel tank to the drive wheels of vehicles, and most in the internal combustion engine that converts chemical energy of fuel into useful work. The causes of this are numerous, but one of the biggest is that the engine is running in a very wide range of number of revolutions and loads while working with varying degrees of efficiency ratio.



Fig. 2 *Diagram of the relative fuel consumption of a typical internal combustion engine and the paths of energy through a typical gas-powered vehicle in city driving [9].*

Figure 2 shows the relative fuel consumption of a typical ICE and the paths of energy through a typical gas-powered vehicle in city driving. If, for example, the engine delivers 100 kWh of energy from areas of least fuel consumption, it will be spent 22 liters of fuel, and if that same energy draws out from the area of the engine works at low load, it will be spent up to two or even three times more fuel. If the engine could keep the regimes of minimum consumption, which means a load of more than 50% and the number of rotation around the maximum torque, then you could save a considerable amount of fuel for the same usable energy. This is not possible in a classical drive chain (motor-transmission-wheels). It is necessary, therefore, to separate the engine physically from the drive wheels and to establish a completely different structure of the propulsion system, in order to achieve full control of engine operating modes according to the number of rotation and load [9].

There are three basic types of hybrid-electric drive: serial, parallel and plug-in (Fig. 3). A series hybrid uses a gasoline or diesel ICE, coupled with a generator, to generate electricity but not to drive the car. The engine can send the electric current directly to the electric motor or charge a large battery that stores the electricity and delivers it to an electric motor on-demand. The electric motor propels the vehicle, using its power to rotate a driveshaft or a set of drive axles that turn the wheels.

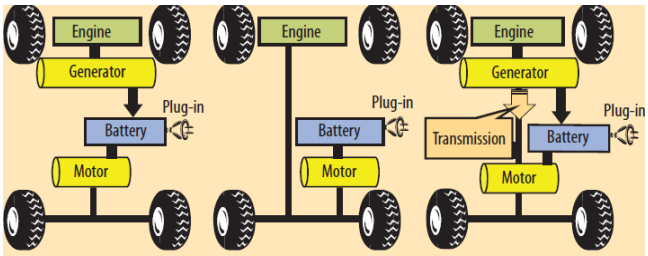


Fig. 3 *The basic structure of serial, parallel and plug-in hybrid-electric drive.*

A parallel hybrid uses both an electric motor and an ICE for propulsion. They can run in tandem, or one can be used as the primary power source with the other kicking in to assist when extra power is needed for starting off, climbing hills, and accelerating to pass other vehicles. Because both are connected to the drive train, they're said to run "in parallel." Because plug-in hybrids feature larger batteries that can be charged at any ordinary electrical socket, they have the capacity to extend the ability of the electric motor to

drive the car farther without the need for starting the ICE and therefore substantially increase the vehicle's fuel efficiency. Estimates have ranged as high as 100 mpg!

2.3. Hydraulic hybrid ground vehicles

Hydraulic hybrid technology has the advantage of high power density and the ability to accept the high rates/high frequencies of charging and discharging, therefore it is well suited for off-road vehicles and heavy-duty trucks. Relatively lower energy density and complicated coordinating operation between two power sources require a special energy control strategy to maximize the fuel saving potential. Kumar [10] has presented a new configuration of parallel hydraulic regenerative vehicle (PHRBV) to improve the braking energy regenerated potential and engine work efficiency. Based on the analysis of optimal energy distribution for the proposed PHRBV over a representative urban driving cycle, a fuzzy torque control strategy based on the vehicle load changes is developed to real-time control the energy distribution for the proposed PHRBV.

The HRB Hydrostatic Regenerative Braking System helps meet increasingly strict environmental regulations and reduces operating costs by saving fuel. The HRB system will provide superior return on investment. The HRB stores a vehicle's kinetic energy, which would otherwise be lost during mechanical braking operation. This energy is then available for powering the vehicle and reducing primary energy use. HRB, the hydraulic hybrid of Rexroth, reduces fuel consumption and CO_2 emissions from heavy commercial vehicles with a high stop & go frequency by up to 25 percent and brake wear by up to 50 percent. This helps to reduce environmental pollution and the total cost of ownership for the operator.

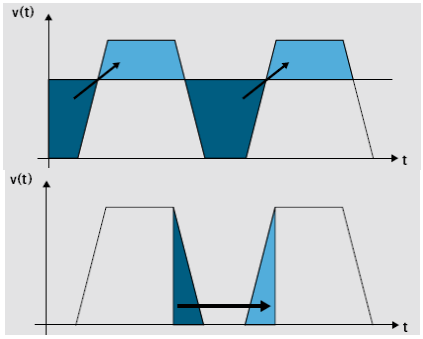


Fig. 4 *Characteristics of an electric hybrid and hydraulic hybrid [11].*

Characteristics of electric hybrid: Excess motor power is continuously accumulated in a battery over a longer time period (blue) and accessed as needed (light blue); High energy density and low power density: The battery can absorb a great deal of energy, but the charge time is relatively long, so it is not possible to fully recapture the braking energy; Energy is stored in batteries; Typically found in passenger cars.

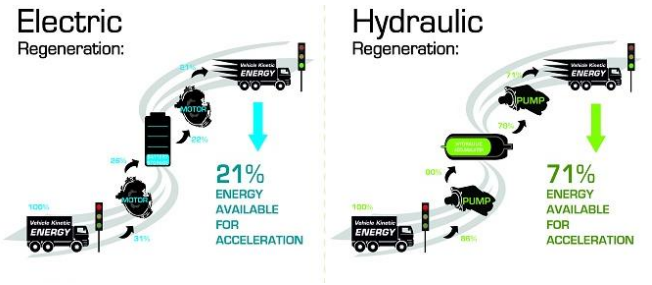


Fig. 5 *A comparison of electric and hybrid regeneration.*

Characteristics of hydraulic hybrid: The kinetic energy from braking is fed to a hydraulic accumulator (blue) and immediately reused for starting (light blue). Hydraulic hybrids are ideal for vehicles with frequent, short start-stop cycles, such as public transit buses, refuse trucks, forklifts, pneumatic tire rollers, telehandlers, swap body movers and much more; High power density and low energy density: there are limits to the amount of energy the system can accumulate. However, it takes less time to collect and store this energy, which can be called upon as needed. The full braking energy is then fed to a hydraulic accumulator and stored.

There is a common consensus that hybrid drive trains can strongly increase the efficiency of a drive train. However, the increased efficiency does not by itself result in a reduction of the fuel consumption or the cost of ownership. The electric drive train components result in an increased vehicle weight, which increases the fuel consumption of the vehicles. Moreover, the added cost for the electric components gives doubt about the cost-benefit-relationship, especially of the full hybrid drive train concepts. Nevertheless, the trend of hybrid electric transmissions has also come to the ground vehicles market. Achten & Innas [5] have proposed "Hydrid" drive and control system that enables the design of a new generation of off-road vehicles with a strongly reduced fuel consumption, while maintaining (or even improving) the productivity. The "Hydrid" completely eliminates the mechanical drive train, thereby creating extra degrees of freedom for the suspension and traction control of the vehicle. The "Hydrid" has hydraulic accumulators for energy storage and power management, hydraulic transformers for efficient power control, and highly efficient and compact in-wheel motors.

2.4. Military Applications of Hybrid Cars and Trucks

Implementing HEV technology in military vehicles offers a number of potential advantages. The possibility to generate an increased amount of electric power is one important advantage that addresses the immediate demand for ever more electric power onboard modern military vehicles. Other advantages may become equally important with time. There are, however, technical challenges related to specific subsystems (components) in a HE drivetrain and to the overall system and vehicle design.

The great interest in military HEVs suggests that it is an important technology for future military vehicles. Compared to a legacy military vehicle, a military HEV will be more complex and an increasingly multidisciplinary system. Given also the large variety of military vehicles, tracked or wheeled, from unarmed to heavy armed, and the relatively immature HE technology, no two systems are alike. It is therefore difficult to draw simple and universally valid conclusions. The relevant time frame also becomes very important. The most viable solution in the short term (5-7 years) might not be the same one as in the long term.

Model-based systems development for military ground vehicles is a key enabler for rapid prototyping and design optimization. Batteh & Tiller [12] have described flexible, modular vehicle model architecture in Modelica to support a range of systems engineering analyses of conventional and hybrid vehicle architectures throughout the product development process. The models and sample simulation results highlight the flexibility of the model architecture and the wide range of engineering analyses that can be supported.

In August 2007, the U.S. Army Tank Automotive Research, Development and Engineering Center (TARDEC) began full-load integration testing of the military's first hybrid electric drive propulsion system designed for combat vehicles [13]. Milner et al. [14] developed and validated a high-fidelity six-degree-of-freedom model to use in a trade study for the development of a prototype autonomous vehicle. The model was developed with extensive capabilities for evaluating both on-road and off-road vehicle performance while allowing the user to modify the components and simulation setup as desired. The model enables the user to assign any desired modifications to virtually all of the major vehicle and simulation parameters.

However, there are important technical challenges that need to be solved before we will see the successful fielding of a mass produced military HEV. A number of military HEVs have been successfully demonstrated, but there are still important limitation related to key technologies such as electric motors, power

electronics and energy storage systems (e.g. batteries). The maturity of the technology depends on the vehicle type (role, weight, tracked or wheeled etc.) and the HEV drivetrain architecture opted for (series, parallel etc.) [15].

Combat vehicles can also have benefit from the hybrid-electric drives. Some of the most important are the following: Fuel savings- As with civilian vehicles and in combat and other vehicles for military purposes, narrowing the area of combustion engines can contribute to significant fuel savings (in some driving conditions even more than 50%). Fuel savings in military vehicles is important not only because of the fuel but also because there are other repercussions: simplifying and reducing costs of logistics, increasing the autonomy of the vehicles and so on. The issue of environmental protection is also not unimportant-lower fuel consumption means lower emissions and other toxic substances. Low acoustic signature of the vehicle-Hybrid-electric drive reduces the possibility of observing the vehicle through a lot of elements. One of the most important is that within the limits of available energy in batteries, the vehicle can be powered purely electrically powered, which means no noise, heat radiation and no emission gases. This ride can be of crucial importance in military operations. But even when the vehicle is driven in a combined operation, observing of the vehicles has been reduced because:

- IC engine runs at lower numbers of rotation, and there is no sudden changes, which means less noise,
- hydraulics for propulsion of the auxiliary systems to power the vehicle can be completely eliminated, thereby eliminating the noise of hydraulic pumps and motors, which is usually considerable,
- reduced noise from cooling fans and others.

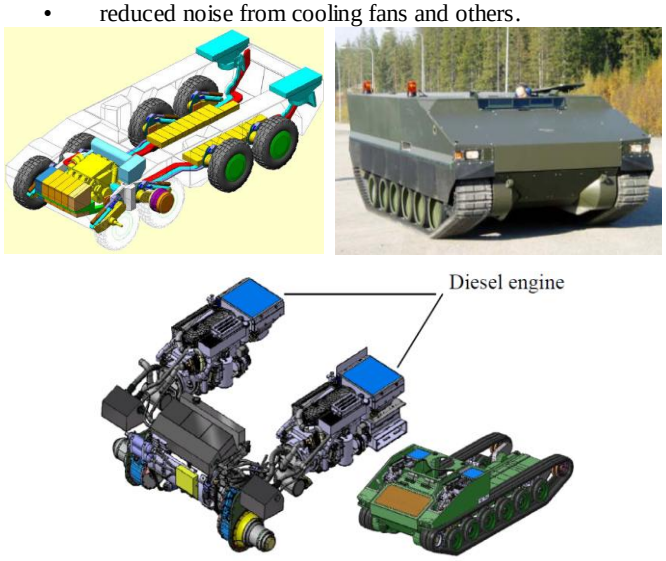


Fig. 6 *Hybrid Electric Combat Systems*.

With hybrid-electric drive, vehicle has electricity available in unlimited quantities that can be used to drive auxiliary devices, and other needs of the dome cars, and even for purposes outside the vehicle. New technologies of electric weapons and electromagnetic protection (EM shielding) are useless without a strong source of power supply. There are many other benefits of hybrid-electric drive as: modularity of the system easier to maintain, complete automation and control reduce the human factor and provide a better diagnosis, flexibility in the design of the propulsion system enables better use of space, and others [16].

3. Conclusion

Automotive engineers may be further ahead in applying hybrid technologies, but some of the most exciting hybrid innovations these days target off-road OEMs and makers of military, agricultural and construction vehicles. Regenerative braking is a major means of hybrid vehicle to reduce consumption of fuel and lower the environment pollution. Comparison of different solutions of hybrid ground vehicles in terms of the percentage of recuperated energy during the regenerative braking phase is done in this paper. The proposed hybrid drive and control system enables the design of a new generation of ground vehicles with a strongly reduced fuel consumption, while maintaining the productivity. Militaries worldwide are also interested in realizing the potential energy savings associated with hybrid vehicles. It is important to note that there are other potential payoffs associated with military hybrid vehicles: the ability to idle and possibly move without the acoustic and thermal signatures of an internal combustion engine. Regenerative braking that incorporates a hydraulic system has the advantage of high power density and the ability to accept the high rates/high frequencies of charging and discharging. This makes hydraulic regenerative braking technology well suited for off-road vehicles and heavy-duty trucks.

This paper was realized within the researching project “The research of vehicle safety as part of a cybernetic system: Driver-Vehicle-Environment” ref. no. 35041, funded by Ministry of Education, Science and Technological Development of the Republic of Serbia.

4. References

1. B. Dudley, BP Energy Outlook 2017 edition. (2017). (https://www.bp.com/content/dam/bp/pdf/ energy-economics/ energy-outlook-2017/bp-energy-outlook-2017.pdf, 10.06.2017)
2. C. Mi, M.A. Masrur, & D.W. Gao, *Hybrid electric vehicles-Principles and applications with practical perspectives*, United Kingdom: A John Wiley & Sons, Ltd., Publication (2011)
3. G. Pistoria, *Electric and hybrid vehicles*. Elsevier, Netherlands (2010)
4. S. Skoog, *Power Sources for Hybrid Electric Vehicles*, Dissertation, Division of Industrial Electrical Engineering and Automation, Faculty of Engineering, Lund University (2009)
5. P. Achten & B.V. Innas, A Series Hydraulic Hybrid Drive Train For Off-Road Vehicles. Fluid Power Journal, Proceedings of Off-Highway Directory, 8-12 (2009)
6. I. Husain, *Electric and hybrid vehicles: Design Fundamentals*, New York, NY: CRC Press, Taylor&Francis Group (2010)
7. M. Ehsani, Y. Gao & A. Emadi, *Modern Electric, Hybrid Electric, and Fuel Cell Vehicles-Fundamentals, Theory, and Design*, New York, NY: CRC Press, Taylor &Francis Group (2010)
8. A.A. Boretti, Improvements of Truck Fuel Economy using Mechanical Regenerative Braking, SAE Technical Paper 2010-01-1980 (2010)
9. Z. Ilijevski, Hibridno-električni pogon vozila za vojne potrebe, from http://www. hrvatski-vojnik.hr/hrvatski-vojnik/0212005/hibrid.asp, accessed on 2010-09-07.
10. ER.A. Kumar, Hydraulic Regenerative Braking System, Int. J. Sci. & Eng. Res. **3**(4), 1-12 (2012)
11. Hydraulic Hybrid from Rexroth: Hydrostatic Regenerative Braking System HRB (2011). from https://www.boschrexroth.com/en/us/products/systems-and-modules/mobile-hydraulic-systems/hydrostatic-regenerative-braking-system-hrb/hrb-function/hrb-function-page, accessed on 2016-07-07
12. J.J. Batteh, & M.M. Tiller, A modular model architecture in modelica for rapid virtual prototyping of conventional and hybrid ground vehicles, *Proceedings of the 2009 Ground Vehicle Systems Engineering and Technology Symposium (GVSETS)*, 1-14 (2009)
13. G.M. Bochenek, & J. Hitchcock, Army Transitions Hybrid Electric Technology to FCS Manned Ground Vehicles, ARMY AL&T, 36-39 (2007)
14. D. Milner, J. Goodell, W. Smith, M. Pozolo & J. Ueda, Modeling and Simulation of an Autonomous Hybrid-Electric Military Vehicle, World Electr. Veh. J. **3**, 1-9 (2009)
15. P. Dalsjo, Hybrid electric propulsion for military vehicles-Overview and status of the technology. FFI-rapport 2008/01220 (2008)
16. D.M. Rizzo, *Military vehicle optimization and control*. Dissertation. Michigan Technological University (2014)